Department of Chemical Engineering

Improvements of Oil-In-Water Analysis for Produced Water Using Membrane Filtration

Khor Ee Huey

This thesis is presented for the Degree of
Doctor of Philosophy
of
Curtin University

February 2011

Declaration

To the best of my knowledge and belief this thesis contains no material previously published by any other person except where due acknowledgment has been made.

This thesis contains no material which has been accepted for the award of any other degree or diploma in any university.

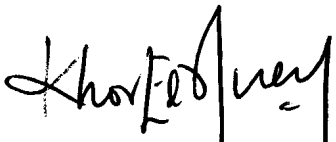

Signature: .....

Date: 21 February 2011

To my parents, beloved husband and two lovely daughters

Abstract

The accuracy of oil-in-water analysis for produced water is increasingly crucial as the regulations for disposal of this water are getting more stringent world wide. Currently, most of the oil producing countries has their own regulations for disposal of this water. The oil-in-water can be distinguished between two types, mainly dispersed and dissolved oil. Among these oils, dispersed oil concentration is the main component under monitoring for the oil-in-water limitation. From literatures, the standard analytical method for oil-in-water measurement has been changed from IR analysis to GC-FID analysis due to solvent restrictions. As a result of the change, a total of dispersed and dissolved oil is measured and this causes the oil-in-water parameter value to be higher. Therefore the removal of dissolved oil before oil-in-water analysis is critical. This issue can be overcome by enhancing current monitoring technique which incorporates a separation technique in removing dissolved oil from the produced water prior to the GC-FID analysis. A thorough review was given to all current available separation techniques that can be employed for dissolved oil removal. Membrane filtration system was proposed in this research to be incorporated into the test method to remove the dissolved oil as it is relatively a small separation unit, easy to operate and very practical in the laboratory scale application. By using membrane filtration, it was found that the removal of dissolved oil is dependent on the pore-size of the membrane where in this case Microfiltration removes more dissolved oil than Ultrafiltration.

However, there is an issue in using this membrane filtration technique. The deposition of dispersed and dissolved oil on the membrane reduces the efficiency of the removal process. In this research, mathematical & computational modelling was done in studying the hydrodynamic effect caused by pressure for the fluid flow profile inside the membrane cartridge. Then, two approaches are proposed in the

prevention of fouling, firstly, by physical or mechanical means and secondly, by chemical means. The use of mechanical means for the prevention of deposition were studied by simulation using computational fluid dynamics (CFD) and mathematical model to visualize the hydrodynamic conditions inside the membrane cartridge. Mathematical model has been developed for the relationship of differential pressure (DP) with the concentration of oils at the wall (Cg). The purpose of this study is to estimate the concentration of oils by changing the differential pressure. Several factors for the reduction of fouling or the concentration of oils at the membrane wall by physical means such as pore sizes, membrane types and operating conditions were studied. The experimental data were analyzed by using statistical method. Through design of experiment (DOE) and the verification of CFD visualization, the optimum conditions for the operation were identified to be at low differential pressure (DP) but at high trans-membrane pressure (TMP). The most suitable type of membrane with 0.2um pore size was found to give highest efficiency in removing dissolved oil.

Despite these findings, the total prevention of oil fouling on the membrane by mechanical means is not possible. Therefore, chemical pre-treatment method and chemical cleaning methods were explored in their capacity to remove the deposition of oil on the membrane. This pre-treatment method enhances the separation by changing the physical properties of the oil towards the membranes. Changes of chemical properties of oil should be avoided in this attempt for accuracy of measurement. pH changes are one of the ways for pre-treatment, and the effects of acidity and alkalinity effect on the solution were studied for the improvement of the separation. Chemical cleaning using NaOH was investigated for its ability to clean off the deposition of oils on the membrane. The duration of the cleaning as well as the volume used were studied experimentally until the optimum conditions were reached. The chemical treatment approaches are integrated into the physical method to enhance the removal of dissolved oil by using membrane filtration. The optimum condition of this integrated techniques were verified experimentally.

In conclusion a new standard analysis method in the oil-in-water parameter monitoring for produced water in the oil and gas sector has been developed. With the incorporation of membrane filtration system, produced water analysis will be improved, which would benefit the oil and gas operators.

Acknowledgement

I quit my permanent job with the government to commence a 4-years journey of PhD endeavour in 2007. With a two year old kid and 6 months old baby, I could not have regretted more at the start of my research. However, life could not have been better without the support from my loving husband, Bernard Chin, who has never lost his faith in me.

I would also want to thank my Supervisor, Prof. Yudi Samyudia whom has given his encouragement and guidance throughout these 4 years of research.

My gratitude also goes to fellow lecturers in Curtin University of Sarawak Malaysia namely Dr. Alexander Gorin, Mr. Freddie Panau, Mr. Jobrun Nandong, Mr. Rajalingam Sokkalingam, for the contributions in their area of expertise.

Special thanks goes to Dr. Paul for his training in "Advance in Design of Experiment", which has enlightened me in the area of statistical studies.

Last but not least, I thank God for He is the TRUTH which through knowing Him is where the knowledge starts; He is the WAY which He has guided me without err and He is the LIFE which I may have hope when looking forward in completing my PhD. All glory and honour goes to Him in the highest.

Publications

Journal Papers

E.H. Khor, Y. Samyudia, 2009, "*The study of mass transfer coefficient in membrane separation for produced water*", International Journal of Chemical Engineering, Vol. 2, No. 2-3, pp. 143-152.

E.H. Khor, P. Mullenix, Y. Samyudia, 2010, "*Modified film theory model for fouling control in membrane filtration*", Asia Pacific Journal of Chemical Engineering. (Submitted)

E.H. Khor. Y.Samyudia, 2011, "*Improvements of oil in water analysis for produced water using cross-flow membrane filtration*", Journal of Membrane Science. (In preparation)

E.H. Khor, Y.Samyudia, 2011, "*Enhancement of Dissolved Oil Separation by Integrated Mechanical and Chemical Treatment*", Chemical Engineering Science (In preparation)

Conference Papers

E.H. Khor, Y. Samyudia, 2007, "*Review on produced water treatment technology*", Proceedings of the 21st symposium of Malaysian chemical engineers (SOMChE 2007), Kuala Lumpur, Malaysia, December 2007.

E.H. Khor, Y. Samyudia, 2009, "*The study of mass transfer coefficient in membrane separation for produced water*", CHEMECA 2009, Perth, Australia, September 2009.

E.H. Khor, P. Kumar, Y. Samyudia, 2009, "*CFD modelling of crossflow membrane filtration –Integration of filtration model and fluid transport model*", 2nd CUTSE International Conference 2009, Miri, Malaysia, November 2009.

E.H. Khor, Y. Samyudia, 2010, "*Optimization of dissolved oil separation for produced water analysis*", 5th International Symposium on Design, Operation and Control of Chemical Processes (PSE Asia), Singapore, July, 2010.

E.H. Khor, Y. Samyudia, 2010, "*A comparison of the separation efficiency of dissolved and dispersed oil using microfiltration and ultrafiltration membrane*", CHEMECA 2010, Adelaide, Australia, September 2010.

TABLE OF CONTENTS

List of Tables

List of Figures

Nomenclature

C_g	Concentration at the wall or gel concentration
C_b	Bulk concentration
DP	Differential pressure or crossflow pressure
MF	Microfiltration
MTC/ *k*	Mass transfer coefficient
TMP	Trans-membrane pressure
UF	Ultrafiltration
R_o	Observed Rejection
δ	Boundary layer
MWCO	Molecular weight cut-off
Permeate	Filtrate
kDa	kilo Dalton
EDTA	ethylenediaminetetraacetate
SDS	Sodium Dodecyl Sulfate
ANOVA	Analysis of Variance
r^2	Coefficient of determination
DI	Distilled Water
N	Normality, number of reactive units in 1L

Chapter 1: *Introduction*

1.1. Background

Produced water is the water that is being extracted from the subsurface during oil and gas production. During early production, the amount of water present may be insignificant. However, as time goes by, a sizeable amount of water will be produced by old oil wells [1]. According to a study done by Kemmer [2], every barrel of oil extracted yield approximately 6-8 barrels of produced water. This produced water originates from the water that is trapped in permeable sedimentary rocks within the well bore. It includes the water that has been injected into the formation to maintain reservoir pressure and any chemicals added during the production/treatment processes. Due to the high salinity and oil content, the disposal of such waste water at the bay can have a great impact on the ecologically sensitive environment. Nevertheless, experience to date has shown that re-injecting produced water is an attractive and more environmentally-sound solution to water disposal.

To protect the environment, before deep water disposal or reinjection, the water needs to be separated from the oil [3] because the oil from the water has the tendency to cause sediment contamination, acute toxicity, oxygen depletion and ecosystem instability [4]. Oil-in-water analysis techniques are therefore very crucial especially in the accuracy of detecting the oil content to meet the stringent regulations and standards stipulated by individual country. The laboratory analysis methods that are currently available are explained in the following section.

1.2. Oil-in-water Analysis Method

The laboratory analysis techniques available are listed below [5]:

- Infrared analysis (IR)
- Gravimetric analysis
- Liquid-liquid extraction and gas chromatography using flame ionisation detection (LE-GC-FID)
- Ultraviolet (UV) fluorescence
- Ultraviolet (UV) absorbance
- Colorimetry
- Supercritical fluid extraction coupled on-line with infrared spectroscopy
- Fibre optic chemical sensor

Most of these techniques are not oil-specific as they respond to any suspended particles. UV fluorescence spectroscopy is partly oil-specific, because it only measures accurately when the oil is dissolved or emulsified [6]. When oils are in droplets or dispersed form, the measurement will not be accurate. Currently, the standard methods for oil-in-water analysis in laboratory are based on IR absorbance, gravimetric, GC-FID and calorimetric techniques. These techniques have their advantages and disadvantages. Table 1.1 shows the summary of the most widely used analytical method in oil and gas industry with their pros and cons.

Table 1.1 Advantages and limitations for different types of analytical methods

Analytical Method	Advantages	Limitations	References
Infrared (IR)	Simple, inexpensive. Well established.	Freon is prohibited for use in laboratory. TTCE substitute for Freon is carcinogenic.	[7]
Gravimetric	Simple, quick, inexpensive.	Not sensitive. For very oily sludge/ waste only. Not suitable for light HC.	[8]
UV absorbance/ fluorescence	Easy to use, no extraction needed.	Detect only aromatic organic matter. Affected by non-petroleum products that fluoresce e.g. chlorophyll.	[9]; [10]
Liquid-liquid extraction and gas chromatography using flame ionisation detection (LE-GC-FID)	Best replacement for IR; Qualitative and quantitative information can be provided.	Difficult procedures. Need skilled laboratory operators to interpret the spectrum.	[11]

1.3. Regulations and Standards

Currently, most of the oil producing countries has their own regulations for the disposal of this water (Table 1.2). However, some oil operators observe their own regulations which are more stringent compared to what the country has stipulated. For instance, Shell Company operating in Malaysia will observe Shell Global Standard as their dispersed oil limit in produced water for disposal (Table 1.3). This ensures that the standard limit set by the country is not being violated. For the oil-in-water standard, dispersed oil concentration is the main component for the monitoring.

In oil and gas terms, dispersed oil refers to the free oil in produced water which is in the form of small droplets, and may range from sub-microns to hundreds of microns. Large amount of dispersed oil is harmful to the environment, as they can agglomerate to form a thin film on the surface of the water and prevent oxygen from dissolving into the sea water thus threatening the marine lives [12]. Another type of oil which is not under the regulation is termed dissolved oil – such as BETX (benzene, ethyl-benzene, toluene and xylene), NPD (napthalene, phenanthren, dibenzothiophene) and/ or some of the PAHs (polyaromatic hydrocarbons) that are partially soluble and can be present in dissolved form in the water.

Table 1.2 Dispersed oil level in produced water for disposal

Locations	Discharge limits (mg/l)
Australia	30 average and 50 Max
Brazil	20 Max
Brunei	30 (Horiba single wavelength IR method)
Canada	40 average (30 days rolling), 60 max for any 48 hrs.
Caspian Sea	20
China	30 for inner sea and 50 for outer sea, 40 and 75 max
Egypt	15 max
Gabon	20 ASTMD3921-85, UV/Vis Spec
Indian Ocean (Bombay High Field)	48
Indonesia	50
Italy	40
Malaysia	100 (APHA 5520-B Gravimetric)
Nigeria	10-20
Thailand	100 max
Tunisia	10 max
Sultanate of Oman	5 (coastal) (UV/Vis Spec)
USA (EPA)	29 average (30 days) and 42 max
Venezuela	20
Vietnam	40

Table 1.3 Shell Global Standard for dispersed oil limit

Shell Global Standard	Pollutant Parameter	Onshore Limit	Offshore Limit
Daily maximum	Oil and grease	40mg/L	70mg/L
Monthly average	Oil and grease	15mg/L	30mg/L

1.4. Issues in Regulatory Control Standard for Produced Water

As illustrated in Section 1.3, the disposal of the produced water is being regulated under strict environmental regulations and therefore produced water needs to go through primary and secondary treatments. As a rough guide, the allowable limit set by regulatory body for the disposal of hydrocarbon content in the water is currently limited to a range of 15mg/L to 50mg/L for offshore disposal [13]. In most instances, produced water cannot be disposed off onshore, due to possible salt contamination, and must be injected into an acceptable disposal formation normally oil wells or disposed of by evaporation. Experience to date has shown that re-injecting produced water is an attractive economical way and environmentally-sound solution to water disposal [14, 15]. Moreover, reinjected water could stabilize the pressure of the oil well after excavation and could even increase oil production.

In 1975, initiated by 15 countries in the western coasts of Europe, OSPAR (Oslo and Paris) Commission was formed to protect marine environment and to date, most of the oil and gas operators, especially in the North Sea, are still following the disposal criteria given by this organization. The determination of oil in produced water has been carried out for nearly two decades using solvent based extraction followed by infra-red quantification. However, following the ban on the use of Freon due to ozone depletion and the concerns over health and safety of its replacement Tetrachloroethylene (TTCE), OSLO-PARIS Commission (OSPAR) implemented a new standard method across North Sea in 2007. This method is called OSPAR GC-FID method. However, an issue arises in this OSPAR method on the monitoring of produced water disposal because of the limitation in the analytical technique used. OSPAR stated a disposal limit of oil in terms of dispersed oil concentration; but with the current analytical method (GC-FID), the total of dissolved and dispersed oil is measured as no distinction of dissolved oil is made during the measurement process. Therefore, the readings will be higher than the actual, resulting in non-compliance to the regulatory standard.

There are two possible improvements to this analytical method, namely a) subtraction of dissolved oil peaks from the Total Ionic Chromatogram (TIC) spectrum but this requires skilled laboratory operators, or b) incorporation of a treatment technique in the analytical method to remove the dissolved oil. In normal laboratory, it is neither feasible nor economical to employ skilled laboratory operators who are able to identify and subtract dissolved oil peaks and these require on-going operational. Moreover, to perform this operation is very time-consuming. The latter option on the other hand requires only an initial one-off capital cost. Therefore, the practicality of the second option which is the incorporation of a separation method to remove the dissolved oil becomes more viable and is the basis or motivation for this research.

1.5. Current Treatment Techniques for the Removal of Dissolved Oil from Produced Water

Produced water needs to be separated from the oil during production and before their discharge. According to Hansen and Davies [16], the traditional treatment methods such as flocculation or clarification performed badly in the removal of dissolved oil as compared to emulsified/ dispersed oil components. Currently, there are two parameters in the separation of oil from produced water. The first parameter is by using the density difference between oil and water. The specific gravity of oil is 0.8 [17, 18] and hydrocyclone is one of the application of separation technique by density difference. The second parameter is separation by the size of oil droplet. The size of oil droplet varies in time. As oil droplets increase in size the rising rate (buoyancy) of the droplets increases too. Figure 1.1 shows the histogram of oil droplet distribution [19]. An example of applications using this droplet size parameter is by coalescence technique. Currently after extraction, produced water is being sent to the skimmer or hydrocyclone for the separation of oil and water followed by secondary separation process using induced gas floatation. Table 1.4 summarises the produced water treating system configuration with their approximate minimum droplet size removal. Current produced water treating technologies are designed to remove discrete droplets of oil from the water, and not the soluble oil [3].

A tertiary treatment by membrane filtration may further reduce the contaminants to an acceptable level suitable for water reuse. A review on produced water treatment by Khor and Samyudia [20] commented on the possible integration of membrane filtration system as a tertiary process to remove the dissolved oil.

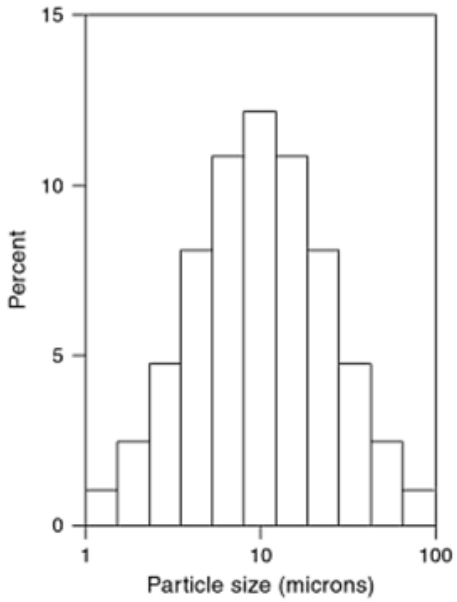

Figure 1.1 Histogram of oil droplet distribution [19]

Table 1.4 Produced water treating methods and equipments [13, 21, 22]

Method	**Equipment Type**	**Approximate Minimum Drop Size Removal Capabilities (Microns)**
Gravity Separation	Skimmer Tanks and Vessels	100-150
	API Separators	
	Disposal Piles	
	Skim Piles	
Plate Coalescence	Parallel Plate Interceptors	30-50
	Corrugated Plate Interceptors	
	Cross-flow Separators	

	Mixed-flow Separators	
Enhanced Coalescence	Precipitators	10-15
	Filter/Coalescers	
	Free-flow Turbulent Coalescers	
Gas Floatation	Dissolved Gas	4-20
	Hydraulic Dispersed Gas	
	Mechanical Dispersed Gas	
Enhanced Gravity Separation	Hydrocyclones	5-15
	Centrifuges	
Advance Oxidation Process	UV and Ozonation	10-15
Filtration	Multi-media	<1-10
	Membrane	
Surfactant modified Zeolite	Granular particles	BTEX

Other possible treatment methods to remove dissolved oil includes chemical clarification, bubble separation, photocatalytic oxidation, phytoremediation and sorption on altered clay minerals, carbonaceous sorbents and granular activated carbon (GAC) [22].

1.6. Research Gap

According to Price [23], Treaty of the Metre has conducted a strategic review from 1998 to 2007 with the aim to resolve problems regarding accuracy of measurements. Accuracy has vital importance concerning metrology in chemistry. For this reason, a new area in chemistry was spawned some time in 1990s i.e. analytical chemistry to meet the global metrological needs. At this juncture, a research idea is drawn to our attention: Current produced water treatment methods such as free-water-knock-out system, hydrocyclone, dissolved gas floatation or biological treatment are not able to remove fully dissolved oil from the produced water. The oil-in-water still consists of

non-polar oil and dissolved oil. Current analytical method measures the concentration of both types of oil despite that only dispersed oil is monitored by governmental regulation [3, 5]. Motivated by this idea, a separation system is proposed to be integrated into the standard analytical method so that the accuracy of oil-in-water measurement can be improved. Filtration process especially membrane filtrations has the advantage in this application because a good degree of separation can be achieved [16]. Furthermore, its application in the laboratory scale can eliminate the problem of high operational cost and degradation of the filters elements when used in plant application for produced water treatment. Therefore, in this research, the use of membrane filtration is proposed in removing dissolved oil in the produced water.

1.7. Research Questions and Thesis Objectives

Five specific research questions which form the basis of the literature review in Chapter 2 are being addressed in this thesis and the main findings from each study are presented in the following section. The research questions highlighted below outlined the five objectives of this study, surrounding the main purpose of removing the dissolved oil from the produced water using membrane filtration. All these five topics will be elaborated in Chapters 4 to 8.

1.7.1. Is membrane filtration a feasible technology for the separation of dissolved oil from the produced water?

The practicality of incorporating membrane filtration into standard test method has not been explored. However, studies have shown that reversed osmosis filtration technique is applicable in the removal of dissolved oil [24]. In another study of produced water treatment using membrane filtration, Santos and Wiesner [25] were not able to demonstrate the overall technical and economical effectiveness of ultrafiltration due to unpredictability of influent water quality. In Chapter 4 of this thesis, microfiltration and ultrafiltration membranes are compared for their efficiency in the removal of the dissolved oil in permeate. For the measured efficiency in this study, the dispersed oil should remain in the retentate as much as possible.

1.7.2. Fouling is the main concern for membrane filtration. What are the models that describe the fouling phenomena in the membrane cartridge?

Film theory model [26] can explain very well the concentration polarization occurring on the membrane surface. However, to use this model, the estimation of the mass transfer coefficient (MTC) in the application of membrane filtration is crucial. This is because the hydrodynamic effects on the fouling of the membrane can be studied by monitoring the MTC. In Chapter 5, linear regression was performed to estimate the MTC using two models namely Film Theory (FT) model and Solution Diffusion Theory [27]. These two models were then compared and the model which fits the experimental data was chosen and the MTC estimated are then used for subsequent studies. The FT model was being analyzed by using a statistical tool i.e. Respond Surface Methodology (RSM) to improve and formulate a new model. The correlation between the differential pressure (DP) and the MTC were established using the modified FT model.

1.7.3. Differential pressure (DP) is an important parameter to control the fouling. How does the DP affect the fluid flow pattern inside the membrane?

In membrane filtration, the possibility of dispersed oil attaching on the membrane surface is the main concern. The strategy to minimise this gel layer on the membrane by DP was studied by looking at the fluid flow pattern through the use of Computational Fluid Dynamics (CFD) in Chapter 6. By using computational simulation, the condition inside the membrane cassette can be visualised and the turbulent condition, pressure and velocity can be estimated at the outlet. The fundamental understanding of the fouling phenomena was studied through modelling of two sub-models which are the Navier-Stokes equation and Darcy‘s law. The flow profile for clean water flux was studied as a standard with reference to the flow profile of produced water flux at a later stage. These models were simulated using a commercial solver called Fluent.

1.7.4. What are the optimum conditions for the enhancement of the separation by physical method?

After analysing the fluid flow pattern inside the membrane cartridge, the design of physical enhancement technique by using hydrodynamic effect to control the fouling is obviously feasible. In Chapter 7, physical and mechanical parameters such as membrane material, membrane pore sizes, trans-membrane pressure (TMP) and DP for the improvement of the dissolved oil separation are identified. The effects of physical parameters and operating conditions on controlling the fouling are optimized to improve the dissolved oil separation by using statistical tool.

1.7.5. What are the optimum conditions for the enhancement of the separation by combined physical and chemical treatment?

Physical or mechanical means are not able to completely prevent the deposition of oil or prevent concentration polarization from occurring. To improve oil-in-water measurement, dissolved and dispersed oil should not remain deposited on the membrane surface after the separation. Therefore, this research is designed to change the surface properties of the oil and the membrane by using chemicals so that it prevents the oil from adhering onto the membrane surface. This is called a pre-treatment process. pH adjustment is used in the pre-treatment process to change the electrostatic properties of membrane surface and solubility of the oil thus preventing the fouling. Besides pre-treatment process, chemical cleaning method is also performed to wash out the remaining oils that were left on the membrane surface. The oil content that has been washed out by NaOH will be measured, thus improving the accuracy of measurement. To improve the accuracy of measurement, a combined physical-chemical pre-treatment and cleaning process techniques are incorporated into the analytical method. These will be discussed in Chapter 8.

1.8. Assumptions and Thesis Scope

In this thesis, the removal of dissolved oil is very critical for the improvement of current standard analytical method for oil-in-water analysis. The removal based on size exclusions and polarity using isothermal membrane filtration technique was enhanced by physical and chemical approach. Based on the fact that this is a small scale operation with low concentration of feed, this research assumes that the fouling is reversible. It also assumes that during the separation using membrane filtration, there are no interactions between other components such as heavy metals and radioactive materials with the oil components in the produced water. Therefore, the sample used in this research is simulated produced water, containing 100ppm of crude oil and the main focus of the studies is the oil components in produced water. The scope of the thesis is outlined in Figure 1.2. The aim of this thesis is to propose a novel membrane filtration integrated standard test method for the testing of dispersed oil concentration for produced water treatment. The application of membrane separation is enhanced by using physical and chemical approach.

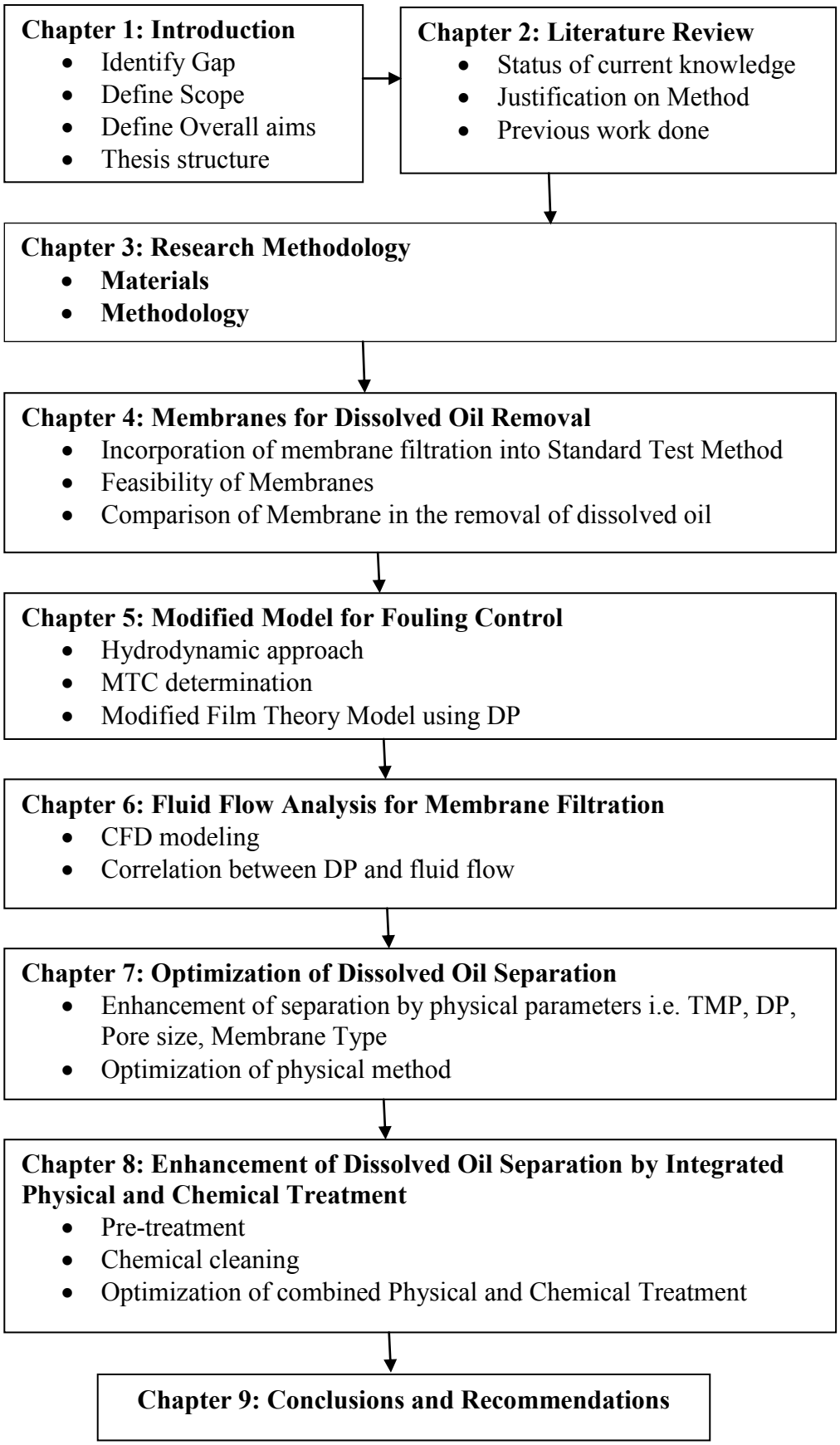

Figure 1.2 Summary of thesis structure

Chapter 2: *Literature Review*

2.1. Introduction

Produced water from oil and gas production is a complex mixture consisting of formation water, re-produced injection water as well as any chemicals added during the production and/or the treatment processes [28]. Currently, dispersed oil concentration is used as the monitoring criteria for the disposal of produced water. Gas Chromatographic flame ionization detector (GC–FID) reference method has been enforced as a standard method to measure the dispersed oil contents in produced water by the Oslo-Paris (OSPAR) convention - signed by nations in the North Sea [29]. However, the drawback of this GC-FID method is that it does not only measure the concentration of dispersed oil but also the dissolved oil concentration. As a result, the reading can be higher than the actual dispersed oil content in the analyzed produced water. This monitoring can lead to the violation of the limit as set by the regulatory bodies. Improvement on the analysis method would be of benefits to many operators of oil exploration.

If membrane (ultra/micro) filtration can be embedded as the pre-processing stage in the OSPAR method, it is expected that the dissolved oil will be contained mainly in permeate while the dispersed oil will be in the retentate. This is because dissolved oil are composed of low molecular weight organic compounds (C2-C5) and medium molecular weight compounds (C6-C15) such as BTEX whereas dispersed oil has longer carbon chains [4]. The retentate is then taken for the oil-in-water analysis using the OSPAR method. This improved produced water analysis would therefore have a more accurate measurement for monitoring purposes.

Figure 2.1 shows the application of membrane filtration incorporated into the GC-FID test method.

Figure 2.1(a) Current oil-in-water analysis process

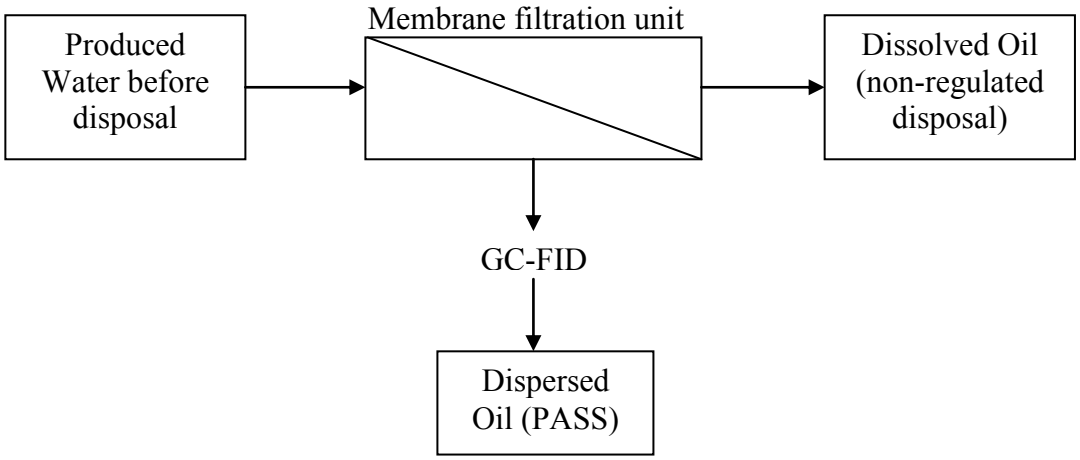

Figure 2.1(b) Integrated analysis process

However for the success of the integrated analysis process, the challenge is to minimise the fouling of the membrane. As shown in Figure 2.2, the deposition of oil onto the surface of membrane could have caused the oil content reading to be lower than the actual.

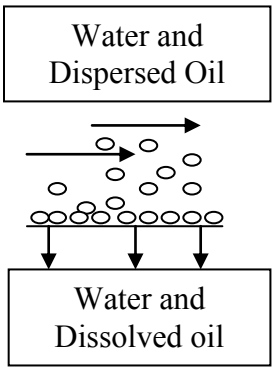

Figure 2.2 Deposition of oil on membrane surface in a crossflow membrane system

In this chapter, the issues of fouling for dissolved oil separation are addressed and solutions to deal with these issues are explored. First of all, identification of both the dispersed and dissolved oil properties from produced water is discussed in detail following a discussion on the current treatment methods for the oils-in-water separations. Secondly, current test method is discussed and the possibility of membrane-incorporated-GC-test-method technique is explored. Thirdly, previous work done for the identification and modelling of fouling is reviewed. Fourthly, possible methods to improve the separation of dissolved oil are investigated through literature review.

2.1.1. Produced Water from Petroleum Industry

The industrial wastewater in the oil and gas context is called the produced water. Produced water is the water extracted from the subsurface together with oil and gas during production. It includes water from the oil and gas reservoir that has been reinjected into the formation to maintain reservoir pressure and any chemicals added during the production/treatment processes [30]. Produced water contains not only the emulsified oil, but also a variety of dissolved substances such as aromatics compound, heavy metals, dissolved organic matter (DOM), de-foamers as well as suspended solids such as sands and natural organic matter (NOM). During early oil and gas production, the water may be insignificant. Over time, percentage of water in the well increases and the petroleum product declines. According to Khatib and Verbeek, [31] water from Shell operating units has increased from 2.1 million bbl per day in 1990 to more than 6 million bbl per day in 2002. With this magnitude of

volumes, disposal of the water becomes an important issue towards the operation as well as the environment.

2.1.2. Produced Water Constituents – Oil in Produced Water

The physical and chemical properties of produced water vary considerably depending on the geographical location of the field, geological host formation and the type of hydrocarbon produced. The properties and volume of produced water could also vary throughout the lifetime of a reservoir. Generally in Malaysia, according to Shell Malaysia Berhad, the properties of the produced water prior to any treatment processes consist of 25% water, 3% emulsified oil and the rest solids and hydrocarbon vapour such as H_2S, NH_3, HCN, phenols, and mercaptans. Table 2.1 shows the produced water characteristics following treatment. These data are collected by EPA (Environmental Protection Agency) during the development of its offshore discharge regulations. Best Practicable Technology (BPT) is the most basic level of treatment and Best Available Technology (BAT) represents a more comprehensive level of treatment.

A very comprehensive study on produced water constituents has been done by Stephenson [12] mainly on the water from Gulf of Mexico. According to the author [12], oil-in-water is a term used to categorize organic matter which exists in two forms in the water at the time of disposal, namely the dispersed (hydrophobic) and dissolved (hydrophilic) organic matter. The dispersed oil and dissolved oil can be illustrated as in Figure 2.3. The following chapters focus on these two types of oil, as these constituents are the main concern of this research.

Figure 2.3 Oil-in-water emulsion: Dispersed oil on the surface of the water (Left) and dissolved oil-in-water (Right)

Table 2.1 Produced water characteristics following treatment [32]

Category	Constituent	Concentration after BPT-Level Treatment (mg/L)	Concentration after BAT- Level Treatment (mg/L) - Gas Floatation Treatment
Dispersed oils	Oil and grease	25	23.5
	n-Alkanes	1.03	0.41
Dissolved oils	2, 4-Dimethylphenol	0.32	0.25
	Anthracene	0.018	0.007
	Benzene	2.98	1.22
	Benzo(a)pyrene	0.012	0.005
	Chlorobenzene	0.019	0.008
	Di-n-butylphthalate	0.016	0.006
	Ethylbenzene	0.32	0.062
	2-Butananone	1.64	0.66
	Naphthalene	0.24	0.092
	p-Chloro-m-cresol	0.25	0.010
	Phenol	1.54	0.54
	Steranes	0.077	0.033
	Toluene	1.901	0.83
	Triterpanes	0.078	0.031
	Total xylenes	0.7	0.38
Heavy Metals	Aluminium	0.078	0.05
	Arsenic	0.11	0.073
	Barium	55.6	35.6
	Boron	25.7	16.5
	Cadmium	0.023	0.014
	Copper	0.45	0.28
	Iron	4.9	3.1
	Lead	0.19	0.12
	Manganese	0.12	0.074
	Nickel	1.7	1.1
	Titanium	0.007	0.004
	Zinc	1.2	0.13

Radioactive materials	Radium 226 (in pCi/L)	0.00023	0.00020
	Radium 228 (in pCi/L)	0.00028	0.00025

2.1.2.1. Dispersed Oil

Dispersed oil consists of small discrete droplets suspended in the aqueous phase or water. Normally dispersed oils are made up of long straight chain carbons, e.g. Figure 2.4. When in contact with the ocean floors, the oil accumulates and contaminates the ocean sediments and causes disorder to the benthic community. On the other hand, if the dispersed oil rises to the surface and spreads, it will cause sheening and will increase biological oxygen demand near the mixing zone. Figure 2.5 shows a picture of dispersed oil layer on the ocean after an oil spill. The amount of dispersed oil in the produced water stream will vary depending on different factors during production. These factors include oil density, interfacial tension between oil and water phases, type of chemical treatment, size and efficiency of the physical separation equipment [33] and the amount of oil precipitation [12]. There are currently many researches on dispersed oil elimination being carried out in all parts of the world particularly by Coastal Response Research Centre [34] This shows the utmost importance in the proper disposal of dispersed oil.

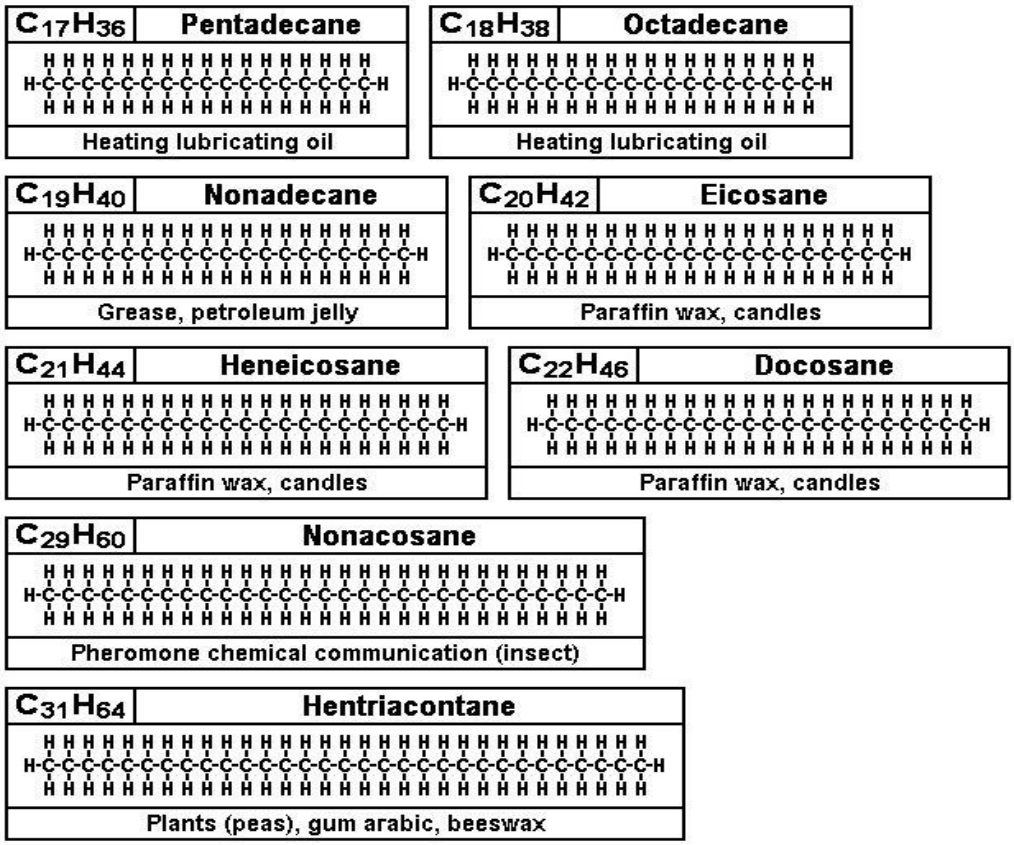

Figure 2.4 Long chain carbons of tetracontane

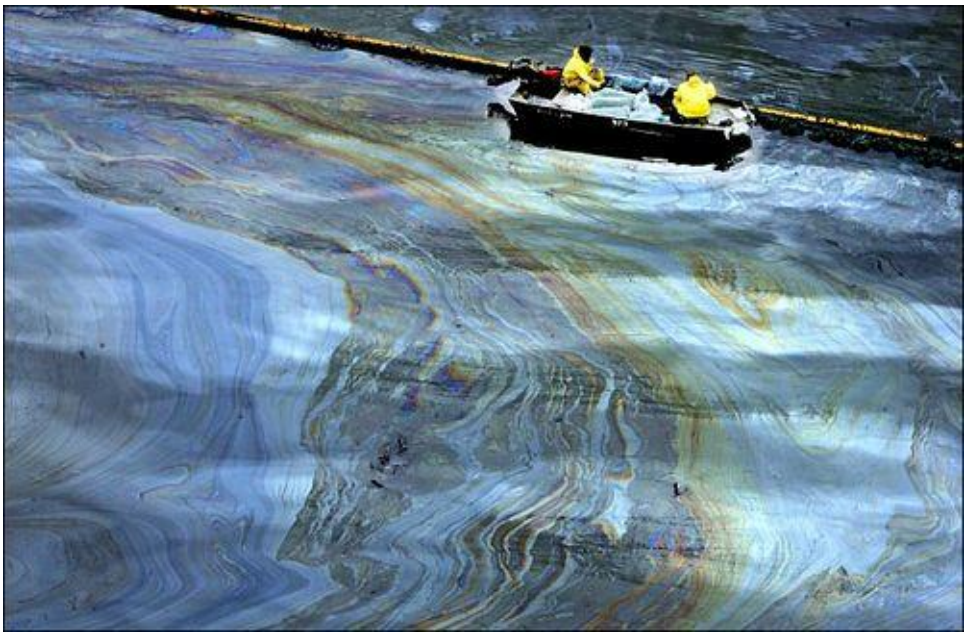

Figure 2.5 Dispersed oil layer floating on the water after an oil spill in 2004. [35]

Dispersed oil in the crude usually consists of long chain (sometimes branched) alkanes and therefore higher in molecular weight. This characteristic causes it to be non-polar. Dispersed oil can be categorised by its droplet size. According to Ma and co-workers [36], a microscope integrated ultraviolet epi-fluorescence illumination technique is an easy and inexpensive way to measure droplet sizes for dispersed oil with a detection limit of 1μm. The dispersed droplet size in oil spills is around 50μm and up to a few thousand microns after an hour of settlement.

Dispersed oil which also known as oil-mineral-aggregates (OMA) can be distinguished from its behaviour as it normally floats on the surface of water as a layer or dispersed layer [37]. Sometimes it can appear and can be characterised as several types of OMA structure such as solid, droplet, flake and oily strands [36]. When agitated, the layer usually breaks up in the water but slowly gathers together again when met. Dispersed oil is hydrophobic in nature and dissolves very well in non-polar solutions.

2.1.2.2. Dissolved Oil

This type of organic matter is water soluble and can be present as dissolved form in water. The concentration and nature of soluble oil present in produced water will vary depending on several different factors such as type of oil, volume of water production, artificial lift technique and age of production [12]. Chemical characteristics of the soluble oil compounds are generally aliphatic hydrocarbons, phenols, carboxylic acids and low molecular weight aromatic compounds. Dissolved benzene, ethyl-benzene, toluene and xylene (BTEX) are among the most abundant polar hydrocarbon and are extractable by oil and grease extractable solvent. The concentration ranges from 68ug/L to 600,000ug/L for different produced waters [38]. Among other dissolved oils are NPD (naphthalene, phenanthrene, dibenzothiophene) and PAHs (poly-aromatic hydrocarbons). In these examples of dissolved oil molecules, the hydrogen and oxygen atoms present in their structure tend to be solvated by water [39]. Figure 2.6 shows the common dissolved oils and their structures. They are hydrophilic in nature and can easily seep into the ground, consequently causing soil and ground water pollution if dumping were not done

properly. They do not normally form any droplets in the water and thus are not categorised in droplet sizes. However, from their molecular structures, the molecular weight can be calculated. Soluble oils are not easily removed by current treatment methods and therefore they are generally being reinjected into the deep sea and are not being monitored [4].

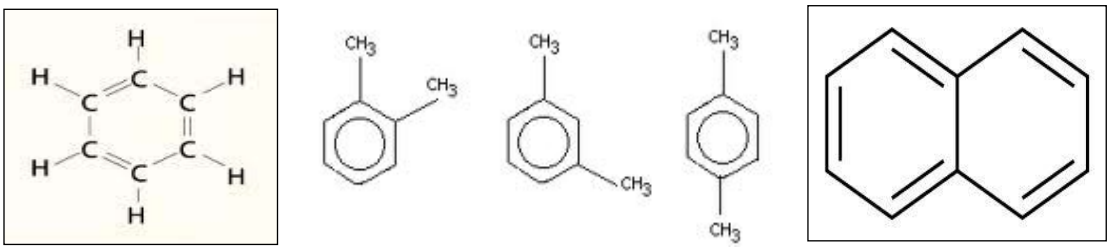

Benzene o-xylene m-xylene p-xylene naphthalene

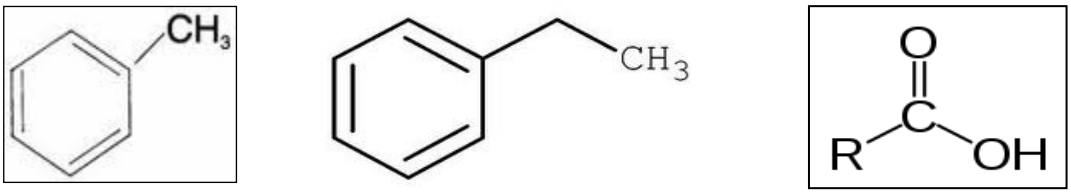

Toluene ethylenebenzene carboxylic acid

Figure 2.6 Common composition of dissolved oils and their structures

Other organic components that are very soluble in produced water consist of low molecular weight i.e. C2-C5 such as carboxylic acids (fatty acids), ketones, and alcohols. These include acetic and propionic acid, acetone, and methanol. In some produced waters, the concentrations of these components are greater than 5,000 ppm [4]. However, these smaller organic compounds are not of interest in this study as they are normally not extractable by oil and grease extraction solvent and thus do not contribute significantly to the measurement [33].

2.2. Analytical Techniques for Oil Content Determination

2.2.1. Previous and Current Analysis Method

As far as oil concentration in produced water is concerned, the value assigned to it is method dependent [2]. Without specifying the method used in the determination of the oil concentration, the value given can be misleading. The following three techniques are the most popular oil-in-water analysis reference methods [2]: Infrared (IR), gravimetric, and gas chromatographic (GC) based methods. Yet, infrared spectroscopy suffered from having difficulty of choices and availability of suitable solvents, in particular, Freon. Moreover, the IR based methods only provide non-specific composition results while gravimetric based methods only become useful for very oily sludge or wastewater. All these leads to GC based methods being more popular in recent years due to the fact that GC based methods could provide information about the types of petroleum hydrocarbons which appeared in samples other than the total amount.

Currently gas chromatographic flame ionisation detector (GC-FID) method is being used world-wide, especially by the countries in North-Sea based on OSPAR method [40]. Using GC-FID as a new analytical method generally required more skill to operate than the IR based method [41]. However, GC-FID does not require the use of solvent that might have potential hazard to the environment and human health.

2.2.2. Gas Chromatographic Mass Spectrophotometer (GC-MS) Analysis

Gas chromatography (GC) is the physical separation phase where it separates the components in the mixture selectively. Different components are distributed between mobile phase (carrier gas) and stationary phase (the column packing or the column wall) [42]. The columns of the GC play an important role in the separations. Therefore the choice of specific type of column for oil separation in this study is very crucial.

The principle of Mass Spectrometry (MS) is the production of gas-phase ions from the samples that are subsequently being separated according to their mass-to-charge (m/z) ratio and being detected. The resulting mass spectrum is a plot of the (relative) abundance of the generated ions as a function of the m/z ratio. Extreme selectivity can be obtained from this analysis method, which is very important in quantitative trace analysis.

Gas chromatography-mass spectrometry (GC-MS) is a combination of two powerful analytical tools: gas chromatography for the highly efficient gas-phase separation of components in complex mixtures, and mass spectrometry for the confirmation of identity of these components as well as for the identification of unknowns.

GCMS analysis is performed by the injection of solvent with the solute of interest. Water or polar molecules should not be present inside GC. Therefore before any water or waste water analysis using GC, solvent extraction must be performed. These extraction procedures for the experiments are customised from the OSPAR GC–FID method [40] modified from the ISO 9377–2 method and APHA 5520B method [43]. A summary of liquid-liquid extraction method is explained in Section 3.5.1.

2.3. Membrane Filtration

Membrane filtration is a type of separation process which uses synthetic membranes as selective medium to separate two or more fluids. The application of this technology was considered important starting in the 70‘s. Since then membrane processes are used in an array of applications such as biotechnology, whey processing, cheese making, water treatment etc. and the number of such applications are still increasing.

2.3.1. Membrane Materials

Membranes are made of a large number of different materials. The synthetic membranes which are used in the industry can be divided into organic (polymeric)

and inorganic membranes. Table 2.2 shows the membrane material types with their respective properties.

Table 2.2 Types of membrane materials

	Cellulose triacetate	**Polyethersulfone**	**Hydrosart®**
Main component	Cellulose	Polymer	Patented product
Characteristics	Hydrophilic	Non hydrophilic or hydrophobic interactions	No information
pH tolerance (pH)	1-14	1-14	2-14
Binding properties	Low non-specific		Low protein binding
Supporting material	Non	Yes	
Cost	High	Low	Medium
Temperature Limit	> 50°C	< 50°C	< 50°C

Understanding of the membrane material is important in choosing a suitable membrane type for this study. Oil is an organic compound, and as a preventive measure of oil attachment onto the membrane surface, therefore polymeric type membrane is more suitable. Moreover polymeric membrane is cheaper in cost compared with cellulose type of membrane. Sections below illustrate in detail the several material types and their suitability.

2.3.1.1. Cellulose Triacetate

According to the manufacturer [44], this type of material is characterized as highly hydrophilic and with low non-specific binding. It is casted without membrane support that could trap passing micro-solute. Therefore, adsorption of the membrane is the only mechanism for separation. It is used when high recovery of filtrate solution is required. Figure 2.7 shows the structure of cellulose triacetate membrane

in microscopic view. The figure also shows the organic molecular structure of cellulose triacetate and there is a large possibility that oil which is organic will adsorbed onto the surface of the membrane, and it is not suitable for this study.

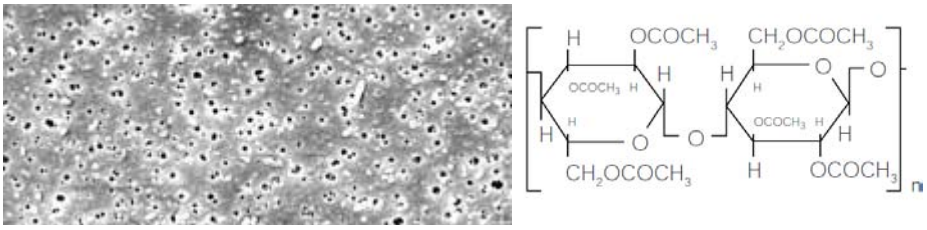

Figure 2.7 Microscopic view of cellulose triacetate membrane and its molecular structure [45]

2.3.1.2. Polyethersulfone (PESU)

This is a general purpose non-ionic inorganic membrane that provides excellent performance when retentate recovery is of primary importance. It has a pH tolerance of 1 to 14 and exhibits no hydrophobic or hydrophilic interactions [44] and is usually preferred for its low fouling characteristics, exceptional flux and broad pH range. This type of membrane is suitable for this study as it is low in fouling and has a broad pH range. Figure 2.8 shows the microscopic view of polyethersulfone membrane and its molecular structure.

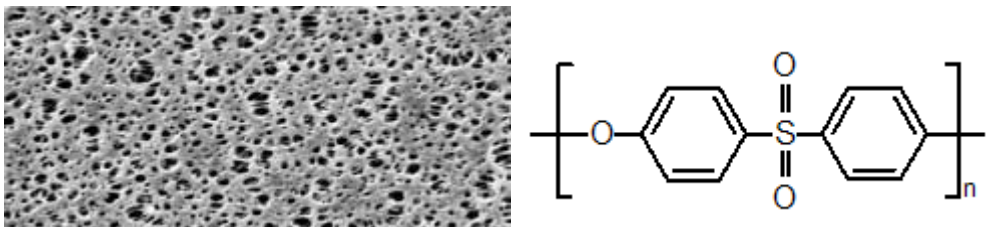

Figure 2.8 Microscopic view of polyethersulfone membrane and its molecular structure [45]

2.3.1.3. Hydrosart®

Hydrosart® is a patented product which demonstrates the same properties as cellulose-based membrane, but with the added benefit of enhanced performance characteristics and extremely low protein binding. Usually this is used for applications such as concentrating and desalting of immunoglobulin fractions.

2.3.2. Operating Mode

In membrane filtration, oils in the feed will over time foul and clog the membrane pore and membrane surface resulting in reduction of permeate flux. In dead-end filtration (Figure 2.9a), the flow is orthogonal to the surface of the filter and the particulates in the feed accumulate as a "cake" on the top of the membrane thus causing the flux to reduce to approximately zero [46]. Dead-end filtration is suitable only for dealing with suspensions with very low solids content [47].

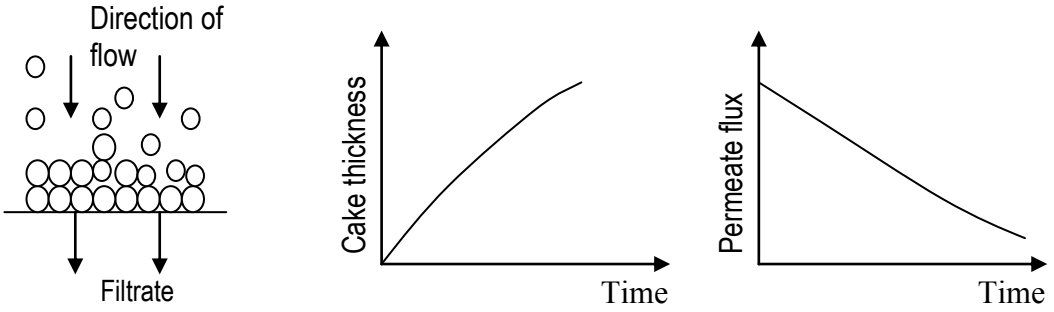

Figure 2.9 (a) Dead-end filtration [47]

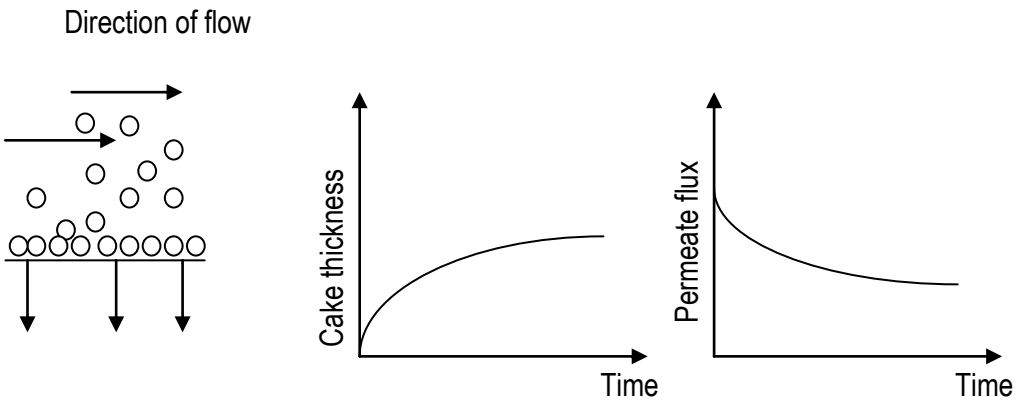

Figure 2.9 (b) Cross-flow filtration [47]

In contrast to dead-end filtration, feed flows parallel to the membrane surface in cross-flow filtration (XF) thereby creating turbulence and shear forces along the membrane surface which slows the deposit of retained molecules and thus slows down the filter –cake" formation (Figure 2.9b). It can be used for much higher concentrations, as deposits on the membrane are swept away by membrane-parallel flow.

In dead-end filtration, all of the fluid entering the filter emerges as permeates, and so the conversion is about 100%. However, for XF filter, more feed passes by the membrane as retentate than passing through it as permeate and the conversion per pass is often less than 20% [48]. However, by maintaining velocity across the membrane, material retained by the membrane is being swept off its surface, hence, little accumulation and fewer tendencies to block the membrane pores. Therefore, the output can be maintained at a level higher than is possible for the same system operating in dead-end flow [49]. Furthermore, another study by Yazhen and co-workers [50] concluded that by using cross-flow microfiltration, the cake layers formed are more permeable, compressible and finer particle size distribution than those formed by using dead-end filtration.

2.3.3. Membrane Pore Size

Listed below is the table (Table 2.3) of different pore sizes of polymeric membranes and their respective characteristics.

Table 2.3 Characteristics of different types of membranes and their applications

Properties	**Microfiltration**	**Ultrafiltration**	**Nanofiltration**	**Reversed Osmosis**
Pore size	0.1 - 10μm	0.001-0.1μm	In between of UF and RO	0.0001-0.001μm
Operating mode	Dead-end and cross-flow		Cross-flow	

Manufactur-ing process	Phase inversion process	Loeb-sourirajam phase separation process	Grafting on ultrafiltration membrane	Phase inversion process
Membrane material*	Polysulfone Polycarbonate Poly(vinylidene -fluoride) Polytetrafluoro-ethylene Polypropylene Polyamid Cellulose-esters Poly(ether-imide) Polyetherether-ketone	Polysulfone/poly (ether sulfone) Polyacrylonitrile Cellulose esters Polyimide/poly-(ester imide) Polyamide(alipha tic) Poly(vinylidene fluoride) polyetheretherket one	Polyamide, Polysulfone, Cellulose acetate	Cellulose triacetate, polyamide,
Driving force	Pressure driven			
Membrane Interface	Isotropic microporous membrane	Anisotropic microporous membrane	Asymmetrical	Asymmetrical or thin-film composite membrane
Potential separation	Suspensions, emulsions	Macromolecular solutions, emulsions	Monovalent salts, viruses, microbes	Aqueous low molecular mass solution
Application	Sterile filtration, wide application	Whey separation, water treatment, food industry etc.	Desalting and deacidification food products, microbiology	Desalting water

* extracted from [51]

2.3.4. Membrane Filtration in Removal of Dissolved Oil

In the past 30 years, membrane filtration has been studied extensively in the treatment of oily wastewater. Figure 2.10 shows the components that could be removed by membrane processes according to membrane pore size ranges. The oil components are categorised in the organic compounds. According to Choong and co-workers [52], reverse osmosis (RO) is very effective in removing dissolved oils. The effluent after this process is eliminated from most of the oils. However, it is seldom used in treatment plants due to high capital and operating costs. From literature studies, most of the researches are done by using RO and ultrafiltration for their dissolved oil separation [53-56]. Claudia and colleagues [57] reported their study for natural effluent organic matter filtration using low-pressure membrane systems namely microfiltration (MF) and ultrafiltration (UF) membranes.

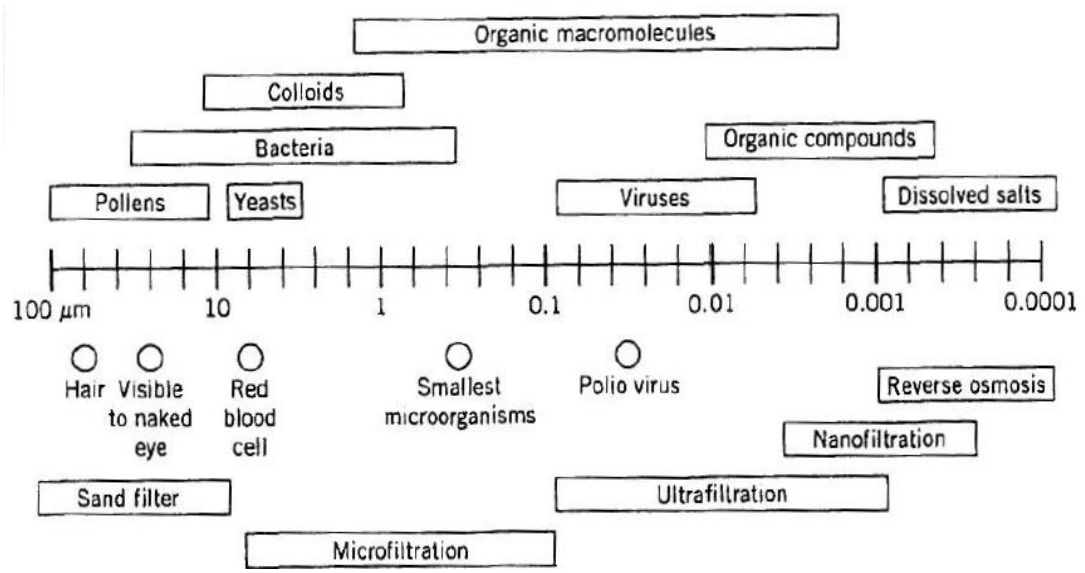

Figure 2.10 Particle size ranges removed by membrane processes [58]

Other studies have been reported using MF [59] for filtration of organic matter and these applications are limited to edible oil such as vegetable oil, which in characteristics is different from crude oil. Therefore, there is still a very wide area to study for the separation of dissolved (BTEX) and dispersed oil in produced water. For this study, to retain the dispersed oil in the feed and separate the dissolved oil, MF and UF are the most promising membranes as far as their pore sizes are

concerned as shown in Table 2.3. Dispersed oils are classified as organic macromolecular structures (Figure 2.10) and are in average 100 times bigger than dissolved organic compounds. Therefore, in the experiments, both MF and UF membranes will be investigated in the dissolved oil separation.

2.4. Fouling issue

Membrane fouling is indicated by a reduction of permeate flux with time, caused by the accumulation of feed components in the pores and on the membrane surface. Fouling will result in an increase of the Transmembrane Pressure (TMP) over time. The fouling mechanism can be expressed by the filtration resistance, R (Figure 2.11). The resistance to filtration can be described by Darcy's Law (2-1):

$$\Delta p = \frac{\mu}{A} R \frac{dv}{dt} \tag{2-1}$$

Where Δp is the TMP, μ is the viscosity, A is the permeability area, v is the velocity of fluid flow, t is the time and R is the resistance in series, which is

$$R = R_m + R_c + R_{pb} + R_a \tag{2-2}$$

R_m is the membrane resistance. The retained components can form a cake layer (R_c) on top of the membrane surface, and block the membrane pores (R_{pb}) or adsorb (R_a) at the membrane surface or in the membrane pores, depending on their chemical and physical properties

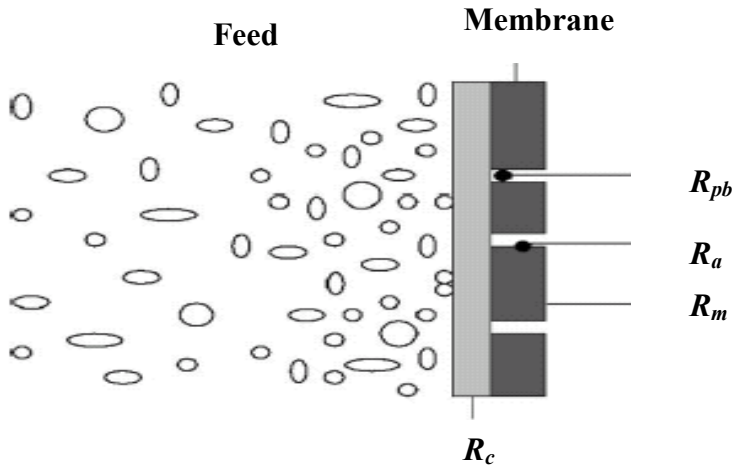

Figure 2.11 Schematic drawing of filtration resistances [60]

2.4.1. Fouling and Modeling

There are many models formulated to represent the phenomena behind flux decline in membrane filtration. For microfiltration, normally flux decline is attributed to cake formation by the retained particles on the membrane and this classical theory is called the standard cake filtration theory [61]. On the other hand, ultrafiltration theories attribute the flux decline to concentration polarization, thus mass transfer mechanism is involved. The pore sizes of reversed osmosis and nanofiltration are at similar ranges and they show similar characteristics in terms of permeation. In general, there are three types of foulant: organic precipitates (macromolecules, oil, biological substances, etc), inorganic precipitates (metal hydroxides, calcium salts, etc) and particulates.

2.4.2. Cake Filtration Theory

In the cake filtration model, the solutes form a ~~"c~~ake" or a layer of deposition of particles at the membrane wall of constant concentration. Total cake layer resistance (R_c) is the product of specific cake resistance (r_c) multiplied by the cake thickness (l_c).

$$R_c = l_c r_c \tag{2-3}$$

with

$$r_c = 180 \frac{(1-\varepsilon)^2}{[(d_s)^2 \varepsilon^3]} \tag{2-4}$$

$$l_c = \frac{m}{[\rho_s (1-\varepsilon) A]} \tag{2-5}$$

Where d is the diameter of the solute particle, ε is the porosity of the cake layer, m is the mass of the cake, ρ is the density of the solute and A is the membrane area. However this model is not practical to be used as the mass of the cake, diameter of the solutes are difficult to estimate. Therefore, assuming that complete solute

rejection, there will be zero solutes in the permeate; in this case, we can obtain the cake layer resistance, R_c, from the mass balance:

$$R_c = \frac{r_c C_b V}{C_c A} \tag{2-6}$$

Where V is the volume of the cake layer, C_b is the bulk concentration and C_c is the cake concentration.

This cake filtration model is usually used for dead-end filtration operation [49].

2.4.3. Concentration Polarization Theory or Film Model Theory

A key factor for determining the performance of membranes is concentration polarization, which causes membrane fouling due to deposition of retained colloidal and macromolecular material on the ultrafiltration or microfiltration membrane surface. Recently, gel layer polarization and concentration polarization is often used in literature interchangeably when referring to fouling of UF and MF [62], [59]. The Film theory model is shown in Equation 2-7:

$$J = k \ln(\frac{C_g}{C_b}) \tag{2-7}$$

where J is the permeate flux; k is the mass transfer coefficient; C_g is the gel concentration; C_b is the bulk concentration. From a hydraulic perspective, membrane fouling is the loss of membrane flux, which is the volume of water that can be passed through a membrane surface unit per unit of pressure. However from a dynamic point of view, membrane fouling is a dynamic process of particle deposition from non-equilibrium to equilibrium [46, 63].

There are two types of fouling: biofouling and abiotic fouling. Biofouling is the accumulation of microorganisms on the membrane surface while abiotic fouling is the formation of a _cake layer‘ consisting of rejected material on the surface. This

cake layer is formed by consolidation of the layer caused by concentration polarization on the membrane surface [64].

2.4.4. Interporous Plugging

Besides the formation of a blocking layer on top of membrane caused by concentration polarization, fouling can be due to blockage or partial blockage of membrane pores [65]. In concentration polarization or the cake layer, pressure can be recovered after backwash and it is described as reversible fouling [66]; whereas interporous plugging is normally an irreversible fouling. However, it is important to note that since concentration of material on membrane surface is very high due to concentration polarization, aggregation or precipitation, the probability for irreversible fouling increases [67].

2.5. Enhancement Technique for the Dissolved Oil Removal Process by Membrane Filtration

In this research, the fouling issue is assumed to be partially reversible as have explained in Chapter 1. According to the literature, optimum transmembrane pressure (TMP) is the combination of pressures in feed, retentate, and permeate channels that will give a critical permeate flux below which minimal foulant deposition occurs [65, 68]. TMP is the driving force for solution to pass through membrane. A gel layer will be formed when the solute present in feed has been dragged towards the membrane followed by the building up of retained solute on the membrane. These solutes in the layer may diffuse back into the cross-flow stream by inertial lift [63].

The growth of gel layer ceases at optimum TMP where the rate of solute deposition equals to the rate of solute diffusion back into the feed stream [46]. Beyond the optimum TMP values, the permeate flux will have already sustained an approximate constant level (i.e. steady state) due to the saturated retention of fouling particles or solute molecules on the membrane surface. The optimum TMP is a function of the feed concentration, the membrane size, and the cross-flow velocity of feed solution

[65]. According to the literature, cross-flow velocity is proportional to retentate flow rate and, in practice, equivalent to the differential pressure (DP, i.e. pressure drop) [46]. Therefore in this work, TMP and DP are studied for the enhancement of separation by preventing fouling.

2.5.1. Computational Fluid Dynamic (CFD)

Computational Fluid Dynamic (CFD) is a research tool which helps in the interpretation and understanding of the results of theory and experiment [69]. Rahimi and colleagues modelled the permeate flux in cross-flow microfiltration using 3D CFD code [70]. The application of CFD in this thesis serves to simulate the flow of fluid inside the membrane cartridge for different operating condition such as DPs and TMPs and to visualise their effects on the fluid during the cross-flow membrane filtration process. The CFD is based on the fundamental governing equations of fluid dynamics – the continuity, momentum and energy equations which are solved by commercial software Fluent 6.1 with finite control volume method.

2.5.2. Physical and Mechanical Treatment Process

The effects of operational conditions such as filtration time, ceasing time and aeration intensity on the membrane permeability and organic removals were investigated by Li Mo and co-workers [71]. The operational conditions such as flux and pressure have certain effect on fouling. Membrane filtration can be done either by constant pressure or constant flux. Field and co-workers [72] has discovered that constant flux filtration was realized at a constant TMP which was below a critical value. Constant flux filtration was maintained by moderately increasing TMP, and this approach is shown to have some advantages over normal constant-pressure filtration because it provides the possibility of avoiding over-fouling and thus reduced the severity of fouling.

Howell [72] also hypothesized of a critical flux below which there is no fouling by colloidal particle. Contrary to the findings of Howell, Pollice and colleagues [73] reviewed that sub-critical flux fouling was observed in certain experiments under

certain operating conditions. Therefore, there is still a gap for research in correlating operating conditions with critical flux. In Chapter 6, computational simulation is used to model the flow inside the membrane cartridge and the effect of DP towards the flow pattern is studied. Vigorous flow could decrease fouling due to shearing effect [74]. By understanding the flow pattern in the cartridge corresponding to the DP, it will help us in understanding the insight of critical flux as critical flux is related to the fouling of membrane.

Besides the physical method for enhancing the separation mentioned, the possibility of chemical treatment to enhance the separation is explored and this would be discussed in great detail in the following section.

2.5.3. Chemical Treatment Process

In reality, fouling is unavoidable and the most suitable solution in accurate measurement is to clean out the deposited dissolved oil from the membrane walls either physically or chemically. Oil was extracted from the cleaning process and quantification of oil was done by using GC-MS method.

Membranes perform exactly what they are able to do under given circumstances. Therefore pre-treatment is an extremely important process prior to membrane filtration. For our case, oil is the main concern in the separation and pre-treatment can improve the solubility of dissolved oil and thus helping it to be separated into the permeate with the solvent. To increase the solubility, adjusting the pH is one of the pre-treatment methods [75]. On the other hand, change in pH can also affect the electrostatic interactions/ repulsions between the membrane wall and solutes, and thus prevent fouling [76].

As mentioned earlier, cleaning is an important stage of membrane filtration as fouling is inevitable. Chemical cleaning can be done to eliminate the stubborn foulant deposited on the membrane which otherwise could not be removed by mechanical cleaning [77], [78]. Studies suggest that an alkaline solution such as NaOH does not only increase the pH of solution, but it can hydrolyse and emulsify

the organic molecules [79], [80]. Through emulsifying the foulant particles on the membrane, the foulant is dispersed into the solution. Besides identifying chemical cleaning agents, optimizing the chemical cleaning regime is equally vital because excessive cleaning will not only have an adverse effect on membrane life, it would also increase the cost of chemicals used and the volume of water required [75]. In this research, the work is separated into two stages, with chemicals pre-treatment being the first stage and chemical cleaning in the second stage to recover the remaining dispersed and dissolved oil. Optimized values of the variables such as trans-membrane pressure (TMP), pH, time of circulation and chemical volume are being determined by simultaneous approach for maximum dissolved and dispersed oil in permeate and retentate respectively.

2.5.3.1. Streaming Current Potential and Zeta Potential

Membrane will develop electric surface charge when in contact with aqueous solution. These electric surface charges cause distribution of ions in the solution due to electric-neutrality of the system forming ―electrical double layer". These double layers of electrical charges consist of the charged surface and the counter ions in the adjacent solutions [81]. The transport of these counter ions along with the pressure-driven fluid flow gives rise to a net charge transport, which is called the streaming current. This information is vital for reducing fouling because the interaction of membrane surface material with the molecules in the solution is the final cause to fouling. Nystrom and colleagues [67] developed a new method to study the flux reduction by correlating it with membrane charges measured using streaming/ zeta-potentials. This streaming potential was later compared with other operating condition such as the pH to see their relationship with flux and foulant properties When charges in the solution can be made the same type of charges as the membrane surface charges or vice versa, the membrane will be less susceptible to be fouled [82, 83]. Zeta potential and streaming potential are related by the Helmholtz-Smoluchowski equation:

$$\zeta = \frac{\eta K}{D\varepsilon_{\mathrm{O}}} \frac{\Delta E}{\Delta P} \tag{2-8}$$

where ζ is the apparent zeta potential, D the electric constant of the medium, ε_o the

permeability of vacuum, η and K the viscosity and conductivity of the bulk solution respectively, and $\Delta E/\Delta P$ is the streaming potential developed as a result of an applied pressure gradient.

2.6. Optimization

The optimistic future for membrane technology relies on its technical and cost issues being addressed properly. Of these issues, the fouling of membranes by rejecting chemical particles and microbes continue to demand considerable attention from research community. The measures for avoidance of fouling are dependent on the specific membrane process due to the complexities of fouling phenomena. As a summary, three major approaches can be identified: hydrodynamic (changing flow regime across the membrane surface), surface modification (changing the surface/foulants affinity) and regular cleaning [65].

There are many researchers investigating fervently on the fabrication of membranes which possess the properties that can resist fouling [84-86], hydrolysis, biological attack, and degradation in the presence of oxidants by altering the membrane surface composition. Recent developments have focused on surface modifications of existing materials to improve selectivity while maintaining high productivity [87]. All these techniques mentioned require extensive time and money but the output is not guaranteed. In this research, however, emphasis is given to the overall process optimization of membrane operation, in terms of operating conditions, cleaning process and optimized pre-treatment conditions. One of the optimization techniques is by statistical approach using design of experiment (DOE). One of the DOE techniques for optimization is by Respond Surface Methodology (RSM) and it will be discussed further in the following sections.

2.6.1. Statistical Method and Design of Experiment (DOE)

Experiments are a component of the scientific learning process. Learning through experiments is a complex entity which involves knowledge, experimentation based on the knowledge, production of data, analysis of collected data which will consequently lead to new knowledge, new experiments, new data, and new

knowledge based on the data [88]. However, the entire process can be subject to experimental ‗noise' and errors. Thus, statistical methods are utilized during data analysis that can combine the roles of hypotheses, data, inferences, and uncertainty. The development of computational technology has also made statistical DOE method an attractive option. The statistical software today are capable of performing statistical experiment design, regression analysis, industrial quality control, multivariate analyses, and provide graphical displays of data. According to Tanco and co-workers [89], design of experiments (DOE) is simply a method of applying statistics onto experiments. There are two groups of DOE i.e.[89]:

- Classical technique
  - Developed in the U.K. and the U.S. in the 1920's with the introduction of factorial designs and fractional designs. The development of optimizing techniques was achieved when G.E.P. Box and W.E. Deming developed the RSM technique. The further development of this technique continues even today.

- Taguchi method
  - Developed by Genechi Taguchi in Japan during the 1950's. This method introduces statistical method for quality from an engineering perspective.

The benefit of statistics in DOE is twofold; first it aids in experimental design that produces data or sometimes a wide smattering of data that is compact with information. Secondly, it plays an important role in aiding the analysis of the data where the valuable information is sifted out [88].

2.6.2. Experimental Variables, Variable Interactions, and Replicates

A key component of DOE is the identification of variables. These variables are the factors that influence the experiment response. Each experiment is an enquiry to a process or system. Thus, the responses of the system must be recorded in quantifiable terms of response variables [90]. The most significant variables are the variables

whose effects on the response variables need to be measured. These variables are known as the experimental factors and are the reason that the experimentation was conducted [91]. The variables can be quantitative or qualitative. Some variables are held constant throughout the experiment and thus are aptly known as constant variables. Holding a variable constant limits the scope and complexity of the experiment and the resulting inferences [91].

However, the results of experiments that are quantified by the response variables are subject to disturbances. These disturbances are hard to control or sometimes uncontrollable and sometimes may not even be known at all [90]. Thus, the experimenter needs to take into account the effects of the disturbance variables to nullify their impacts on the experiment data. Therefore replication needs to be done. The measured responses during experimental replication are known as replicates. Replicates make results more reliable by considering all possible disturbances that leads to the variation of the response variables.

Another factor that needs to be addressed is where there is a joint effect between experimental factors on the response variables. This situation is known as variable interaction and is described as whereby changing one factor causes a change in the response variable that is subject to the setting of the second factor [90]. In other words, interaction between two experimental factors measures how much the change of one of the experimental factor that causes change of the response variable depends on the level of the second factor. One fact that is important is that the interaction between factors is not to be associated with the correlation between factors. According to Soravia and Orth [90] correlation between two factors is when a change in one factor accounts for an increase or decrease in the other factor.

It is mentioned by Hunter [88] that another simple technique for data analysis of 2^k factorial designs is the half-normal plot. This technique consists of plotting the experiment factors on a normal probability paper. From this plot, effects that are indistinguishable from noise will fall along a straight line while effects that are statistically significant will be the outliers of the plot. Thus, half-normal plots are a useful statistical analysis tool.

2.6.3. 2^k Factorial Design

Factorial designs are popular for applications that involve two or more experimental factors. Factorial designs allow for the estimation of the individual effects and the interaction effects for a k number of factors in an experimental procedure where the total amount of factors (k denotes the amount of factors) are varied simultaneously in an organized experiment to obtain maximum precision [88]. The number 2 denotes the fact that there are two levels of each of the k factors. The term two levels indicates that there are two levels of settings, a lower and an upper level for each of the experimental factors [90]. An advantage of factorial designs is that they provide a good setting for data analysis that can show the effects of the factor variations and how these effects depend on other factors [90]. A factorial design also allows not only continuous variables (such as temperature, pressure, concentration) but also categorical variables such as equipment type and solvent type.

Fractional (Factorial) design of the 2^k variation has enormous industrial applicability. The fractional design has less number of runs compared with a full factorial design. However this advantage will be compensated by the confounding effect. By decreasing the number of runs, there will be a higher chance of getting aliased or masked effect. Therefore, to avoid this, a full normal factorial design is preferred. For normal full factorial design, the total run of experiments is determined from the total combinations of the lower and upper levels of the factors.

2.6.4. Response Surface Method (RSM)

Response surface methodology (RSM) is developed by Box and Wilson [92]. The key ideas that were proposed by Box and Wilson were developed by using linear polynomial models (mainly first- and second-degree models), with an assumption of continuous response variables, and to be independently and normally distributed with constant error variances [93]. The main objective is to optimize the response according to the type of response surface formed from the result of factorial design tests [94].

RSM applies to relate the dependent variables to the response variables. The first step to achieve this is by fitting the data into a model, using low order model such as a first- or second-order model. The function is first-order model if the response is well modelled by a linear function of the independent variables [95].

$$y = \beta_o + \sum_{j=1}^{k} \beta_j x_j + \varepsilon \tag{2-9}$$

If there is curvature in the system, then a polynomial of higher degree such as the second order model must be used.

$$y = \beta_o + \sum_{j=1}^{k} \beta_j x_j + \sum_{j=1}^{k} \beta_{jj} x^2{}_j + \sum_{i} \sum_{<j=2}^{k} \beta_{ij} x_i x_j + \varepsilon \tag{2-10}$$

Where y is the predicted response; β_0 a constant; β_j the linear coefficient; β_{jj} the squared coefficient; and β_{ij} the cross-product coefficient, k is the number of factors and to be normally distributed with a constant variance, y is the response and x is the experimental factors. In factorial designs they are coded as +1 and -1. This is known as coding variables and is essentially a simple linear transformation of the factor range onto the interval [-1, +1] [90]. The transformation is called centering and scaling and the equation to illustrate this is:

$$x_{centered\&scaled} = \frac{2\left(x - x_{center}\right)}{\left(x_{\max} - x_{\min}\right)} \tag{2-11}$$

Centering and scaling allows for comparison of factors with different scales to be compared. The experimental results are used to estimate the value of β using least-squares regression analysis. RSM is a sequential procedure. The ultimate objective of RSM is to obtain the local optimum by the hill climbing process known as Path of Steepest Ascent (POA). The choice of model lies with the statistician but a general rule of thumb is that the first-order model is chosen for its simplicity. The second-order model is only used when the first-order model is inadequate. The model is then tested for its sufficiency by checking its R^2 and adjusted R^2 value to test out the quality of fit, its F-value, Lack-of-Fit (LOF) tests to assess the model adequacy, and ANOVA to check for statistical significance of the model [90]. If the model is

insufficient, in some cases, a transformation of the x's over a logarithmic scale or a reciprocal scale might be necessary [91].

If the model is deemed adequate, then we move to the second step, which is the POA. The POA for a first order model follows the vector equation below.

$$\overline{\beta} = (\beta_1, \beta_2, ..., \beta_k) \times 1 / \left(\overline{\beta}' \overline{\beta}\right)^{1/2} \tag{2-12}$$

The POA is conducted to analyze the data for presence of curvature and perform normal or half-normal plots analysis from which we can determine and the significant experimental factors. After POA, if there is a presence of curvature, we move on to the third step, augmenting the design to fit a second order model (Equation 2-10). Among the augmentative methods available are Central Composite Designs (CCD), Box-Behnken Designs and Optimal Designs. Augmented designs call for more experimental runs and even in some cases more replicates. The data from the new experimental runs are combined with the previously obtained data and is fitted accordingly to a second order model. However, the appropriateness of higher order models such as cubic and quadratic models to the data is also a possibility. Once the model is fit, we can determine the optimum point from the resulting response surface. The final step is to confirm the optimum that is obtained from the response surface contours via an experimental run.

Conventional RSM includes Central Composite Design (CCD), and Box-Behnken Design. A rather not so classical one is D-optimal design. In the following section, each design is studied extensively and the best design suitable for this research will be proposed.

2.6.4.1. Central Composite Design

Central Composite Design (CCD) is used to calibrate full quadratic models by using only 2 levels. It is developed by Box and Wilson. There are three types of CCDs—circumscribed, inscribed, and faced. Each design consists of a factorial design (the corners of a cube) together with centre and star points that allow for estimation of second-order effects. For a full quadratic model with n factors, CCDs have enough

design points to estimate the (n+2)(n+1)/2 coefficients in a full quadratic model with n factors.

The type of CCD used (the position of the factorial and star points) is determined by the number of factors and the desired properties of the design. This design gives good accuracy of estimates over the entire design space. However, the drawback of this design is that it requires a substantial number of runs e.g. it requires 30 runs for a 4-factor with 2-response design.

2.6.4.2. Box-Behnken Design

Similar to CCD, Box-Behnken designs are used to calibrate full quadratic models. Box-Behnken designs are rotatable and, for a small number of factors (four or less), require fewer runs than CCDs. By avoiding the corners of the design space, they allow experimenters to work around extreme factor combinations. Similar to an inscribed CCD, however, extremes are then poorly estimated. Nevertheless the constraint of this design is it requires a minimum of 3 numerical factors.

2.6.4.3. D-Optimal Design

Optimal designs are used in certain quarters for response surface exploration [91]. Optimal designs were introduced during the 1900‘s as an alternative to the more traditional designs such as the factorial, fractional factorial, Box, and Box-Behnken [96]. Specifically, optimal designs are used when there is an irregular experimental region, when a non-standard model is used, when accounting for non-linearity, or when there is a restriction on the number of samples that can be tested. To elaborate, optimal designs are used for situations when one needs to fit a non-standard model which is a model that assumes something other than a first- or second- order polynomial model [91]. Several optimality criteria have been developed over the years including D-, A-, E-, G-, T-, and V-optimal [96].

D-Optimal designs minimize the volume of the joint confidence interval for the model parameters. According to Mannarswami and colleagues [96], a D-optimal design does not change under non-singular linear transformation and provides

accurate estimates of model parameters. To illustrate the D-optimal design method, consider the matrix X in Equation 2-13:

$$\boldsymbol{X}=\begin{bmatrix} a_{11} & b_{12} \\ a_{21} & b_{22} \end{bmatrix} \tag{2-13}$$

The first and second columns represent the experimental factors. To select the best combination of the factors we use the D-optimal criterion. According to de Aguiar and co-workers [97] the D-criterion was proposed by K. Smith and states that the model matrix *X* that minimizes the determinant of the dispersion matrix $(X'X)^{-1}$, is optimal. Minimizing the determinant of the dispersion matrix is also equal to maximizing the determinant of the information matrix (X'X) [97]. The determinant of the information matrix is exemplified in Equation 2-14.

$$\det (\boldsymbol{X'X})^{-1} = \frac{1}{(\det(X'X))^{-1}} \tag{2-14}$$

2.6.5. Analysis of Variance (ANOVA)

ANOVA is a statistical tool to analyse and compare variability in two or more sets of data [90]. Within DOE, ANOVA can be used as a counterpart to regression analysis and to compare the _desired' variability caused by the experimental factors with the _undesired' variability caused by experimental errors. To illustrate further, ANOVA breaks down the total observed variability in the response variable into two parts; one that is caused by the main effects of each of the experimental variables and the other their interactions [91]. The aim of ANOVA is to judge the model and to check if the model sufficiently explains the data and is statistically significant. ANOVA requires the residual sum of square (SSres) and error sum of square (SSE) to be calculated and be made comparable by considering the degrees of freedom [90]. ANOVA then compares the model to the residuals to decide if the model is statistically significant.

2.7. Conclusions

On review of the literatures, conclusions can be made that:

- Dissolved oil remains in the treated produced water despite treatment from current best available technology.
- This dissolved oil content which is not regulated is often calculated into the monitored dispersed oil content due to the inadequacy of current analytical monitoring system. An integration of membrane filtration system into the standard analytical method is recommended to remove the dissolved oil and improve the accuracy of the monitoring.
- Physical aspect of membrane filtration such as membrane materials, operating mode, operating pressures, and membrane pore size, will greatly affect the efficiency of dissolved oil removal.
- Model visualization on the fluid flow inside the membrane will also give us the insight of the correlation with operating pressure.
- A combined physical and chemical treatment process such as pre-treatment of feed, and chemical cleaning at certain mode are also able to wash out the deposited oils thus improving the accuracy of oils measurement.
- This study involves heavy experimental work as for each experimental runs it requires 3 extractions and 3 GCMS analysis. Therefore among other experimental design method for process optimization, RSM D-optimal design best suit this study as it requires the least number of runs, and the dependent variables can be performed within the range of the operating instrument.

Chapter 3: Research Methodology

3.1. Research methodology

This work is pursued to investigate the possibility of incorporating membrane filtration into the analytical method and to find the optimum operating conditions for it. The idea is illustrated in Figure 3.1. The spectrum for 100ppm oil in feed are the total dispersed and dissolved oil. The permeate spectrum shows only dissolved oil and retentate spectrum shows the dispersed oil and the rest of dissolved oil.

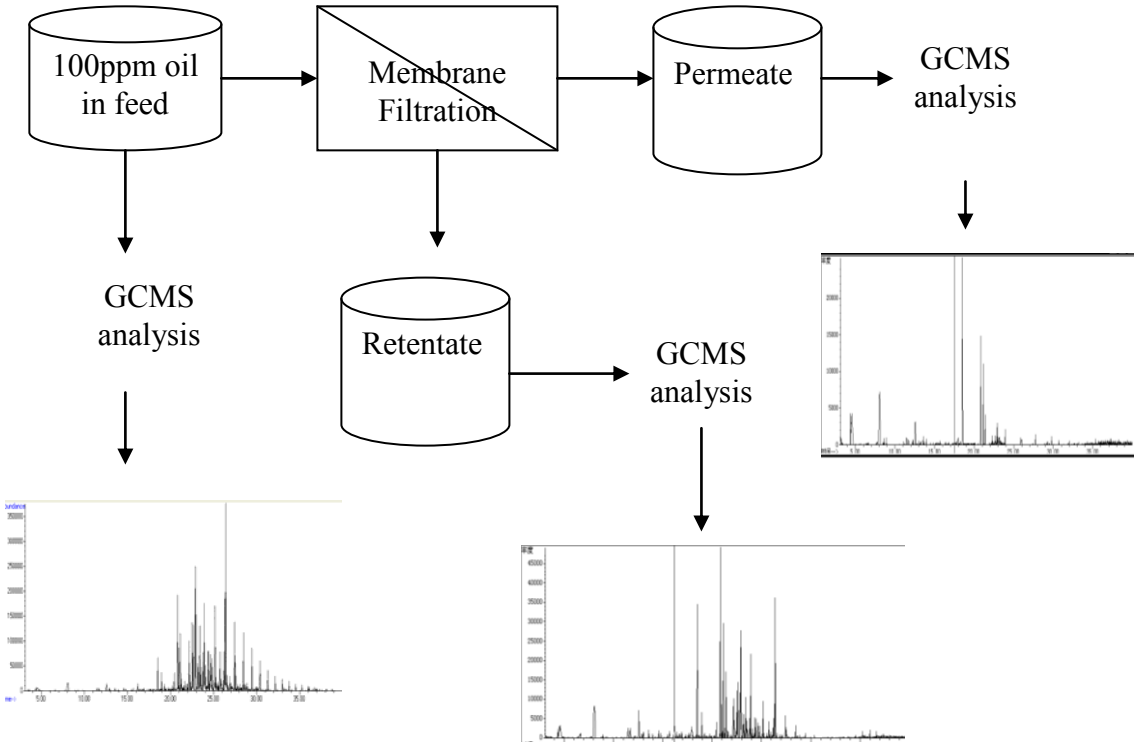

Figure 3.1 Methodology for incorporation of membrane filtration in current GC analysis technique.

An overall research approach used in this thesis to achieve the objective is illustrated below:

1) Firstly the feasibility of membrane in this study was investigated and membrane pore size was screened with respect to dissolved oil content in permeate.
2) After the suitable membranes were found to be able to separate the dispersed oil with dissolved oil, the modelling explaining the fouling phenomena was studied relating the cross-flow pressure (DP) with MTC.
3) By using the model developed together with Darcy‘s equation and Navier-stokes equation, DP and TMP were correlated with the flow pattern inside the membrane by CFD simulation.
4) After simulation, the range of DPs which could help in the shearing effect was used in finding the optimized value for maximum dissolved and dispersed oil in permeate and retentate respectively.
5) Lastly, chemical cleanings and pH adjustment were studied to enhance the dissolved and dispersed oil removal from membrane surface.

3.2. Membrane Material and Operational Mode

Synthetic polymeric membranes such as polyethersulfone and Hydrosart® membranes are chosen for studies as it is the most available membrane from the manufacturer with the required pore sizes and their properties are desired for prevention of oil adsorption (Section 2.3.1). These membranes are manufactured by Sartorius Stedim Biotech and therefore the membrane materials are limited to those that are listed in Table 2.2. In Section 2.3.2, the operational mode is being evaluated and cross-flow operating mode is proposed for this research as it can reduce the effect of declination of the flux as compared to dead-end filtration.

3.3. Membrane Filtration Set-up

3.3.1. Before Filtration

A picture of the flat-sheet membrane filtration unit used in this research is shown in Figure 3.2. Once the membrane is securely fixed in the holding device, distilled water is fed into the membrane system to calculate the clean water flux (CWF) before starting the first experiment. The CWF is measured by first placing a 2000 ml beaker filled with distilled water as the feed inlet to the membrane system. The pump of the membrane system is switched on and the water is collected at the permeate outlet. Permeate is collected in a 1000 ml cylinder and the time to fill the cylinder is taken at intervals of every 100 ml. This step is repeated for the operating condition specified in Table 3.1 with P_F, as feed pressure; P_R, as retentate pressure and P_P, as permeate pressure.

Table 3.1 Operating condition for CWF

DP (bar)	TMP (bar)	P_F (bar)	P_R (bar)	P_P (bar)
0.5	0.85	1.1	0.6	0.0
0.8	2.00	3.8	3.0	1.5

Figure 3.2 A diagram of the membrane filtration unit

3.3.2. After Filtration

For every filtration done, the membrane was cleaned by circulating 1N of NaOH solution for 20 mins. After that, the CWF was measured again, and compared with the CWF before experiment. The cleaning process is considered successful if the CWF before and after is within ±5%. This is to ensure that the next experiment conducted has very low initial error.

Membrane fouling can cause the reduction of the CWF. This means that once the experiment begins, the CWF will be reduced gradually marking a decline in membrane performance. This is the reason CWF is measured after every experimental runs to determine the membrane condition and filtration performance. By maintaining the CWF of the membrane through caustic cleaning [80], the membrane filtration can be performed at a standard condition to maintain consistency in the experiment.

3.4. Preparation of Dispersed and Dissolved Oil in Produced Water Sample

Correct sample preparation and preservation are very crucial for accurate testing. Sampling devices and containers must be thoroughly cleaned to prevent contamination from previous samples. The main components for this research are the oils-in-produced water before the disposal. Currently, the maximum daily disposal limits for total oil-in-water are 70ppm and 100ppm regulated by Shell Global Standard and Malaysian local authority respectively [98, 99]. Therefore the simulated produced water with a concentration of 100ppm of crude oil can be taken to represent the actual maximum disposal limit of produced water samples in terms of oil-in-water content. The 100ppm of crude oil is also a reference standard acting as a control in this experiment.

Standard 100ppm of pseudo-produced water was mixed by adding 0.5g of crude oil with 5000ml of distilled water. The mixture was agitated vigorously using electrical mixer for 30 minutes to form dispersed and dissolved oil mixture. This mixture will

be the feedstock for the experiments in Chapter 7 and 8. Figure 3.3 shows the simulated produced water sample and the permeate after filtration.

Figure 3.3 The left flask shows the produced water sample and the right flask shows the permeate from membrane filtration

3.5. Analytical Method by Gas Chromatographic Mass Spectrophotometer (GC-MS)

The efficiency of separation between dissolved and dispersed oil contents in produced water using MF and UF membrane will be investigated using Gas Chromatography and Mass Spectrophotometer (GC–MS) analysis method. GC-MS is used instead of GC-FID so that the dispersed and dissolved oil components which

appear in the retentate and permeate can be identified through MS library. Figure 3.4 shows the GC-MS instrument (Agilent technology) used in this research.

Figure 3.4 GC-MS instrument used in this research

Dispersed and dissolved oil components analysis from the crude oil pre-mixed produced water sample were measured by using a HP-Agilent 6890N Model gas chromatograph (GC) with a 30m, 0.25mm I.D. HP-5MS 5% Phenyl Methyl Siloxane capillary column and 5975C Model mass spectrophotometer triple-axis detector (MSD). The column chosen for this study is a non-polar HP-5MS 5% Phenyl Methyl Siloxane manufactured by HP Agilent. This column is specifically used for water analysis and for the detection of trace amount of organo-aromatic compound such as BTEX, PAH, etc [100] .

The carrier gas ~Helium (He), had a constant flow rate of 1.2 mL/min. No makeup gas was utilized. The analyses were performed with a temperature ramping in the oven as follows: 40°C for 5min, 40-100°C at 5°C/min, 100-300°C at 10°C/min, and 300°C for 3min. Inlet temperature is 300°C and with splitless mode. The MSD temperature is set at 280°C. Tuning is done once every day for the MSD, prior to analysis, to ensure no leakage in the vacuum compartment and to maintain accuracy in measurement.

Before filtration feed water was analysed for the total crude oil concentration. Approximately 1µl of the extracted feed sample containing 100ppm crude oil is injected into the GC inlet. The liquid-liquid extraction procedures are performed to obtain the extracted feed sample, and the procedures are explained in Section 3.5.1. After 40 mins, TIC spectrums of total oil components from the feed are obtained as shown in Figure 3.5. The total integration areas on the spectrum are measured by using GCMS. This total area corresponds to 100ppm of oil content. By using GC-MS library, the spectrum is analyzed and dissolved oil peaks are identified. Integration of these dissolved oil peaks‘ areas give the dissolved oil concentration in the original feed. The dispersed oil area can be found by subtracting the total dissolved oil area with the total oil area. Likewise, by using this method, the concentration of both oils from retentate and permeate can be calculated. Therefore, three extraction procedures with GCMS analysis have to be performed for each experimental run. The equation for the calculation of oil concentration can be summarized in (3-1). The reference in this study indicated in equation (3-1) is for the total crude oil in feed. The detailed calculation is attached in Appendix E.

$$\text{Concentration of peaks of interest} = \frac{\text{Area of peaks of interest}}{\text{Area of peaks of reference}} \times \text{Concentration of reference} \quad (3\text{-}1)$$

Before integration, each of the spectrums is reprocessed by ClearView™ software to enhance the identification of trace target analytes and to smooth the spectrum obtained. It is done by minimising GC-MS background ion-contributions and reduces noise but increases the sensitivity in full scan mode. Therefore the oil components are more easily being identified by each of their peaks before integration is done.

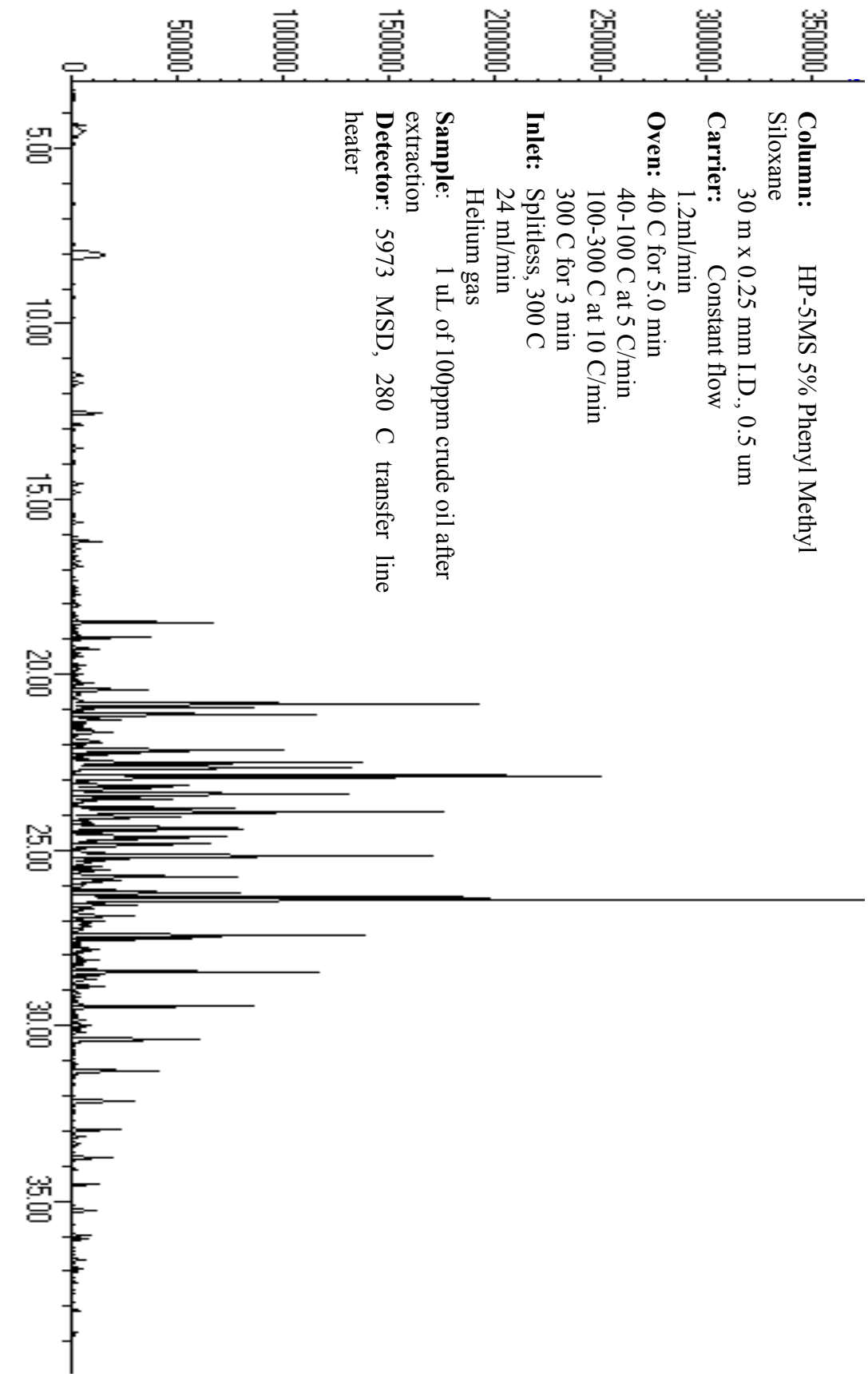

Figure 3.5 GC-MS chromatogram of 100ppm crude oil with the corresponding method used

3.5.1 Liquid-liquid Extraction Method

This section explained the procedure for liquid-liquid extraction method which is outlined in Figures 3.6 to 3.8:

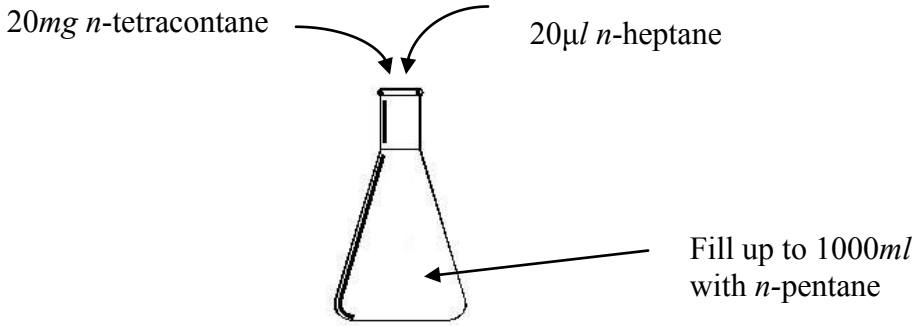

Figure 3.6 Extraction solvent stock solution stored in refrigerator

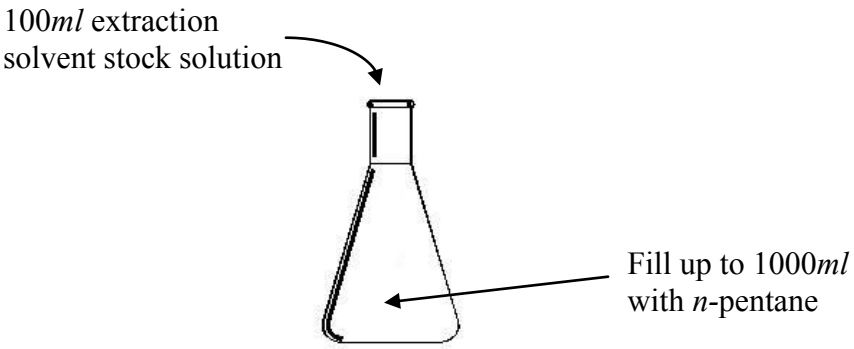

Figure 3.7 Extraction solvent standard solution before use

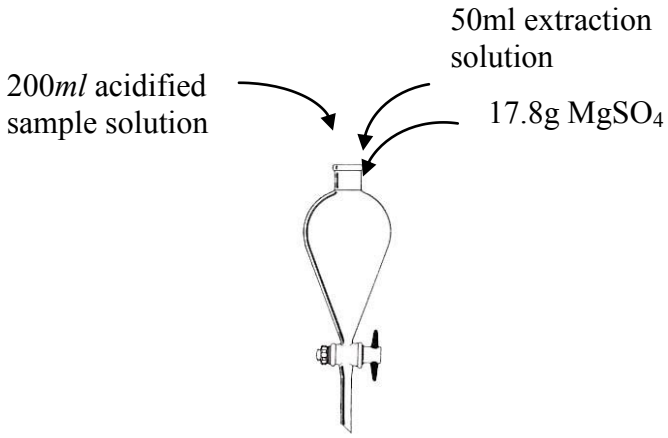

Figure 3.8 Extraction method

Extraction solvent was prepared as illustrated in Figure 3.6-3.8. When doing extraction, samples and the extraction solvent are mixed in the funnel. Funnel was stoppered and mixture was shaken for 10 minutes with regular pressure release. After 10 minutes, the solution was allowed to stand where separation of water and extraction solvent took place. The bottom aqueous layer was drained off and top organic solvent phase was filtered by 2g of Florisil and 2g of sodium sulphate before keeping in a glass bottle for analysis. The purpose of Florisil is to absorb any polar substances that exist in the sample and sodium sulphate is to ensure the analysis sample is dry. Finally, 1µl of analysis sample is injected into the GC for analysis.

3.5.2 Limit of Detection (LOD)

In analytical science, there are two types of detection limit. The Instrument Detection Limit (IDL) and Method Detection Limit (MDL). IDL is the smallest concentration signal that can be distinguished from background noise. Whereas MDL is the minimum concentration of a substance that can be measured and reported with 99% confidence that the analyte concentration is greater than zero. IDL should always smaller than MDL. Therefore, for laboratory accreditation, LOD is approximately equal to MDL [101].

Chapter 4: *Membranes for Dissolved Oil Removal*

4.1. Introduction

Produced water from oil mining industry consists of many constituents. Most of the constituents are treated by ordinary mechanical treatment process except residual oils [1]. The oil-in-water content is the main indicator for produced water monitoring by operators and regulatory authorities before its disposal into the sea. These oils can be classified into two categories: the dissolved oil and dispersed oil. The organic components in the dissolved oil can be divided into four main groups, namely aliphatic, aromatic, polar and fatty acid compounds. The relative quantities and molecular weight distribution of these components vary significantly from field to field. Aromatic components such as BTEX (benzene, toluene, ethylenebenzene and isomers of xylene), PAH (poly aromatic hydrocarbon) which formed the bulk of measurable dissolved oils, are soluble in water due to their polarity. It was documented that dissolved oil leakage into the groundwater or soil will cause acute/lethal effects on health. The acute toxicity effect can be measured by LC_{50} tests which states that the concentration where 50% of the samples are killed during the test period in 8 hours [102]. According to a study by Singer *et. al.* [103] the judgement of whether dispersed or dissolved oil is more toxic is dependent on both the species and oil weathering state. They concluded that weathering reduces the amount water soluble oil compounds to the point where dissolved oil elicited less than 50% effect even at unrealistically high loading rates. Therefore, acute effects of disposal of dissolved oil into the deep sea or reinjection into the oil-wells are generally negligible and relatively safe as these places are far away from land and under the sea bed and susceptible to weathering.

Besides that, aerobic and anaerobic biodegradation by microorganism takes place changing them from harmful organic compounds to CO_2 and H_2O.On the other hand, dispersed oil is very non-polar and hydrophobic. It does not dissolve in water and normally exists in long chains with high molecular weight. In water, it floats on top and forms a layer preventing diffusion of air into the water. This effect causes acute asphyxiation to oceanic creatures [4]. Therefore, the main oil component concerned by the regulatory bodies in the oil-in-water analysis is the dispersed oil content.

From literature studies, current treatment technologies such as hydrocyclones, and gas floatation are not able to separate the soluble oil in produced water [3]. Many researches for the development of inexpensive techniques for the removal of BTEX and other dissolved oil have been on-going for this reason [16, 22, 33]. Success have been achieved in the 90s using combined technique of clarification and reversed osmosis filtration in the removal of dissolved oil [24]. Ultrafiltration has also been demonstrated in the removal of certain dissolved oil [25]. However, there are no reports on the amount of dispersed oil acquired during filtration while removing dissolved oil.

This chapter serves to discuss the feasibility of incorporating membrane filtration as part of oil-in-water analysis to separate dispersed and dissolved oil so that the accuracy of measuring the dispersed oil concentration can be enhanced. From the literature studies, microfiltration (MF) and some ultrafiltration (UF) can be potential tools to separate dissolved oil while maintaining dispersed oil from the produced water due to their pore sizes. The primary aim of this chapter is therefore to improve the efficiency of the separation by exploring different types and sizes of membrane and by adjusting differential pressure. The effectiveness of these membranes in the separation of dissolved oil is measured by its concentration using Gas Chromatography with Mass Spectrophotometer detector (GC-MS). To achieve an efficient separation, two objectives which need to be addressed are: maximizing the amount of dissolved oil in permeate and maximizing the amount of dispersed oil in retentate. The efficiency of separation and the interactions among the factors for these objectives are then statistically analyzed.

4.2. Methodology

4.2.1. Calculation for the Efficiency of Dissolved and Dispersed Oil Separation

As mentioned, there are two types of oil in the produced water namely: dispersed and dissolved oil. The objective is to achieve 100% dissolved oil in permeate; and 100% dispersed oil in retentate. However, some quantity of oil is likely to remain attached or adsorbed on the membrane surface, resulting in unaccounted losses (*error*). In this study, the efficiencies of MF and UF for the separations are being compared. The oil contents are identified and measured by using gas chromatography and mass spectrophotometer detector (GC-MS) as per described in Chapter 3. The efficiency is calculated in terms of percentage and the calculations as shown in Figure 4.1:

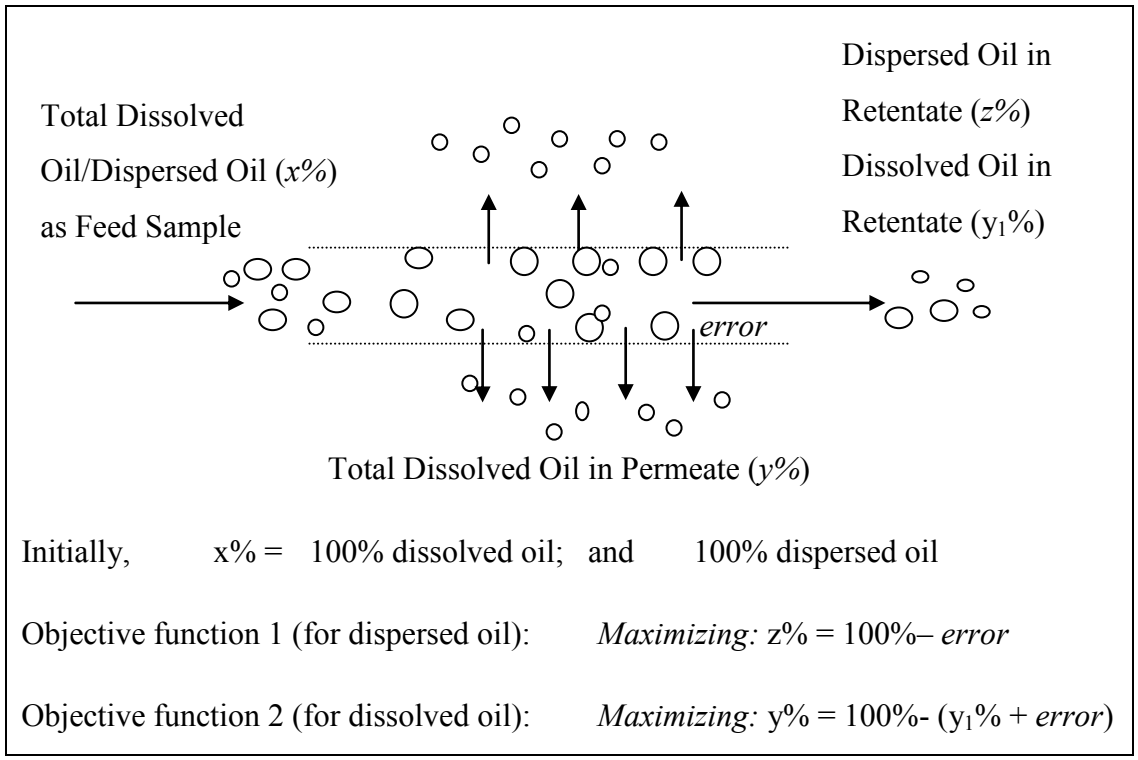

Figure 4.1 Definition of efficiency in the separation of dispersed and dissolved oil

The efficiency in the separation of oils is calculated based on percentage as shown in Figure 4.1. The total dispersed oil concentration from the feed is denoted as 100% dispersed oil and the rest of the concentration will be the dissolved oil concentration which is also 100% dissolved oil. To meet both the objective functions 1 and 2, the error, which is the deposition on the membrane surface, must be as low as possible. Accordingly, qualitative and quantitative GCMS analyses were repeated with retentate and permeate after the filtration experiments.

4.3. Experimental Set-Up

4.3.1. Determination of Optimum TMP for Membrane Filtration

Concentration polarization is the cause for flux reduction and therefore there is a need to increase effective TMP [11] to maintain a constant permeate flux. A higher TMP is required due to the increasing extent of fouling on membrane surface over time where the optimum TMP is dependent on the cycling time of filtration process as well. The filtration system was operated in a fully recycle mode where both retentate and permeate channels were recycled back to the feed beaker containing the sample solution of produced water in order to determine the optimum TMP [12].

A list of TMPs ranging from 0.35 to 3.25 bar, which could be subdivided into four categories of differential pressure, were achieved by adjusting the feed and retentate pressures. The feed pressure (P_F) was manipulated through the pump power while the retentate pressure (P_R) was set by adjusting the control valve on retentate line (Figure 4.2). The system had been left to run for a couple of minutes until the pointer inside the pressure gauges stabilized, or steady state was achieved. The time taken to collect about 200 ml of permeate flow was measured and recorded. For consistency, the readings were taken at least three times. As a result, one could calculate the permeate flow rate and ultimately the permeate flux (J) under different values of TMP. To estimate the optimum values of TMP, the permeate flux was plotted against increasing TMP with different differential pressure categories. Figure A.1 to A.4 in Appendix A show the permeate fluxes vs. TMP for 50 kD (0.1 µm) PESU, 100 kD (0.2 µm) PESU, 100 kD (0.2 µm) Hydrosart® and 0.2 µm Hydrosart® membranes.

According to the graphs, optimum TMPs occurs beyond the instrumental operating limit at 3.5 bar. This is due to the low solute concentration of feed sample which resembles the sample from treated produced water before disposal. Therefore in our study, limiting flux was assumed to occur at a standardized 2.75 bar of TMP for all DPs.

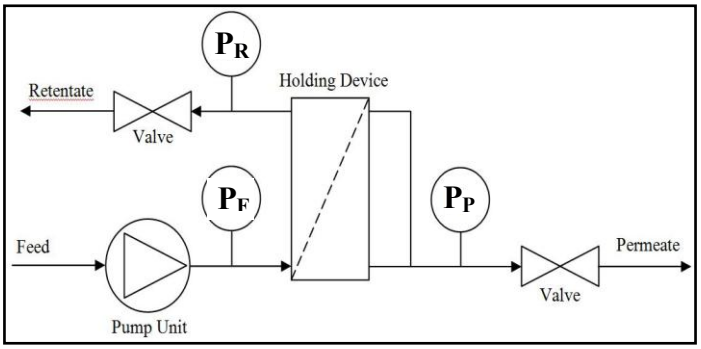

Figure 4.2 A schematic diagram of the filtration unit

4.3.2. MF and UF Membranes

All the membranes used in this research are made by Sartorius AG. Microfiltration membrane with pore size 0.2 μm is used in this study. The ultrafiltrations membranes for the experiments are 0.01 μm (50kDa) and 0.02 μm (100kDa) in pore sizes. Figure 3.2 shows that the crossflow filtration unit that is used in our experiments. Moreover, in our experiment, membrane material type was added as another factor to be considered. Two types of material was used, Polyethersulfone (PESU) and Hydrosart®. The Hydrosart® membrane is a patented product with similar properties as cellulose-based membrane [104]. According to the manufacturer, it can give good separation and prevent fouling.

4.3.3. Produced Water Sample

The simulated produced water of 100 ppm was used in all the experiments as feedstock. The preparation and the choice of using simulated produced water have been discussed in Chapter 3.4.

4.3.4. Dissolved and Dispersed Oil Identification and Separation by Pore Sizes

Calibration curves comprise of Eicosane, Ethyl-benzene and Xylene which are used as the standard reference components representing dispersed and dissolved oil contents, were constructed to quantify the unknown concentrations of respective component in feed, retentate, and permeate. The calibration was done by using MSD software and a sample of the quantification report is shown in the Appendix F. The example of spectrum of 200 ppm Eicosane standard is shown in Figure 4.3. Each of these 200 ppm standard solutions consists of Eicosane, Ethyl-benzene and Xylene is also verified with MSD library. Filtration was performed at DP 0.5 bar with TMP 2.75 bar using 3 different types of membrane discussed in Chapter 4.3.2.

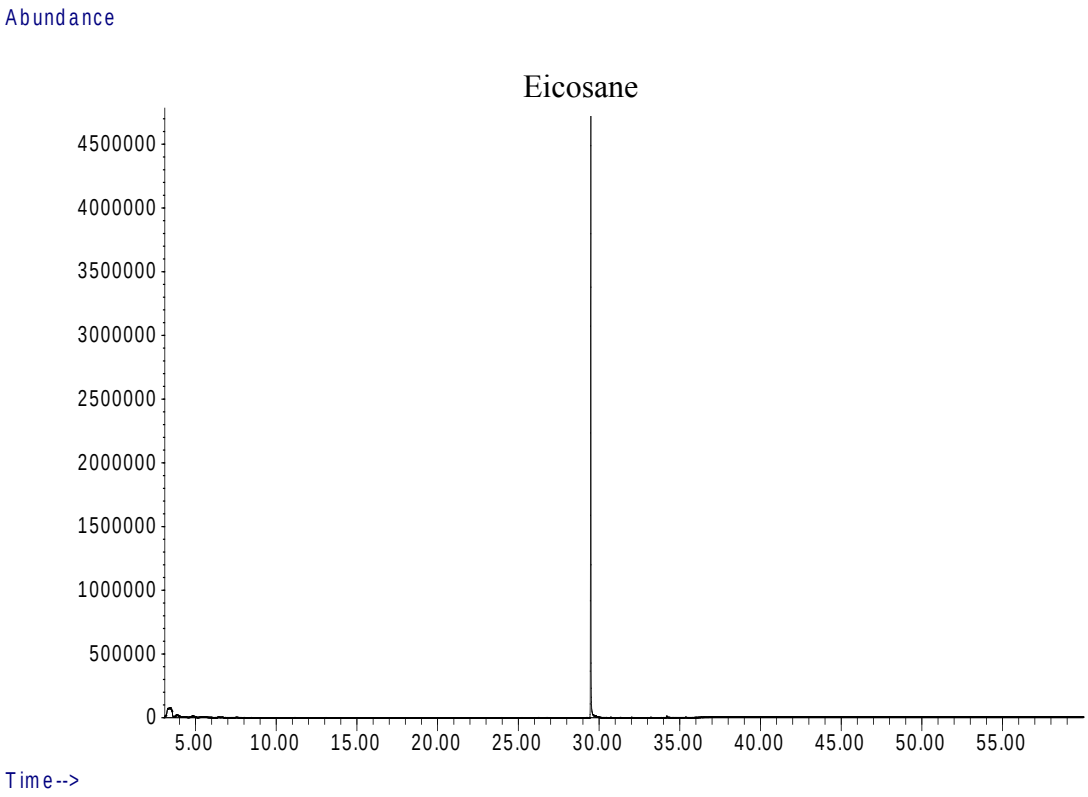

Figure 4.3 Spectrum of Eicosane standards at 200ppm

4.4. Factorial Design Experiments

Factorial design has many advantages over the normal One-Factor-A-Time (OFAT) approach. It does not only offer efficient and economical ways to study the effect of several factors but also the interaction between the factors, thus a better conclusion can be drawn. Three factors that are used in this experiment are membrane pore sizes, membrane types and crossflow pressure/ differential pressure (DP). Since 2 out of the 3 factors are discrete, our approach is to screen the main categorical factors and then establish the best operating numerical factors. Firstly, one categorical factor with one numerical factor (i.e. Size with DP) was analyzed. Next, the other categorical factor with the same numerical factor (i.e. Type with DP) was analyzed. Table 4.1 shows the 2^3 full factorial design with high and low level for the factors within the operating range. There are two objectives for these experiments namely maximizing dispersed oil in retentate and maximizing dissolved oil in permeate. In this work, the results were systematically analyzed using analysis of variance (ANOVA) [105] to determine the main and interaction effects on process behavior. The interaction graphs were studied to estimate the differential pressure to be operated. At a later stage, this analysis results will be used in finding the optimum condition for the operation.

Table 4.1 2^3 factorial design for efficiency of dissolved oil separation

Variables	Code	Low level (-1)	High level (+1)
DP	A	0.5bar	2.0bar
Size	B	0.02µm	0.20µm
Type	C	Hydrosart®	PESU

4.5. Results and Discussions

4.5.1. Effect of Pore Sizes on the Separation of Dissolved and Dispersed Oils

This is a preliminary experiment to study whether the dispersed and dissolved oils can be separated by the membranes. In Table 4.2 these oil components are identified and quantified in –ppm". The qualitative analysis was done by using standard Eicosane, Ethylenebenzene and Xylene, purchased. Any concentration loss in components before and after filtration is assumed to be trapped within membrane sheet. Dispersed oil is non-detectable (ND) in permeate channel because of its larger particle size where the possibility to be retained on membrane surface or to leave the retentate channel are higher. For dissolved oil, a reduction in concentration after membrane filtration could be seen, but the extent might not be that significant if it is compared with dispersed oil.

Figure 4.4 shows that the amount of xylene, ethylenebenzene and eicosane measured in the feed were different due to the method of sample treatment preparation. Multiple –ratio method [103] sample preparation employed in this study represents the constant changing effluent from treatment process.

Table 4.2 Comparison of sizes towards the separation of dispersed and dissolved oils

Oil Type	0.01µm (50kDa) membrane	Feed (ppm)	Retentate (ppm)	Permeate (ppm)
Dissolved	Xylene	3.03	2.82	ND
Dissolved	Ethylenebenzene	10.32	1.96	ND
Dispersed	Eicosane	5.82	ND	ND

Oil Type	0.02µm (100kDa) membrane	Feed (ppm)	Retentate (ppm)	Permeate (ppm)
Dissolved	Xylene	2.84	1.42	0.39
Dissolved	Ethylenebenzene	12.62	0.42	0.07
Dispersed	Eicosane	1.64	ND	ND

Oil Type	0.2µm membrane	Feed (ppm)	Retentate (ppm)	Permeate (ppm)
Dissolved	Xylene	5.85	2.34	2.46
Dissolved	Ethylenebenzene	9.88	1.14	2.28
Dispersed	Eicosane	7.36	1.11	ND

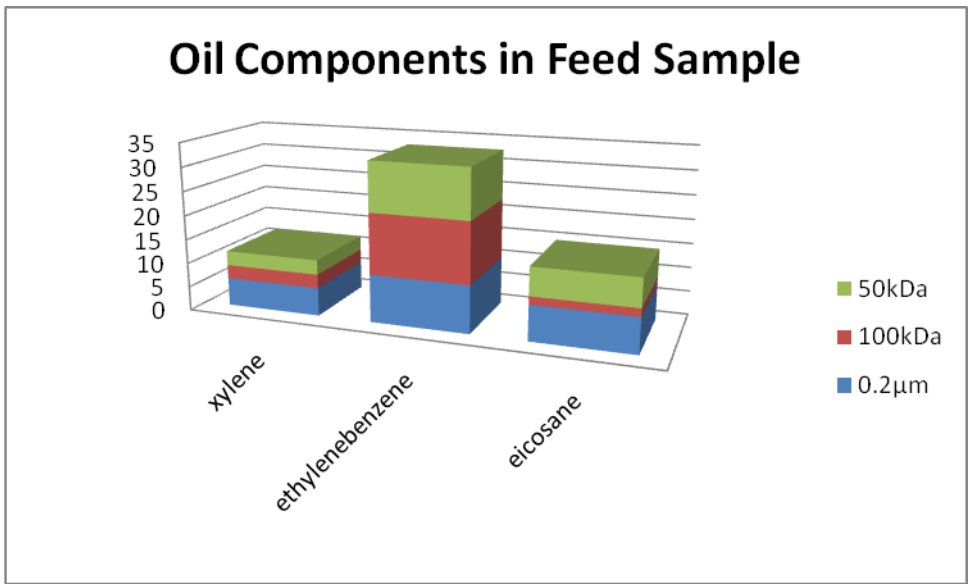

Figure 4.4 Oil components in feed sample

In Table 4.3, a total of dissolved and dispersed oils are identified by using GCMS and their concentrations are measured and reported in percentage. These results show that only 0.02 µm UF and 0.2 µm MF membranes are able to separate the dispersed and dissolved oil in the produced water. Therefore, 0.01 µm UF membrane will be excluded in the comparison in the following experiments.

Table 4.3 Comparison of sizes towards the separation of total dispersed and dissolved oil

Separation Results and Size	0.01µm - Ultrafiltration	0.02µm - Ultrafiltration	0.2µm- Microfiltration
Dispersed oil in retentate (%)	1.3	14.1	23.1
Dissolved oil in permeate (%)	0	0.93	17.3

4.5.2. Comparison of Different Factors

Factorial design is used to generate design of experiment for comparing two factors i.e. membrane size and DPs from which the interactions of two factors for the separation will be studied. In Figure 4.5 & 4.6, Membranes A (MF) and C (UF) are

the same type (Hydrosart®) of membrane with different sizes, i.e. 0.2 μm and 0.02 μm (100 kDa) respectively. The visible line is the best fit for the model, whereas the dotted lines above and below show the range of the data.

From the interaction graph for DP and size of membrane (Figure 4.5), Membrane A (black line) can achieve higher dissolved oil in permeate than Membrane C (red line). Similarly, for high dispersed oil in retentate (Figure 4.6), Membrane A (black line) is more efficient than Membrane C. To get higher dissolved oil in permeate, DP has to be set low for both UF and MF membranes so that with the lower crossflow rate, there will be enough time for dissolved oil to pass through the membrane pores and would not be carried away into retentate. However, to have higher dispersed oil in retentate, DP has to be set high for MF membrane. This indicates that dispersed oil are mostly deposited on the MF membrane surface if the pressure is set low, and when DP was increased, the shear force from the crossflow lifted the dispersed oil on the surface into retentate. However, for the UF membrane, DP is not a significant factor for dispersed oil as has been shown in the ANOVA of dispersed oil in Table 4.4. Table 4.5 shows a summary of operating condition (DP) for maximum dissolved and dispersed oil in permeate and retentate respectively.

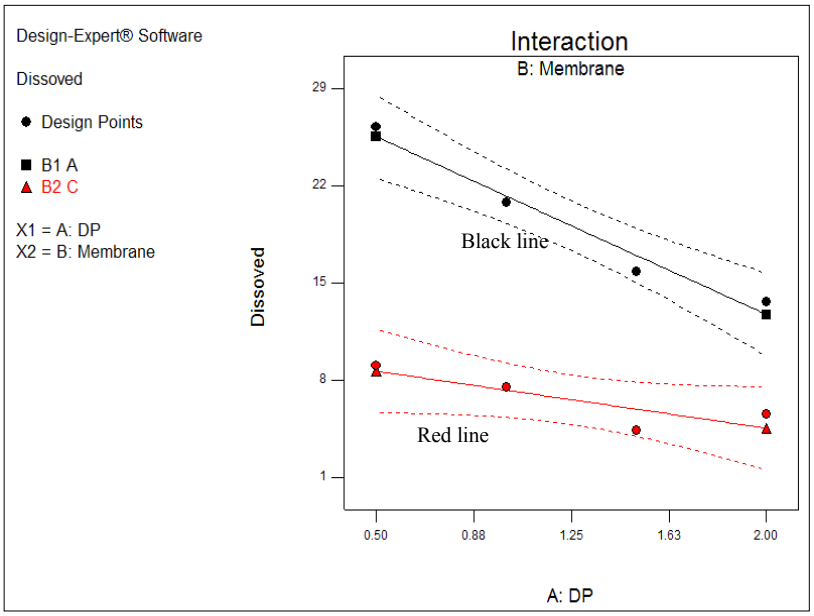

Figure 4.5 Interaction graph for dissolved oil at the permeate (Membrane pore size vs. DP)

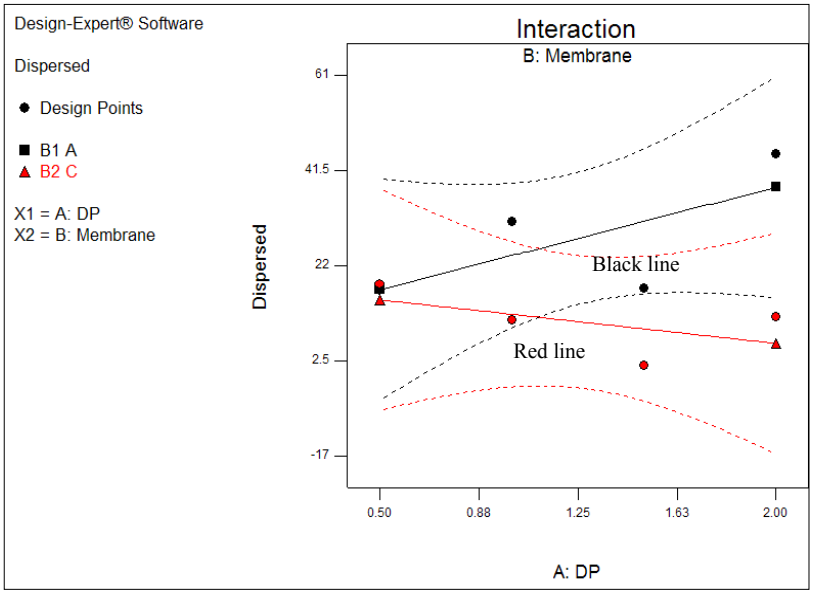

Figure 4.6 Interaction graph for dispersed oil at the retentate (Membrane pore size vs. DP)

Table 4.4 ANOVA for factorial model of DP and pore size for dispersed oil

Source	Sum of Squares	df	Mean Square	F Value	p-value Prob > F	
Model	866.1496	3	288.7165	3.0388	0.1555	
A-DP	40.27724	1	40.27724	0.423926	0.5505	Not significant
B-Membrane	577.9007	1	577.9007	6.082523	0.0692	
AB	247.9716	1	247.9716	2.609952	0.1815	
Residual	380.0401	4	95.01003			
Cor Total	1246.19	7				

Table 4.5 Summary table for operating condition (DP) for maximum dissolved and dispersed oil

	MF	UF
Maximizing oil concentration	DP	DP
Dissolved oil in permeate	Low	Low
Dispersed oil in retentate	High	Not significant

Another experiment design was created to compare two factors i.e. membrane type and DPs so that their interactions for the separations can be studied. In Figure 4.7, Membranes A and C have the same pore size (0.02μm) but different material type, i.e. PESU and Hydrosart® respectively.

From the interaction graph (Figure 4.7), for high dissolved oil in permeate, Membrane C, Hydrosart® (red line) is better than Membrane A, PESU (black line), while the effect of the type of membrane for dispersed oil is not significant (Figure 4.8). The ANOVA in Table 4.6 confirmed the insignificancy of the factor by giving a p-value of 0.8990. As dissolved oil passes through the membrane, more of it was plugged inside the PESU membrane, while lesser dissolved oil plugged the pores inside the Hydrosart® membrane. This shows that Hydrosart® membrane material has non-fouling properties as claimed by the manufacturer. To get higher dissolved oil in permeate, DP has to be set low for both types of membrane. Similarly, DPs have to be set low for both types of membrane to obtain higher dispersed oil in retentate.

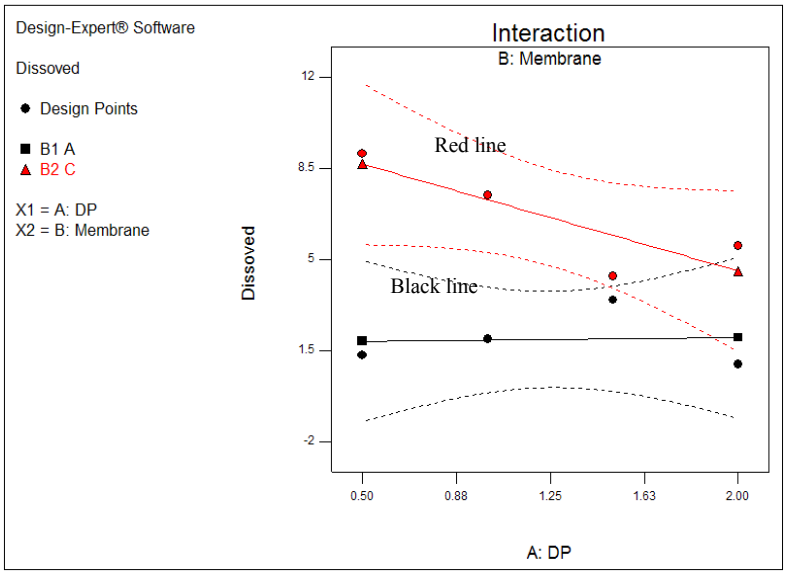

Figure 4.7 Interaction graph for dissolved oil in permeate (Membrane Type vs. DP)

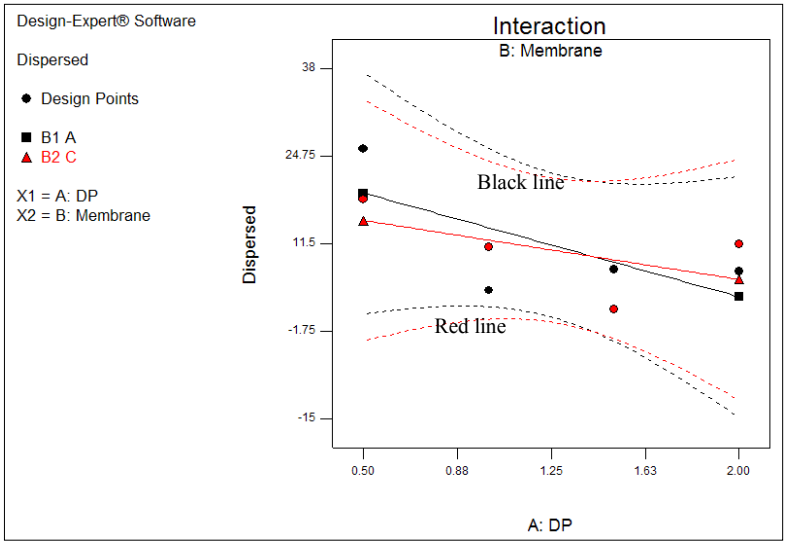

Figure 4.8 Interaction graph for dispersed oil in retentate (Membrane Type vs. DP)

Table 4.6: ANOVA for factorial model of DP and Membrane Type for dispersed oil

Source	Sum of Squares	df	Mean Square	F Value	p-value Prob > F	
Model	181.8171	3	60.60571	0.981559	0.4853	
A-DP	168.0075	1	168.0075	2.721019	0.1744	
B-Membrane	1.128258	1	1.128258	0.018273	0.8990	Not significant
AB	12.68137	1	12.68137	0.205385	0.6739	
Residual	246.9773	4	61.74433			
Cor Total	428.7945	7				

Figure 4.9 shows a summary of the efficiency of dissolved oil separation in permeate for different types and sizes of membranes and the different operating DPs conditions. The legend which shows 0.2µm is the 0.2µm Hydrosart membrane; 100P is the 100kDa (0.02 µm) Polyethersulfone membrane and 100H is the 100kDa (0.02 µm) Hydrosart membrane. With membrane filtration incorporated in the standard test method, more than 25% of dissolved oil can be separated from the treated produced water by using 0.2µm membrane operating at DP 0.5 bar. Without membrane filtration, these 25% of dissolved oil will be measured as dispersed oil thus the chances of violating the disposal regulation limit increases. As DP increases the efficiency of separation dropped. For a similar pore size, efficiency can be improved by using Hydrosart® membrane material.

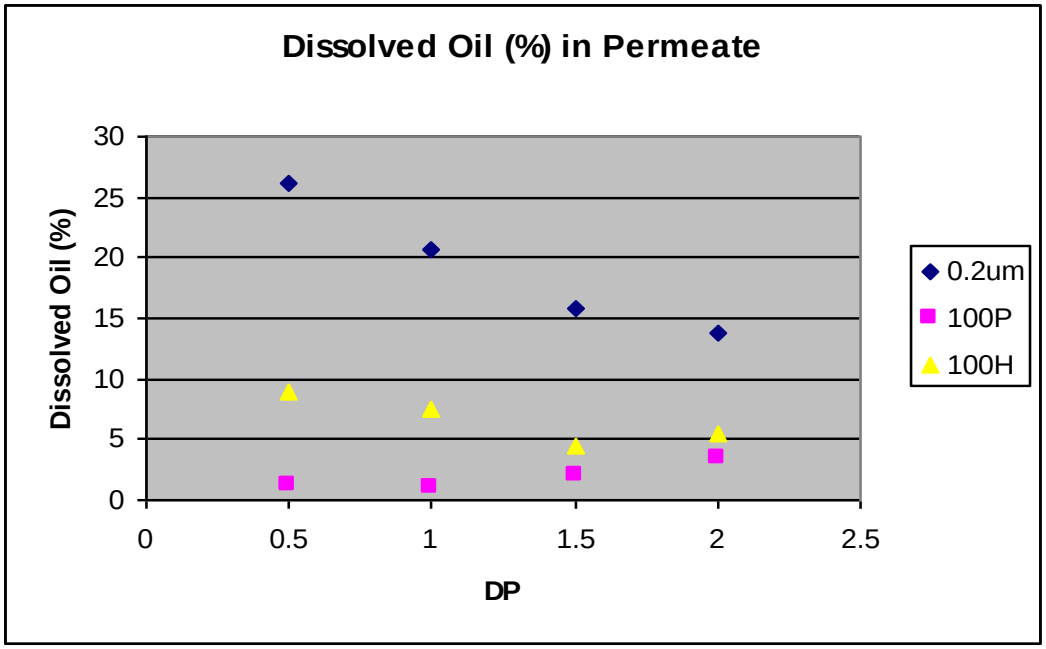

Figure 4.9 Dissolved oil (%) in permeate vs. DP

4.6. Conclusions

In this chapter, the incorporation of membrane filtration into the standard test method has shown improvement in eliminating the dissolved oil from the analysis. The effectiveness of the membrane in terms of pore size and the type of membrane and operating pressure to achieve high dispersed oil in rententate and high dissolved oil in permeate are analysed. From Table 4.2, conclusions can be drawn that 0.01 μm (50kDa) membrane pore size is not suitable for dissolved oil removal. This is because the pore size is too small for the dissolved oil to be removed as permeate. Table 4.2 also shows that dissolved oil is lower in molecular weight than dispersed oil as dispersed oil such as Eicosane is not detectable (ND) in permeate. From the experimental data, it was found that for high dissolved oil in permeate, the pore size and the type of membrane are critical. On the other hand, for high dispersed oil in retentate, the pore size is critical but not the membrane type. Moreover, the polarity of the oil has an effect towards the membrane type as we can see in the case of dissolved oil where cellulose-based Hydrosart® membrane prevent the adsorption of oil plugging the membrane wall. In conclusion, Microfiltration using 0.2μm Hydrosart® membrane can achieve a more efficient separation of dissolved and dispersed oil in permeate and retentate respectively.

Nevertheless, in the determination of suitable DP for separation of dissolved and dispersed oil, the results give conflicting suggestion: low DP is needed for high dissolved oil but high DP is needed for high dispersed oil. Thus, to obtain a good separation by maximizing both the oil contents, it is important to get the best optimum setting of the crossflow pressure. This issue will be addressed in Chapter 7.

Besides that, a combination of operating condition of DP and TMP for the highest permeate flux is important. This is because, the decline of permeate flux is usually an indication of fouling occurring. The prevention of fouling of dispersed oil on the membrane surface is crucial for the accuracy in measurement, and is addressed in the following chapter.

Chapter 5: *Modified Film Theory Model for Fouling Control in Membrane Filtration*

5.1. Introduction

Boundary layer problems are often present in any separation processes. In membrane separation for instance, concentration of solute nearer to the membrane wall will be higher than that of the bulk solution (Figure 5.2). This concentration polarization phenomenon will subsequently result in the undesirable issue i.e. fouling. For that reason, many models are derived explaining this phenomenon such as the boundary layer resistance model [106], osmotic pressure model [107] and the gel polarization model [49]. Many research projects are ongoing to try to minimize the fouling and to increase permeate flux through various means including mechanical techniques such as shear induction [74], vibratory shearing [108], air scouring [109] etc. Process modeling is therefore important before any practical application, to help in identifying the operating range for the optimization of filtration system to overcome fouling.

Models are used to predict and explain the concentration polarization phenomenon occurred during fouling. For most of the models, Mass Transfer Coefficient (MTC) of solute across the membrane is required. MTC is closely related to the hydrodynamic properties of fluid flow and thus studying the MTC could help us in optimizing the filtration process by reducing the gel layer. In this chapter, the model which gives the best estimate of the MTC is identified. The model is then modified and is utilized to control fouling.

According to the Film Theory model [49],

$$J = k \ln(\frac{C_g}{C_b}) \tag{5-1}$$

where J is the permeate flux; k is the mass transfer coefficient; C_g is the gel concentration; C_b is the bulk concentration. Concentration at the membrane wall or in some other literature termed gel concentration, C_g, is hard to measure or estimate. However, by finding the k value, we will be able to estimate the C_g value. The mass transfer coefficient (MTC or k value) in membrane filtration can be varied and optimized because it depends strongly on the hydrodynamics of the system [49].

The k value is an essential but usually unknown parameter. The conventional way of estimating the k value is done by using the Sherwood relation based on the assumption that fluid flows in non-porous and smooth duct [110]. The correlation of the mass transfer coefficient and the Sherwood number is as follow:

$$Sh = \frac{kd_h}{D} = (a \,\mathrm{Re}^b \, Sc^c) \tag{5-2}$$

where Sh is the Sherwood number; k is the mass transfer coefficient; d_h is the hydraulic diameter; D is the diffusion coefficient; a, b, c are constants which are determined from experiment. Re is Reynolds‘s number; Sc is Schmidt‘s number. Therefore, in order to predict the C_g value using the Film Theory model, multiple steps are involved. This may introduce multiple errors in the process. For instance, to predict the mass transfer coefficient from the Sherwood number, the values of Reynold‘s number and Schmidt‘s number need to be determined first. This Reynold‘s number is related to the velocity by the empirical formula:

$$\mathrm{Re} = \frac{\rho v d}{\mu} \tag{5-3}$$

where ρ is the density of the fluid, ν is the velocity of the fluid d is the diameter of the pipe, and μ is the viscosity of the fluid.

However, this Sherwood relationship is again based on the assumption of flow being in a smooth pipe and adapted from heat transfer analogy [110]. Thus this method is not suitable for membrane surfaces which are porous and not smooth, and hence does not fit the assumptions made in the modelling. Furthermore, the problem of fouling could not be controlled directly from this Film Theory model as the adjustable variable is absent in the model. Crossflow pressure in particular, affects directly the mass transfer coefficient of the membrane filtration system. As explained by Van den Berg and colleagues [111] the determination of *k* values by Sherwood relation is very difficult. However, it can be done by evaluating the crossflow velocity with film theory models.

Another notable point is that in other membrane filtration equation by Darcy [49], $J = (\Delta P - \Delta\Pi)/\mu(R_{total})$ the pressure term involved is the trans-membrane-pressure (TMP) and not the differential pressure (DP). Thus, if this DP can be correlated with the mass transfer coefficient, and then integrated directly into the Film Theory model (Equation 4-1), C_g will therefore be easily predicted and controlled.

In this study, a two-stage modelling is pursued. First, the mass transfer coefficient k value is determined using regression techniques [112]. Two models (solution-diffusion model and fluid transport model) are compared and the suitable model for determining the k value is identified. Secondly, by using the k values estimated from the first stage, an empirical model with cross-flow pressure as a function of MTC is derived and coupled into the film theory model equation so that the cross-flow pressure (DP) is a function of concentration at the membrane wall. At a constant permeate flux, one can minimise the concentration at the membrane wall by optimizing the DP. Figure 5.1 shows a schematic diagram for the summary of this work.

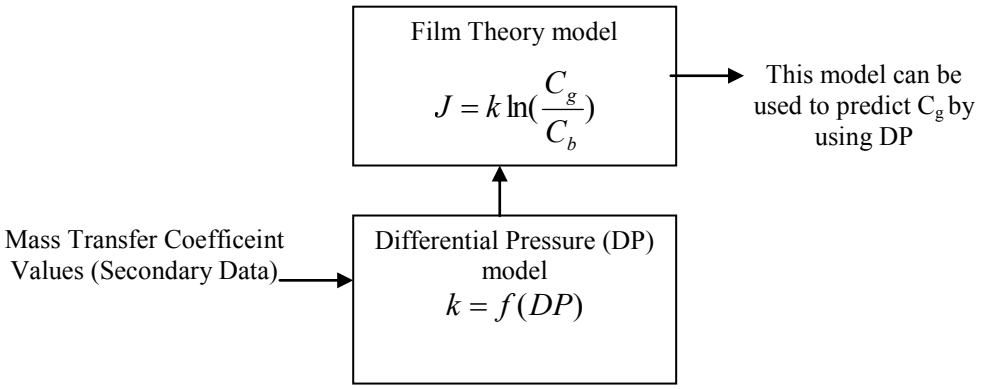

Figure 5.1 Schematic diagram of hybrid modelling for membrane filtration

5.2 First Stage Modelling- Determination of *k* Value [112]

5.2.1 Introduction

In the first stage of modelling, two models which are Film Theory model (5-1), and Solution Diffusion model are compared for the best fit in the estimation of mass transfer coefficient (*k* value). The permeate flux (*J*), concentration of permeate (C_p) and concentration of feed (C_b) data are measured and inserted into respective equations which will be further explained in the following sections. Linear regression is performed to get the *k* value from the slope of the graph. By using different cross-flow pressures (DP) and membrane types, a series of *k* values were estimated. An example is shown in Table 5.4 for DP 0.4 bar.

5.2.2 Film Theory Model

In membrane separation process, particles being rejected by the membrane will build up near the membrane surface thus forming concentration profile [49]. Concentration at the membrane surface will be higher and decay exponentially back to bulk concentration when away from the membrane wall (Figure 5.2).

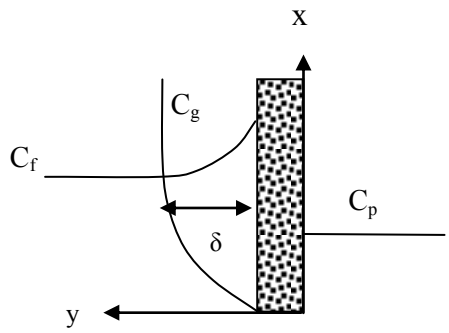

Figure 5.2 Concentration profile develops across a boundary layer (δ) during membrane filtration

Some of the particles near the wall will diffuse back to the bulk/feed until equilibrium is formed [46]. This steady state relationship is represented by:

$$JC = JC_p - D\frac{dC}{dx} \tag{5-4}$$

At the boundary conditions: when $x = \delta$; $C = C_f$ and when $x = 0$; $C = C_g$

Integrating Equation 5-4 with the boundary conditions we have

$$\frac{C_g - C_p}{C_f - C_p} = \exp(\frac{J\delta}{D}) \tag{5-5}$$

When there are complete rejection, *Cp* is equal to 0, and rearranging we have

$$J = \frac{D}{\delta}\ln(\frac{C_g}{C_f}) \tag{5-6}$$

Where $\frac{D}{\delta}$ is equal to mass transfer coefficient (MTC) and can be replaced by *k*.

Expanding Equation 5-6 with *k* incorporated, we have a linear equation (y = c + mx)

$$J = k \ln C_g - k \ln C_f \tag{5-7}$$

This is a linear regression problem. From a set of experimental data on J and C_f, we will be able to estimate k value.

5.2.3 Combined Solution Diffusion/Film Theory Model

An alternative method to estimate the mass transfer coefficient is by using the model derived by Murthy and Gupta [113] from combining solution-diffusion and film theory model [114]. First of all, we define observed rejection coefficient and true rejection coefficient as:

Observed rejection coefficient, $R_o = \dfrac{C_f - C_p}{C_f}$ (5-8)

True rejection coefficient, $R = \dfrac{C_g - C_p}{C_w}$ (5-9)

Rearranging the rejection coefficient with Equation 5-5 will yield

$$\frac{R_o}{1 - R_o} = \left(\frac{R}{1 - R}\right) \exp\left(\frac{-J}{k}\right) \tag{5-10}$$

Equation 4-10 needs to be modified to find the MTC value. The solution-diffusion model can be combined with (4-9) to give

$$\frac{1}{R} = 1 + \left(D\frac{K}{\delta}\right)\left(\frac{1}{J}\right) \tag{5-11}$$

Where $D\dfrac{K}{\delta}$ is considered as a single parameter namely solute transport parameter. Rearranging (11), we have

$$\frac{R}{1 - R} = J / \left(D\frac{K}{\delta}\right) \tag{5-12}$$

Substituting (5-12) into (5-10) yields,

$$\frac{R_o}{1-R_o} = \left[\frac{J}{\left(D\frac{K}{\delta}\right)}\right] \exp\left(\frac{-J}{k}\right) \tag{5-13}$$

(5-13) can be rearranged into linear form as

$$\ln\left(\frac{R_o}{1-R_o}\right) - \ln J = \left(-\frac{1}{k}\right)J - \ln\left(\frac{DK}{\delta}\right) \tag{5-14}$$

Again, this is a linear regression problem. From the same experiment, by plotting $\ln\left(\frac{R_o}{1-R_o}\right) - \ln J$ vs. J, we will be able to estimate k value from the slope.

5.3 Second Stage Modelling

The k values vary with crossflow pressure (DP) and the type of membrane. Therefore, an empirical model of k with DP can be derived using statistical analysis with the following assumptions:

a) The system is operated at the optimum TMP. Optimum TMP is where the limiting flux occurs. For this system, optimum TMP is chosen to be at 2.75 bar for ultrafiltration (Figure A.1 and A.2 in Appendix A) and microfiltration (Figure A.4 in Appendix A) for all the DPs used in our experiments.

b) Maximizing k value to obtain a low concentration membrane wall (C_g) is possible when feed concentration is relatively unchanged.

5.4 Experimental Set-up

5.4.1 Feed Water Sample and Membranes

A produced water sample with 0.04-0.05g/ml (40000-50000 ppm) of solute, from a holding basin in Miri Crude Oil Terminal was filtered using three different membrane sizes of 0.20 μm (3051860701W—SG, Sartorius AG.), 0.01 μm or 50 kDa molecular weight cut-off (MWCO) membrane (3051465001E—SG, Sartorius AG.) and 0.02 μm or 100 kDa MWCO membrane. The 0.20 μm membrane is a microfiltration membrane, while the 0.01 μm and 0.02 μm membrane are ultrafiltration membranes.

5.4.2 Operating Condition of the Membrane Filtration System

The filtration was operated at optimum trans-membrane pressure (TMP). The importance of operating the TMP at optimum has been explained in Chapter 2.5. Optimum TMP is where the highest permeate flux is reached [115]. Table 5.1 shows the operating conditions of TMP for these two types of membranes. TMP is the driving pressure across the membrane. However, by changing the DP, the flow rate in the cross-flow direction will be altered and the mass transfer coefficient will vary. The calculation of TMP (5-15) and DP (5-16) are given as:

$$TMP = [(P_{feed} + P_{ret})/2] - P_{per} \quad (5\text{-}15)$$

$$DP = P_{feed} - P_{ret} \quad (5\text{-}16)$$

where P_{feed}, P_{ret}, and P_{per} are adjusted accordingly to meet the operating conditions stipulated in Table 5.1.

Table 5.1 Operating pressures (in kPa) for cross-flow membrane filtrations

DP	TMP	P_{feed}	P_{ret}	P_{per}
50	275	300	250	0
100	275	330	230	0
150	275	350	200	0

5.4.3 Determination of k Values

The experiments were performed by using cross-flow membrane filtration system from Sartorius with Sartocon Slice Cassette containing Polyethersulfone (PESU) 50 kDa MWCO membrane. The membrane cassette is in the vertical position and the in-flow direction is anti-gravitational, flowing from bottom to top. Figure 4.3 shows the flow diagram of the membrane system used. The filtration was operated at optimum trans-membrane pressure (TMP) which is 2.75 bar at 3 differential pressures (DP) which are 0.5 bar, 1.0 bar and 1.5 bar.

TMP is the driving pressure across the membrane. However, by changing the DP, the flow rate in the cross-flow direction is altered. Initially the weight of 12 empty cylinders was measured and recorded. The raw water and distilled water were weighed separately. During the filtration, 100 ml of permeate were collected in each of the 12 cylinders with the time and weight recorded. The time recorded is used to calculate the permeate flow rate and the flux. Feed concentration changes when volume of feed varies. Therefore the feed volume was measured for each 100 ml of permeate taken so that feed concentration can be determined. The calculations for the experiment are explained in Appendix B. The experiments are repeated with 100 kDa MWCO PESU ultrafiltration membrane and 0.2 μm microfiltration membrane.

5.5 Results and Discussions

5.5.1 First Stage Modelling- Determination of k Values

From the data collected, 6 graphs are plotted using the linear form of Solution-diffusion/film theory model (S-D) and Film theory (FT) model. From the slope of the graphs, the MTCs or k values are calculated using (5-7) and (5-14) accordingly. The MTCs for their respective DPs are summarized in Table 5.2 below:

Table 5.2 MTCs for Solution-diffusion model and Film theory model for 50kDa membrane

MTC	DP 0.5 bar	R^2	DP 1.0 bar	R^2	DP 1.5 bar	R^2
S-D	8.69E-06	0.7232	6.25E-06	0.2725	9.78E-06	0.1038
FT	2.00E-04	0.9635	2.00E-05	0.3778	8.00E-06	0.0535

From Table 5.2, the coefficient of determination, R^2, represents the degree of linear-correlation of variables in regression analysis [116]. The experimental data at DP 0.5 bar fit reasonably well with both the S-D and FT models (R^2 =0.7232 and R^2 =0.9635 respectively). However, the R^2 at DP 1.0 bar and DP 1.5 bar are relatively small for both models, thus the MTCs estimated from the models at these DP are likely to be incorrect. Figure 5.3 and 5.4, shows the fitting of SD and FT model at DP 0.5 bar. FT model in Figure 5.4 has a better fit with the experimental data. Therefore, the estimated MTC value by FT model is closer to the true value as compared with S-D model. Therefore the MTC from FT model operating at DP 0.5 bar is a reliable value and is the best estimated mass transfer coefficient for our membrane system.

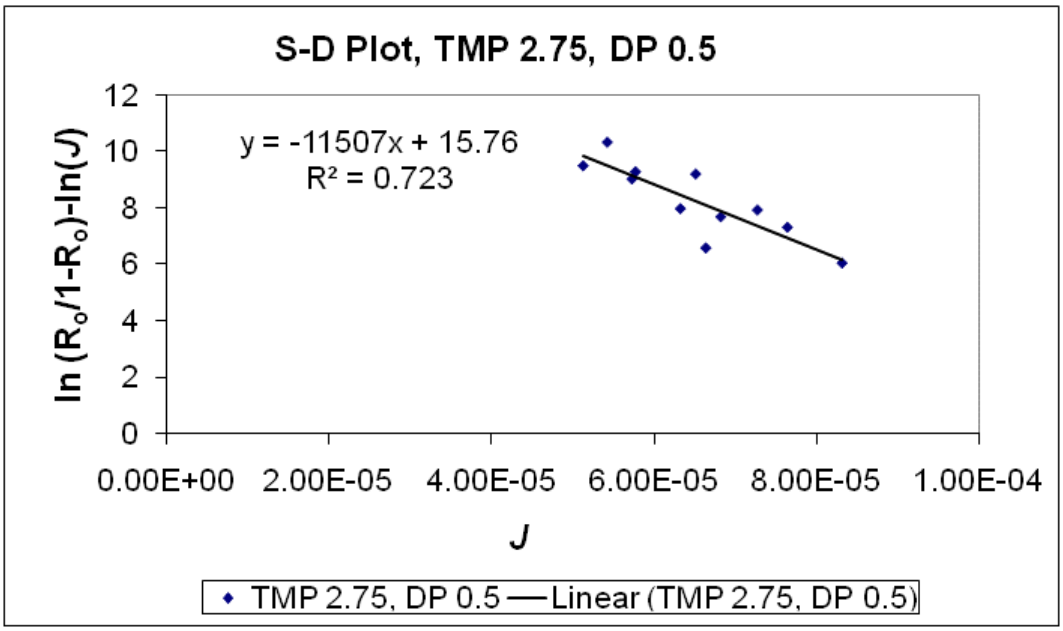

Figure 5.3 $\ln(\frac{R_o}{1-R_o}) - \ln J$ versus J for DP 0.5 bar (50 kDa membrane)

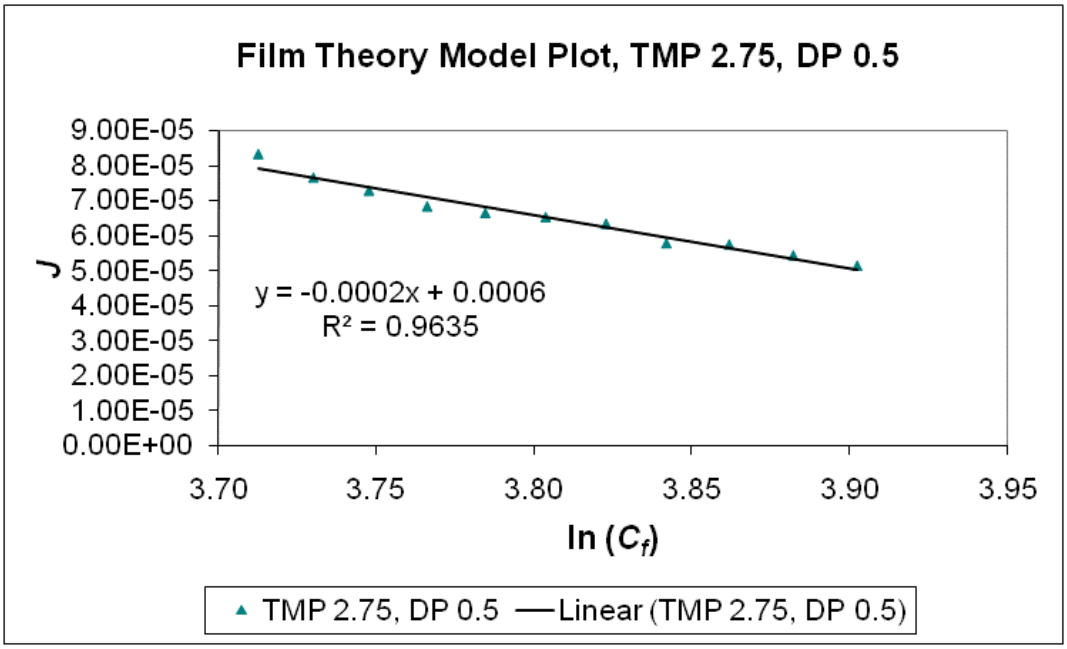

Figure 5.4 J versus ln (C_f) for DP 0.5 bar (50 kDa membrane)

Another important analytical finding was that, the changes in the MTC values for the FT model with varying DP are more significant as compared to the changes seen in MTC values using the S-D model. Therefore, this experiment shows that DP is a significant factor for FT model but not for the S-D model. This is due to the concentration of solute in the produced water passing through as permeate is very small because of the small membrane pore size, thus it is assumed to be negligible which satisfy the assumption made by FT model [49]. Consequently, S-D model may give a better prediction when there is higher concentration of solute in the permeate.

This experiment is repeated with 100 kDa MWCO PESU membrane and the MTC results with their respective R^2 are summarised in Table 5.3.

Table 5.3 MTCs for Solution-diffusion model and Film theory model for 100kDa membrane

MTC	DP 0.5 bar	R^2	DP 1.0 bar	R^2	DP 1.5 bar	R^2
S-D	3.87E-05	0.0433	3.05E-05	0.0445	4.08E-06	0.056
FT	7.00E-05	0.8926	8.00E-05	0.5465	1.00E-05	0.2927

From these two experiments, the results consistently show that the FT model fits well with the experimental data. Also noted that for FT model, it fits particularly well at lower DP range i.e. DP 0.5 bar. As the differential pressure (DP) increases, R^2 values decreases. An additional experiment was performed at DP 0.4 bar for 100 kDa membrane to verify the hypothesis. Linear regression plot for FT model at DP 0.4 bar is shown in Figure 5.5. In fact, the experiment data for lower DP shows relatively good linear correlation with the FT model ($R^2 = 0.7591$).

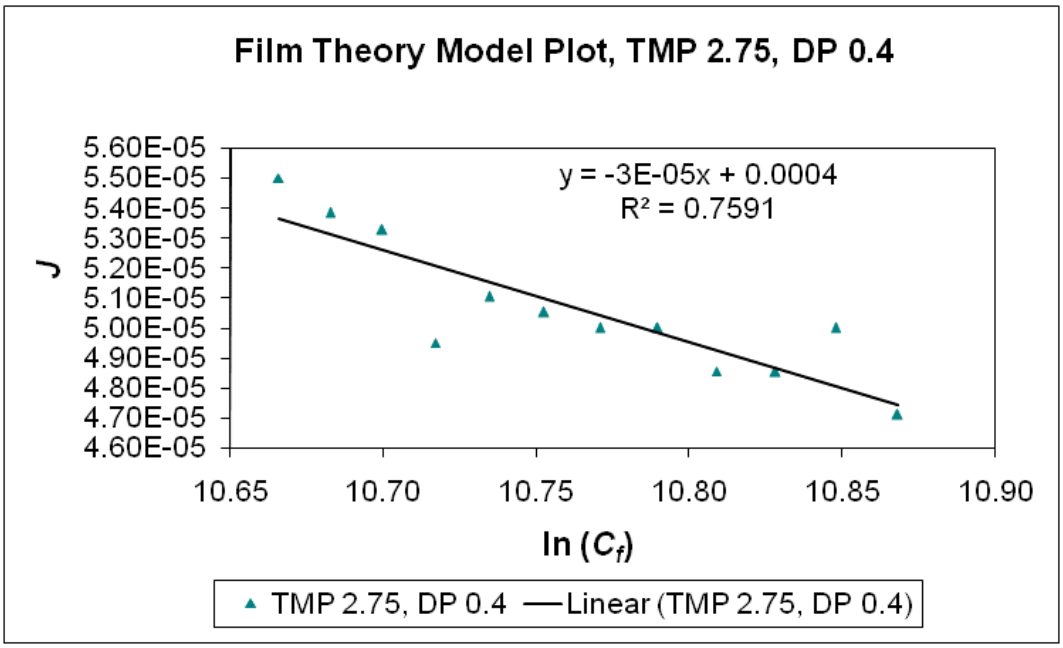

Figure 5.5 J versus ln (C_f) for DP 0.4 (100kDa membrane)

A third membrane i.e. 0.2 µm Hydrosart® membrane is used for the same experiment. Similarly, the result in Table 5.4 shows that FT model fits very well with experimental data which gives an R^2 value of above 0.65 for all the DPs. Due to the steady state assumptions of the model, this model fit particularly well at lower DPs. At lower DPs, the flows achieved steady state sooner than at higher DPs. As the pore size of the membranes increases, the permeate flow through the membrane is much easier and therefore will reach steady flow even at a higher DP.

Table 5.4 MTCs for Solution-diffusion model and Film theory model for 0.2µm membrane

MTC	DP 0.3	R^2	DP 0.5	R^2	DP 1.0	R^2	DP 1.5	R^2
S-D	2.5E-08	0.4648	1.4E-05	0.1292	1.32E-05	0.131	1.8E-05	0.0585
FT	1.0E-07	0.8927	5.0E-05	0.9400	3.0E-05	0.6721	2.0E-05	0.7814

5.5.2 Second Stage Modelling- Correlation Modeling of DP with k Values

In order to evaluate the relationship between the DP and the type of membranes on the mass transfer coefficient, several combinations were run repeatedly. The combinations listed in Table 5.5 were analyzed to determine if a suitable empirical model could be derived. Since multiple levels of DP were run for each membrane type, a quadratic model could be the possible fit for the data. *k* factor for each treatment combination was determined by using Equation (5-1). In this second stage modelling, ANOVA is applied in statistical model fitting using data from 50 kDa (0.01 μm) membrane and 0.2 μm membrane which represents ultrafiltration and microfiltration models respectively.

Table 5.5 Treatment combinations for correlation modeling of DP with *k* values

Combination	DP (bar)	Membrane	k Factor
1	0.4	0.01μm	0.0000600
2	0.5	0.01μm	0.0010000
3	0.7	0.01μm	0.0000300
4	1.0	0.01μm	0.0000200
5	1.5	0.01μm	0.0000075
6	1.5	0.01μm	0.0000080
7	0.3	0.20μm	0.0001000
8	0.5	0.20μm	0.0000500
9	0.7	0.20μm	0.0001000
10	1.0	0.20μm	0.0000300
11	1.5	0.20μm	0.0000150
12	1.5	0.20μm	0.0000200

Table 5.6 Correlations between model factor effects.

	DP	Membrane Type	DP x Membrane Type
DP	1.00	0.018	-0.046
Membrane Type	0.018	1.00	0.055
DP x Membrane Type	-0.046	0.055	1.00

Since the lowest level of DPs were slightly different for the two membrane types as can be seen from combination 1 and 7 of Table 5.5, the treatment combinations deviate slightly from a factorial design and need to be checked to determine if any correlation of factor terms has been introduced. A correlation matrix of model terms in Table 5.6 shows that there are no strong correlations, which is greater than 0.5, between model effects and hence the treatment combinations in Table 5.5 could be used to fit a quadratic statistical model consisting of main effect, interaction and squared terms. The replicated runs were performed in order to obtain an estimate of pure error to test for lack of fit.

A Box-Cox power transformation was utilized to reduce the modelling sum of squares for error, providing an improved fit and better fulfilment of model assumptions. Either a log or inverse square root power transformation are within the confidence interval bounds, marked in red around the lowest log sum of squares on Figure 5.6 and thus may be used to provide a better fit and improve the residuals' properties relative to the assumptions of equal variation, normality and lack of outliers. The class of power transformations is well known [92] and are indexed by the parameter λ in the expression (5-17) for the variable Y with data values Y_j, j=1,...,n,

$$Y^{(\lambda)} = \frac{Y^{\lambda} - 1}{\lambda \prod_{j=1}^{n} Y_j^{\lambda-1}} \quad with \quad Y^{(0)} = \left(\prod_{j=1}^{n} Y_j^{\lambda-1} \right) \ln(Y) \tag{5-17}$$

The inverse square root power transformation (λ=–0.5) actually made the residual plots slightly better than the log transformation (λ=0) and was thus selected. The use of the inverse square root transformation had the double effect of improving the model assumptions and simplifying the fitted model.

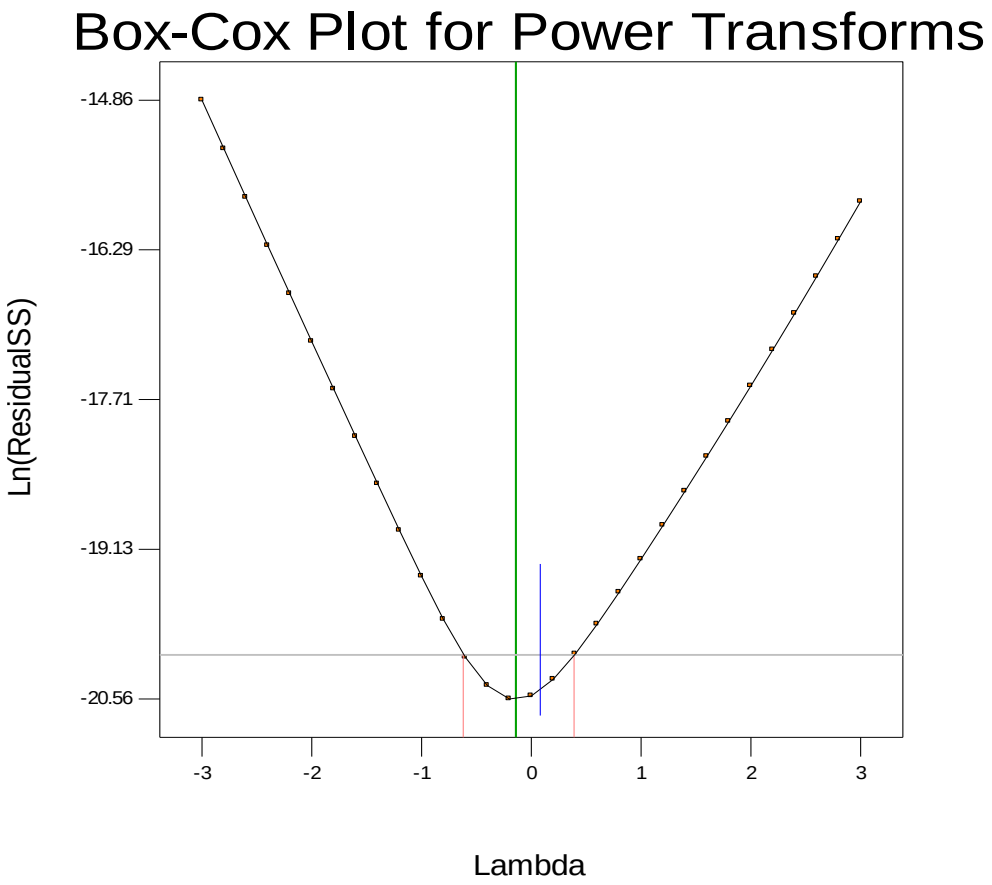

Figure 5.6 Box-Cox power transformation curve

Using Design Expert 7.1.3, the ANOVA for the fitted factorial model with interaction using the inverse square root transformation in Table 5.7 shows that the model contains a significant interaction between DP and Membrane Type without lack of fit. Higher order terms, such as squared terms, were not significant and are not included in Table 5.8. Besides the significant p-values given in Table 5.7, the model fit summary in Table 5.8 also shows a high adjusted R^2 at 0.9294 and the model has good predictive behaviour with a prediction R^2 value of 0.8908.

Table 5.7 ANOVA table for *k* factor model

Source	Sum of Squares	df	Mean Square	F Value	p-value
Model	89445.673	3	29815.224	49.286	< 0.0001
A-DP	74121.507	1	74121.507	122.527	< 0.0001
B-Membrane	8216.913	1	8216.913	13.583	0.0062
AB	7208.155	1	7208.155	11.916	0.0087
Residual	4839.511	8	604.939		
Lack of Fit	4173.983	6	695.664	2.091	0.3584
Pure Error	665.528	2	332.764		
Cor Total	94285.184	11			

Table 5.8 Model summary statistics for *k* factor model

Source	Standard Deviation	R-Squared	Adjusted R-Squared	Predicted R-Squared	PRESS	
Linear	36.5873	0.8722	0.8438	0.7589	22731.34	
2FI	24.5955	0.9487	0.9294	0.8908	10298.93	Suggested

Furthermore, there are no outliers, influential points or high leverage points indicated by model diagnostics. The fitted model describing this relationship can be written as in (5-18a) and (5-18b) for two different type of membranes. Figure 5.7 shows the interaction effect of DP and Membrane Type on the *k* factor using the inverse square root transformation along with the original scale.

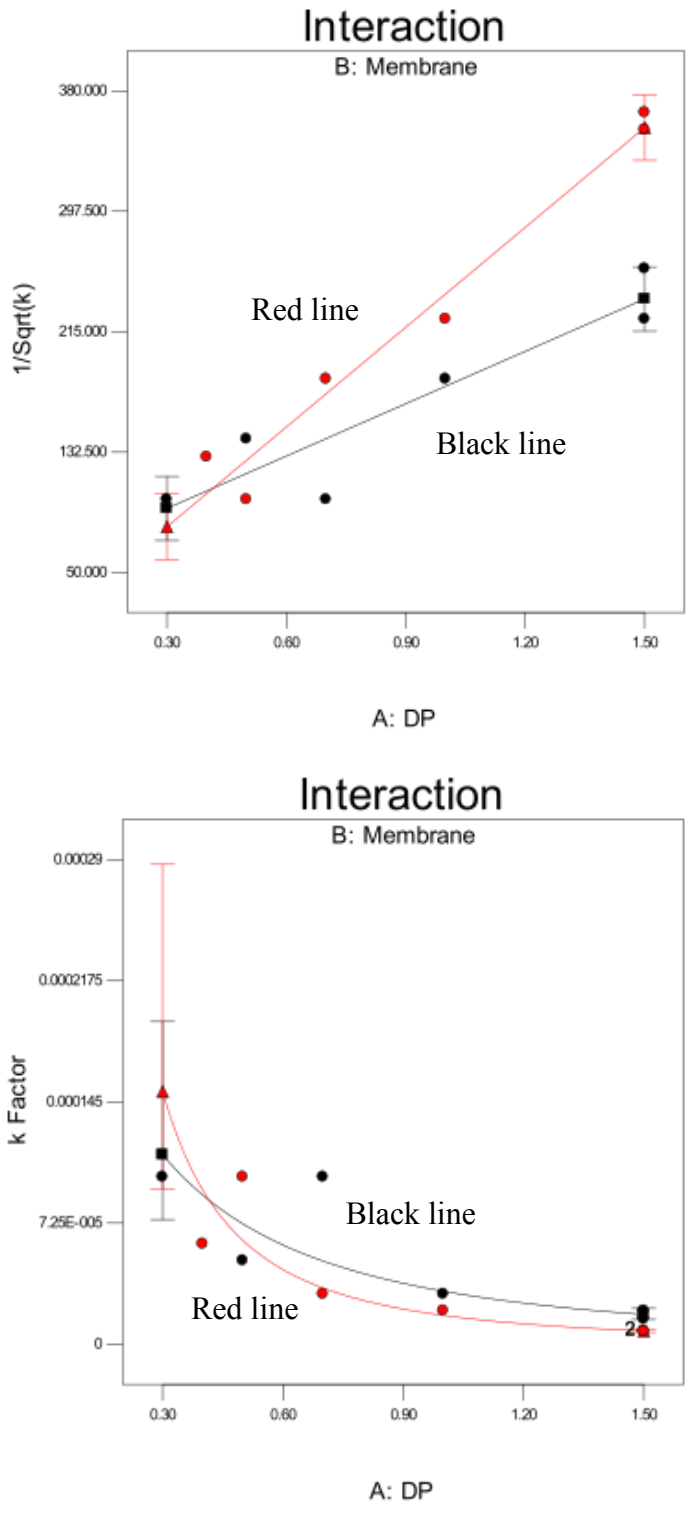

Figure 5.7 Interaction between DP and membrane type on the inverse square root (top) and original scales (bottom). (Black line = 0.20 μm; Red line = 0.01 μm)

It is evident from the error bounds in Figure 5.7 that there is more variation in predicting the *k* factor for low values of differential pressure. Also, the 0.20 μm membrane will have slightly better performance for high values of DP, but at low DP values, the 0.01 μm membrane may actually have a higher mass transfer coefficient. Thus there are two models for predicting the *k* value as a function of DP for each type of membranes (5-18a and 5-18b).

MF membrane (0.20μm): $k = (58.05409 + 119.54122\ DP)^{-2}$ (5-18a)

UF membrane (0.01μm): $k = (12.97153 + 227.88446\ DP)^{-2}$ (5-18b)

5.5.3 Modified Film Theory Model

By coupling (5-18a & 5-18b) with the Film Theory model, empirical models for these two types of membranes are developed as shown in (5-19a & 5-19b). With (5-19a& 5-19b), the gel layer concentration, C_g, can be estimated when flux, DP, and bulk concentration are known. Notably, unlike the *k* value, these three variables can be easily measured from the experiment. These models in (5-19a& 5-19b) are validated with experimental values in the following section.

For MF (0.20 μm): $J_{pred} = (58.05409 + 119.54122DP)^{-2} \ln(\frac{C_g}{C_b})$ (5-19a)

For UF (0.01 μm): $J_{pred} = (12.97153 + 227.88446DP)^{-2} \ln(\frac{C_g}{C_b})$ (5-19b)

5.6 Model Validation

Rearranging (5-19a& 5-19b), gel layer concentration, C_g, can be predicted by the following model:

$$\text{MF membrane: } C_g = C_b \exp[J(58.05409 + 119.54122\,DP)^2] \quad \text{(5-20a)}$$

$$\text{UF membrane: } C_g = C_b \exp[J(112.97153 + 227.88446\,DP)^2] \quad \text{(5-20b)}$$

Using (5-20a & 5-20b), C_g values can be estimated if the DPs are known, with the flux and feed concentration (C_b) remaining constant. Figure 5.8 and 5.9 show the simulated and the experimental C_g values plotted against DP for 0.20 µm and 0.01 µm membranes respectively. The flux (J) and C_b used are 0.00005 m/s and 0.04 mg/m^3 respectively. Clearly, from these graphs, C_g will be lower when DP decreases. The simulated data are close to the experimental results. Gel layer concentration for 0.2 µm membrane is very much lower than 0.01 µm membrane because its pore size is bigger and most of the solute passed through the membrane into the filtrate whereas, the gel layer built up at the membrane wall for 0.01 µm membrane (Figure 5.9). To find the optimum condition for controlling the fouling, an optimization of DP for this operation is performed using the new model (5.20a & 5-20b).

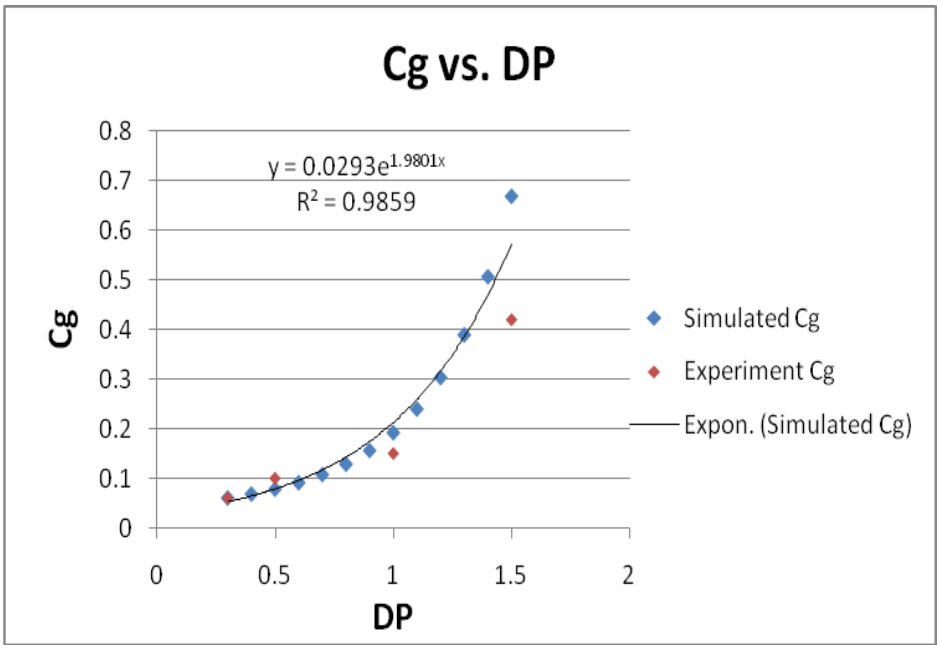

Figure 5.8 Graph of C_g in mg/L is plotted against DP for MF membrane (0.2µm membrane)

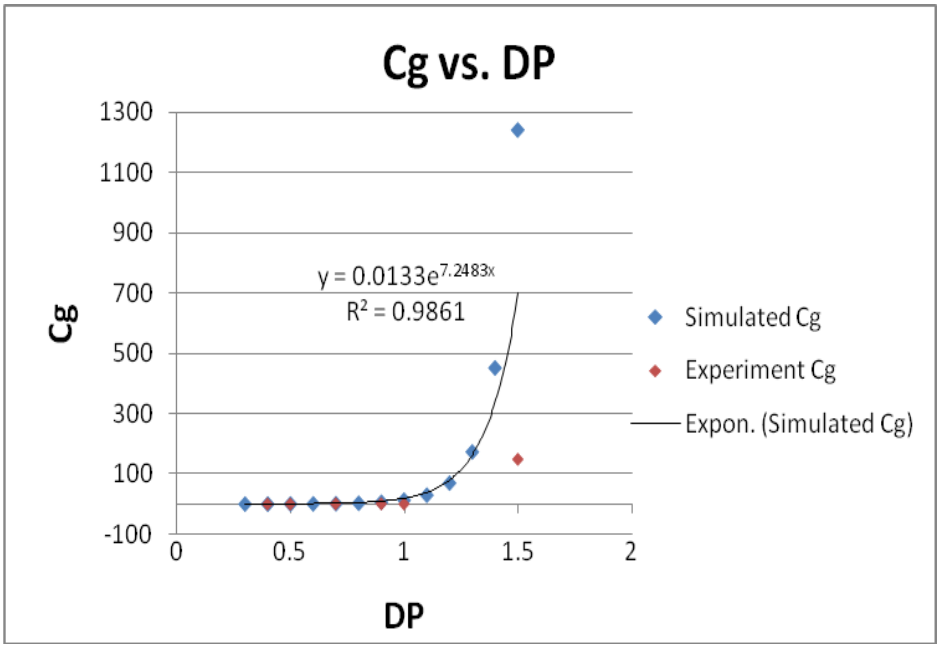

Figure 5.9 Graph of C_g in mg/L is plotted against DP for UF membrane (0.01µm membrane)

5.7 Fouling Minimization

To minimize fouling, the concentration of the gel layer, C_g, should be low. Therefore the objective function is formulated as follows:

$$\text{Minimize} \quad C_g$$

$$\text{DP}$$

$$\text{Subject to} \begin{cases} \text{model (4-20a) or (4-20b)} \\ 0.3 \leq \text{DP} \leq 1.5 \end{cases}$$

Due to the membrane pump constraint, for TMP at 2.75 bar, the lowest operable DP is at 0.3 bars. Therefore, from Figure 5.8 and 5.9, the optimum DP that minimizes fouling is at 0.3 bars for both membranes.

At optimum TMP which is 2.75 bars, low DP has the likelihood of causing turbulence flow inside the membrane cartridge that causes disturbance at the boundary layer of the membrane which reduced the concentration polarization. This fluid flow analysis will be studied in Chapter 6 using CFD technique.

5.8. Conclusion

In this chapter, a modified film theory model has been developed to predict MTC and the concentration of gel layer. The model was developed by combining the film theory model with an empirical statistical model that correlate the MTC with DP. As a result, the models (5-20a & 5-20b) could be used to control fouling by adjusting DP.

Using the developed model, a low cross-flow pressure (DP) was determined to get the maximum k value and also minimum C_g value. Although at low differential pressure there is more variation in the estimates of the k values. The empirical models also showed the interaction between membrane type and DP. This interaction in Figure 5.7 showed that the 0.20 μm membrane had slightly better performance for high values of DP, but at low DP values, the 0.01 μm membrane might actually have a higher mass transfer coefficient. Thus the effect of the membrane type depends on the level of DP. This dependency is comprehended in the two sets of mass transfer coefficient models developed by correlating the DP with k values.

A model validation was done for estimating the C_g values with the results showing that the experimental data are very close to the simulated ones. Finally, the optimum DP was found to be at 0.3 bars which is at the lowest DP operable for this instrument.

Chapter 6: *Fluid Flow Analysis for Membrane Filtration*

6.1 Introduction

Modelling work in Chapter 5 shows that the gel layer concentration can be minimized by manipulating the differential pressure in filtration process. Low DP is found to be desirable to prevent fouling of the membrane. However, the understanding of the effect of DP on the fluid flow pattern inside the membrane cartridge is unknown. This flow visualization is important in order to get qualitative and quantitative information from the flow such as the dynamic behavior, velocity profile, concentration distribution etc. which occurs during pressure change. By knowing this information, more detailed experiment can be designed for the improvement of the efficiency of oil separation. A hypothesis has been formulated that low DP produces turbulent flow inside the membrane cartridge which resulted in the minimum of gel layer concentration. Therefore to prove the hypothesis, in this chapter, Computational Fluid Dynamic (CFD) is used to model and simulate the fluid flow pattern inside the membrane to see the velocity and pressure distribution in the membrane cassette. Study was done by using distilled water in the simulation to visualize the fluid flow. Thereafter the simulated results were verified by experiments. From the CFD simulation, the turbulence intensity can be estimated for various differential pressures occurring at the turbulence outlet.

Most of the works done on modeling are on the flow across the membrane and flux decline during filtration. Fouling models are based mainly on pore-blocking law, concentration polarization [117] and cake formation [118]. Particle deposition on the membrane had also been studied very extensively, such as in the modeling work of Elimelech and Song [119]. Many of the authors who were investigating the hydrodynamics of fluid relating to the membrane filtration process used models from the combination of Navier-Stokes equations and Darcy‘s law [120, 121]. Different approaches were performed to simulate the combined models such as finite element method [121], finite difference scheme [120], and finite volume method [122]. Finite volume method and SIMPLE algorithm are commonly used in problems dealing with fluid flow. For this simulation, the fluid flow pattern inside a concealed membrane is studied. The membrane cartridge as shown in Figure 6.2 is rectangular in shape and made up of several flat sheet membranes with small fluid flow channels in between. Fluid flows anti-gravitationally from bottom to top. Commercial finite volume package FLUENT solver is used to visualize the fluid flow pattern inside the membrane at steady state.

6.2 Numerical Model Formulation

Models are defined within the region of the membrane cassette as shown in Figure 6.1. The first sub-model describes the fluid transport of flow parallel to the membrane while the second one describes the filtration across the membrane. For the first part of the modeling work, the flows of fluid through the slit between two membrane sheets are modeled as seen in Figure 6.1. The models done by Damak and coworkers [120] are modified to fit the membrane system that are used in this experiment. The flow is anti-gravitational; the in-let is from the bottom and out through the top of the rectangular slit of two membranes. Most people doing modeling for membrane filtration assumed that the fluid was laminar flow inside the membrane [123, 124]. According to Belfort and colleague [125] turbulent flow started at Re 4000 for porous tubes instead of Re 2100 in non-porous tubes. The dimensions in the membrane cassette are complicated and therefore it is difficult for Re calculations. However, due to the high pressure exerted at the feed inlet (> 3.25 bar) and retentate (> 1.75 bar)

outlet in this experiment settings, the flow would be disturbed and eddies were assumed to be formed. This would in turn induce higher turbulence intensities. The calculation of turbulence intensity [126] is by using the equation (6-1)

$$I = \frac{u'}{u_{avg}} = 0.16(\mathrm{Re}_{DH})^{-\frac{1}{8}} \tag{6-1}$$

where u‘ is the root mean square of the velocity fluctuation, and u_{avg} is the mean flow velocity.

Flow in the porous slits is therefore expected to be in turbulent state.

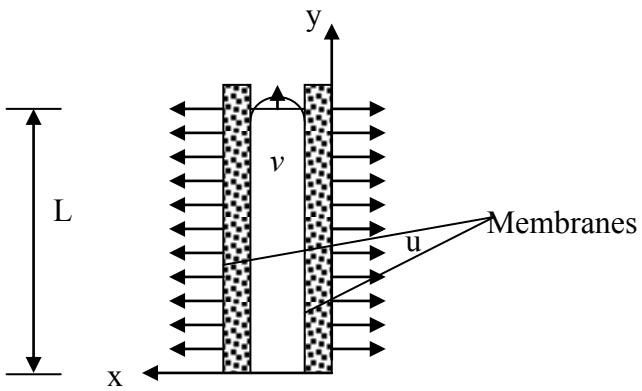

Figure 6.1 Modeling region in between two membrane sheets
(Dimension is not proportional to the actual setup)

6.2.1 Flow Regime in the Slit

According to continuity equation and Navier-Stokes equation,

$$\frac{\partial u}{\partial x} + \frac{\partial v}{\partial y} = 0 \tag{6-2}$$

The u-component is

$$\rho(u\frac{\partial u}{\partial x} + v\frac{\partial u}{\partial y}) = \mu(\frac{\partial^2 u}{\partial x^2} + \frac{\partial^2 u}{\partial y^2}) - \frac{\partial P}{\partial x} + \rho g_x \tag{6-3}$$

The v-component is

$$\rho(u\frac{\partial v}{\partial x}+v\frac{\partial v}{\partial y})=\mu(\frac{\partial^2 v}{\partial x^2}+\frac{\partial^2 v}{\partial y^2})-\frac{\partial P}{\partial y}+\rho g_y \tag{6-4}$$

where u is the velocity at x direction; v is the velocity at y direction; P is the TMP; ρ is the fluid density; g is the gravity and μ is the fluid viscosity.

6.2.2 Flow Regime at the Porous Wall

The momentum equation across porous zone, i.e. Darcy‘s law, is written as:

$$u=-\frac{\kappa}{\mu}\frac{\partial P}{\partial x} \tag{6-5}$$

where u is the permeate flux, v is the retentate velocity, μ is the dynamic viscosity, κ is the permeability, P is the pressure drop and x is the length of the channel where the pressure drop is taking place.

Porous wall in the membrane is assumed to be homogenous and isotropic and the flow through porous wall can be treated as the boundary condition of the free flow through a tube.

6.2.3 Boundary Conditions

At the inlet, the inlet pressure is

$$p_o = p_s + \frac{1}{2}\rho|v|^2 \tag{6-6}$$

where p_o is the total pressure gauge at the inlet, p_s is the static pressure and v is the initial velocity which is zero.

At the exit, fully developed profile is assumed.

$$y = L, 0 < x < X: \quad \frac{\partial v}{\partial y} = 0; u = 0 \tag{6-7}$$

At the axis of symmetry there are no momentum fluxes crossing the boundary.

$$x = 0, 0 \le y \le L: \quad \frac{\partial v}{\partial x} = 0, u = 0 \tag{6-8}$$

At the porous wall, the wall suction velocity is given by Darcy's law and no slip velocity is applied as follows,

$$x = X, 0 \le y \le L: \quad u = \frac{\kappa}{\mu}\frac{P - P_e}{e}, v = 0 \tag{6-9}$$

$$u = R(P - P_e), \; R = \frac{\kappa}{\mu}.\frac{1}{e} \tag{6-10}$$

where κ is the permeability of the membrane, μ is the viscosity of the fluid and e is the thickness of the porous wall. These three parameters can be determined empirically and they are summed in the term R, resistance. P is the TMP and P_e is the external pressure which includes osmotic pressure.

The numerical model assumed that the filtration is at steady state, with a turbulent flow type. There are six classical turbulence models in FLUENT and these are mixing length, standard k-ε, RNG k-ε, realizable k-ε, Reynolds's stress and algebraic stress models [126].

Standard k-ε model was selected because the membrane geometry is not complex and the flow is assumed to be fully turbulent with negligible effects of molecular viscosity [127]. The standard k-ε model is a semi-empirical model based on model transport equations for the turbulence kinetic energy (k) and its dissipation rate (ε). The model transport equation for k is derived from the exact equation, while the

model transport equation for ε was obtained using physical reasoning and bears little resemblance to its mathematically exact counterpart. The transport equations for k and ε are as follows:

As
$$\mu_t = \rho C_\mu \frac{k^2}{\varepsilon}; \tag{6-11}$$

$$\frac{\partial(\rho k)}{\partial t} + \frac{\partial}{\partial x_i}(\rho k u_i) = \frac{\partial}{\partial x_j}\left[\left(\mu + \frac{\mu_t}{\sigma_k}\right)\frac{\partial k}{\partial x_j}\right] - \rho\overline{u_i u_j}\frac{\partial u_j}{\partial x_i} - \rho\varepsilon \tag{6-12}$$

And

$$\frac{\partial(\rho\varepsilon)}{\partial t} + \frac{\partial}{\partial x_i}(\rho\varepsilon u_i) = \frac{\partial}{\partial x_j}\left[\left(\mu + \frac{\mu_t}{\sigma_\varepsilon}\right)\frac{\partial\varepsilon}{\partial x_j}\right] + C_{1\varepsilon}\frac{\varepsilon}{k}(-\rho\overline{u_i u_j}\frac{\partial u_j}{\partial x_i}) - C_{2\varepsilon}\rho\frac{\varepsilon^2}{k} \tag{6-13}$$

where $C_1\varepsilon$ and $C_2\varepsilon$ are constants, σ_k and $\sigma\varepsilon$ are the turbulent Prandtl numbers for k and ε, respectively. When differential pressure (DP) increases from 0.5 bar to 2.0 bar, at an interval of 0.5 bar; the turbulent intensity decreases as described in Table 6.2.

As mentioned in previous section, we use the Darcy‘s equation in modeling the filtration of distilled water across the membrane. In FLUENT, Darcy‘s equation is under the porous jump boundary condition with the numeric model described as follows:

$$\Delta p = -\left(\frac{\mu}{\alpha} v\right)\Delta m \tag{6-14}$$

where Δp is the Trans-membrane Pressure (TMP), μ is the viscosity of the fluid, α is the permeability of the medium, v is the filtration flux, and m is the thickness of the membrane. TMP and DP equations can be found in (5-15) and (5-16).

In the FLUENT geometry, a representation of 2 slices of membrane separating 3 rectangular compartments are used to model the fluid flow pattern inside the membrane cassette as illustrated in Figure 6.1. This geometry is developed by using GAMBIT. In order to capture all flow characteristics, a two dimensional tetrahedral grid was built with a total of 30,526 mesh numbers.

6.3 Experimental Set-up

For experimental validation, Sartocon Slice Cassette containing Polyethersulfone (PESU) membrane with 50 kDa molecular-weight-cut-off (MWCO) is used. The dimensions of the cassettes are given in the Figure 6.2. Each membrane cassette contains 20 slices of membrane sheets. The distance between each membrane sheet is approximately 1mm.

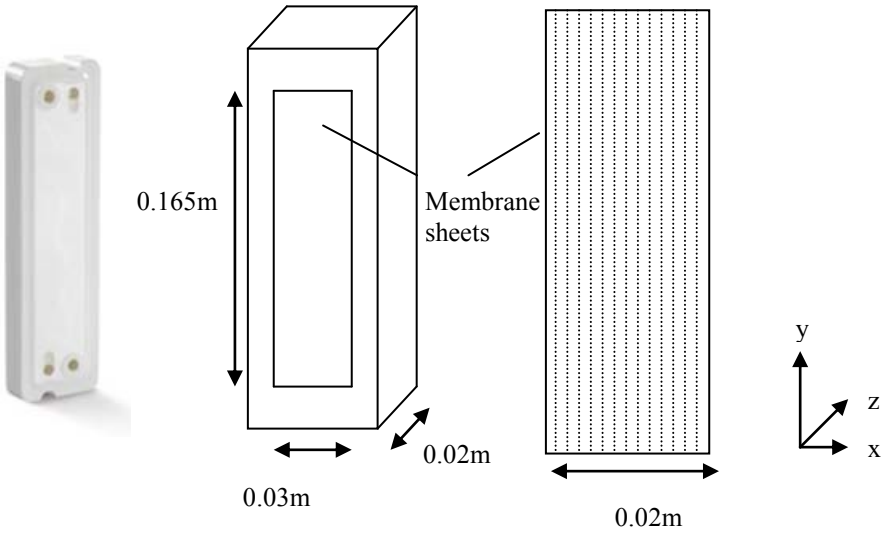

Figure 6.2 Picture of the membrane cartridge (left); Dimension of membrane cartridge (centre); Side view illustration of 20 membrane sheets (right)

The empirical data of the permeability of the membrane, κ is calculated based on the formula,

$$\kappa = u/(P.\mu) \tag{6-15}$$

where u is the permeate flux, P is the trans-membrane pressure (TMP) and μ is the viscosity of the fluid which in this case is 0.001 $kgm^{-1}s^{-1}$. All these information are included in the simulation. The simulated results from FLUENT are then validated with experimental data.

6.3.1 Operating Pressures for Membrane Filtration

Experiments are performed at constant TMP of 2.75 bars and DP changes from 0.5 bars to 2.0 bars. The operating pressures used in the experimental set-up are as shown in Table 6.1 with P_f is feed pressure, P_r is retentate pressure and P_p is permeate pressure. The flow rates for permeate, rententate and feed for distilled water are measured for each differential pressure.

Table 6.1 Operating pressures for the experiments

Pressure term (bar)				
P_f	**P_r**	**P_p**	**DP**	**TMP**
3.80	3.30	0.80	0.50	2.75
3.25	2.25	0.00	1.00	2.75
3.50	2.00	0.00	1.50	2.75
3.75	1.75	0.00	2.00	2.75

6.4 Results and Discussions

Darcy‘s equation and Navier-Stokes transport equation associated with the boundary conditions given in Section 6.2.3 were solved by using finite volume method from a commercial software FLUENT.

Table 6.2 Experimental data for mass flow rates for DP 0.5 bar to 2.0 bar at constant TMP

DP (bar)	TMP (bar)	Feed mass flowrate (kg/s)	Permeate mass flowrate (kg/s)	Retentate mass flowrate (kg/s)
0.5	2.75	0.04952	0.04584	0.00368
1.0	2.75	0.06910	0.04450	0.02510
1.5	2.75	0.08504	0.04233	0.04271
2.0	2.75	0.09375	0.04100	0.05280

Table 6.2 shows how the experimental feed, permeate and retentate mass flow rate (kg/s) change under different operating differential pressure and Trans-membrane Pressure (TMP). Assuming turbulence condition occurs in the membrane cartridge, the turbulence intensity conditions are adjusted to fit the experimental data.

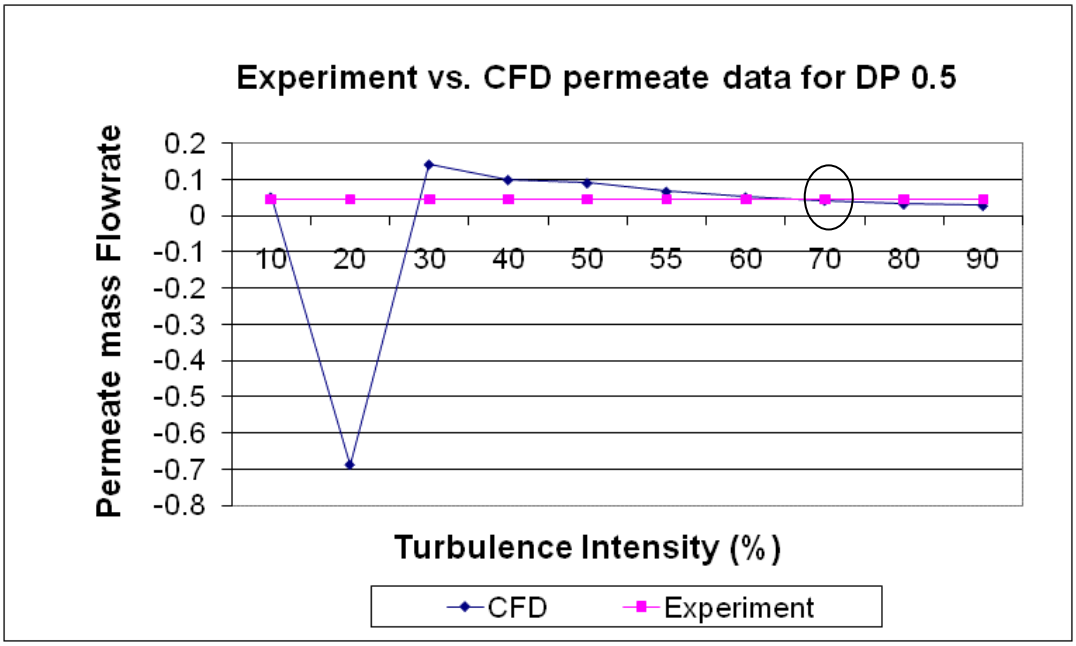

Figure 6.3 CFD vs. experiment at different turbulence intensity for DP 0.5 bar

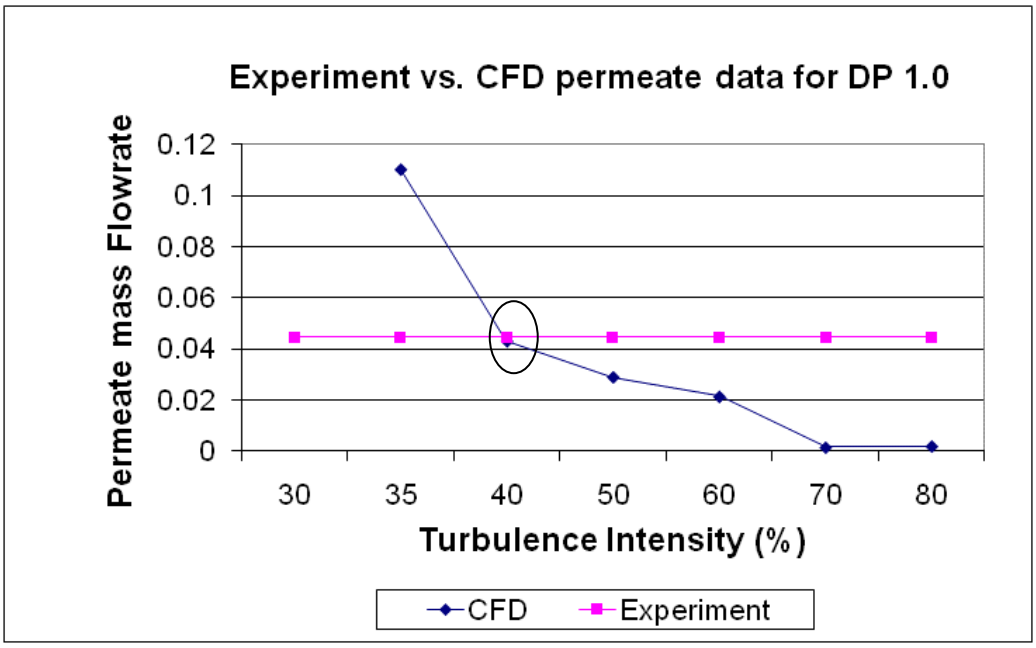

Figure 6.4 CFD vs. experiment at different turbulence intensity for DP 1.0 bar

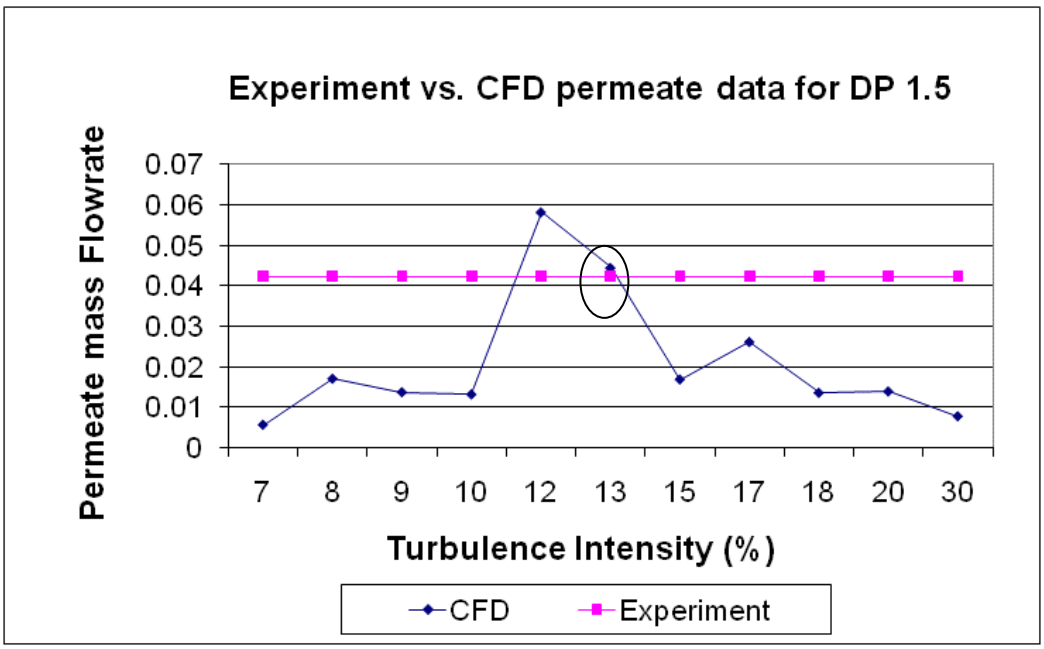

Figure 6.5 CFD vs. experiment at different turbulence intensity for DP 1.5 bar

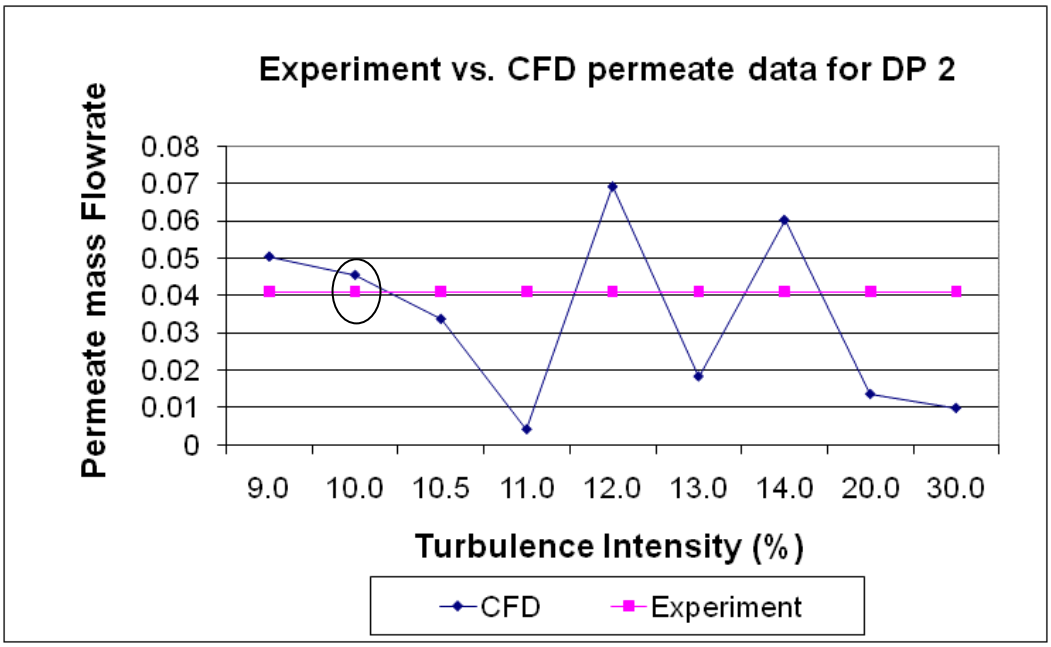

Figure 6.6 CFD vs. experiment at different turbulence intensity for DP 2.0 bar

Figure 6.3 to 6.6 showed the effect of the changes in turbulence intensity towards the permeate fluxes. However the most suitable turbulence intensity conditions to have the CFD data verified with experimental data are identified and listed in Table 6.3.

Table 6.3 shows the CFD and experimental results for feed, retentate and permeate mass flow rates. To avoid confusions, Figure 6.7 was plotted for permeate only for both CFD data and experimental data. From the CFD results all the DPs fits well with the experimental results and they are within a difference of 10% range. The CFD result at DP 1.0 bar is much lower than the experimental data. This may be attributed to the turbulent flow assumption made. Nevertheless, the simulation predicts the same trend as the experimental data.

Table 6.3 Experimental data and CFD data for mass flow rates (kg/s) of feed, retentate and permeate for various DPs

		CFD			Experiment		
DP	Condition*	Feed	Permeate	Retentate	Feed	Permeate	Retentate
0.5	70	0.04952	0.04604	0.00348	0.04952	0.04584	0.00368
1.0	40	0.06910	0.04303	0.02528	0.06910	0.04450	0.02510
1.5	13	0.08504	0.04207	0.04348	0.08504	0.04233	0.04271
2.0	10	0.09375	0.04150	0.06009	0.09375	0.04100	0.05280

*Condition – turbulence intensity (%)

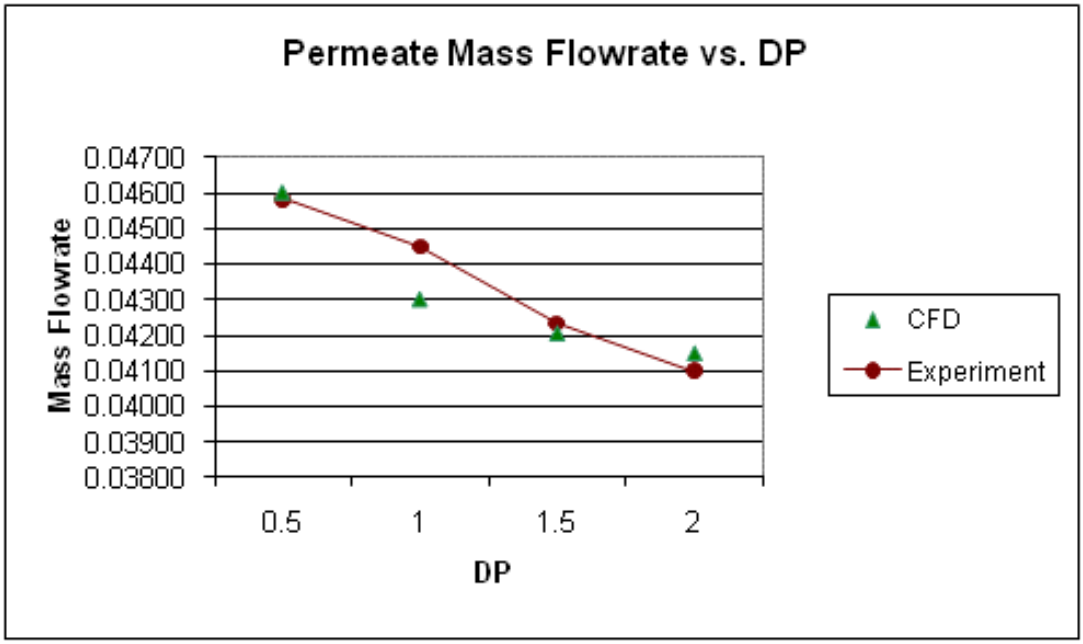

Figure 6.7 Comparison of permeate flux from experiment and CFD

Figure 6.8 shows the velocity plot at the outlet for DP 0.5 bar at TMP 2.75 bar. The velocity plot from -0.5 to 0.5mm are the retentate fluxes (red plot) and the rest are permeate fluxes (green and black plot). This diagram shows that permeate fluxes are higher than the retentate fluxes at DP 0.5 bar. As DP increases from 0.5 to 2.0 bar (Figure 6.8 to 6.11), retentate fluxes increase whereas the permeate fluxes decreases. This trend is in agreement with the experiment which can be seen from Table 6.3. As DP increases, fluid flow in the retentate slit becomes easier without creating vortexes.

From Table 6.3, it can be seen that as DP increases, the turbulence intensity decreases. This indicates that lower DP has higher turbulence intensity than higher DP. This is due to the high operating pressures (Table 6.1) both at the feed, P_f and at the retentate, P_r for DP 0.5 bar. The high inlet velocity is suddenly disrupted by the high pressure exerted at the retentate outlet, causing a disturbance in the flow velocity and creating eddies as has been explained in Section 7.2.

Further illustration from the simulation can be seen from Figure 6.12 where turbulence occurs at the retentate outlet only. Figure 6.12 shows that the turbulence kinetic energy is high at the retentate outlet for all the DPs. The turbulence intensity decreases from lower DP to higher DP as can be seen from Table 6.3, because pressure exerted at the retentate outlet decreases as DP increases. This turbulence effect is desired for helping in the reduction of oil deposition on the membrane by shearing effect during filtration.

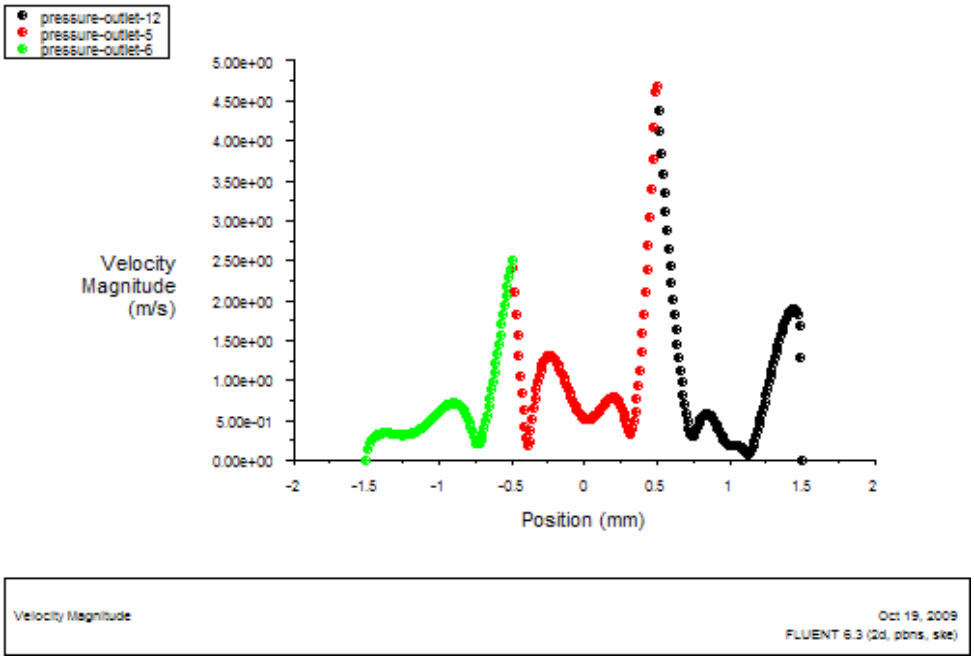

Figure 6.8 Velocity plot at the outlet for condition DP=0.5, TMP=2.75 at 70% turbulence intensity

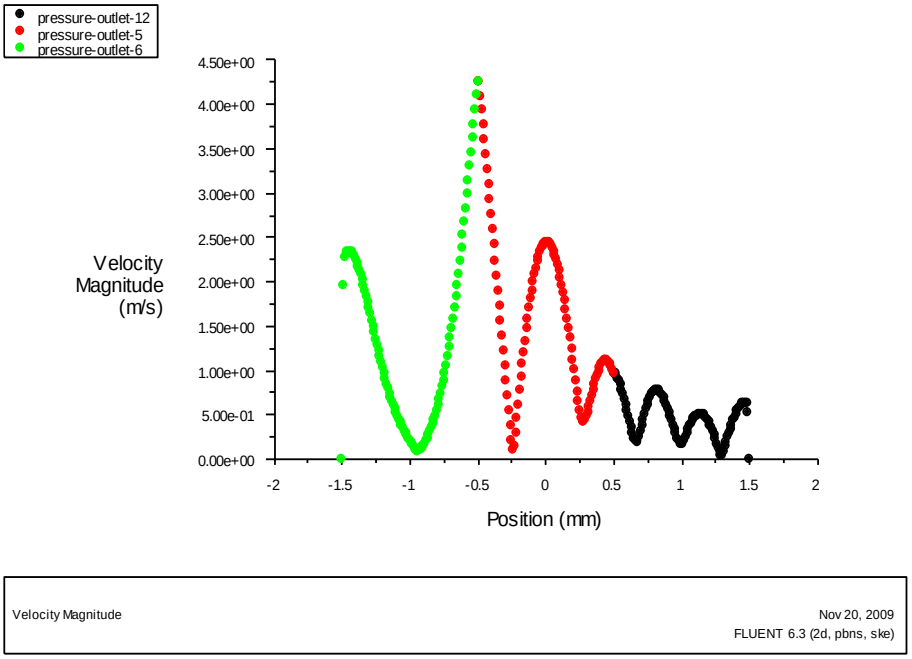

Figure 6.9 Velocity plot at the outlet for condition DP=1.0, TMP=2.75 at 40% turbulence intensity

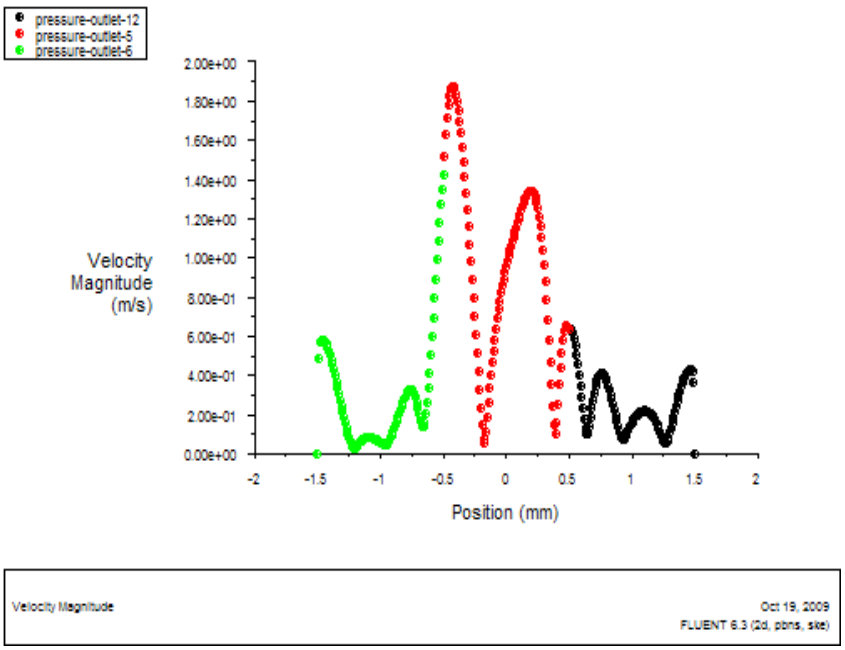

Figure 6.10 Velocity plot at the outlet for condition DP=1.5, TMP=2.75 at 13% turbulence intensity

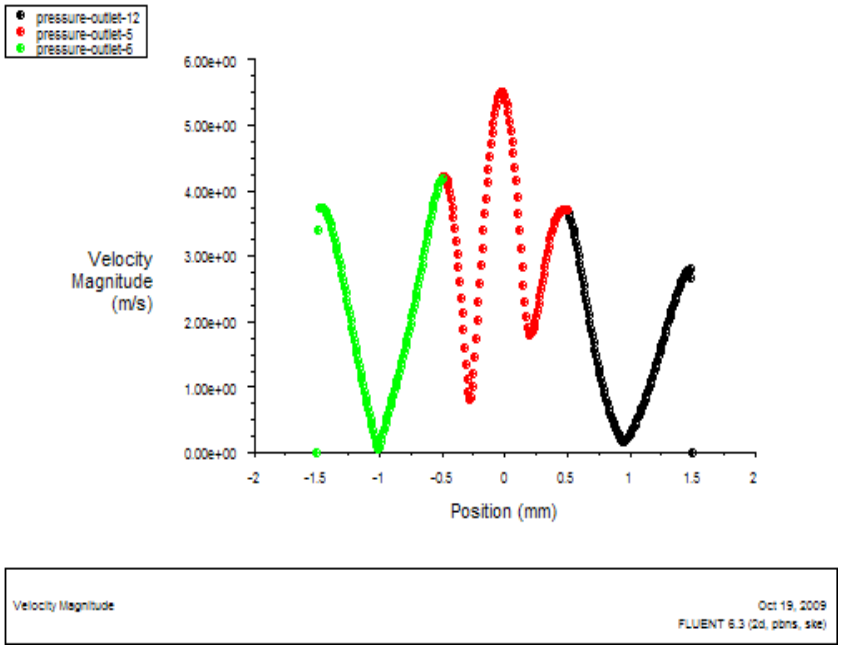

Figure 6.11 Velocity plot at the outlet for condition DP=2.0, TMP=2.75 at 10% turbulence intensity

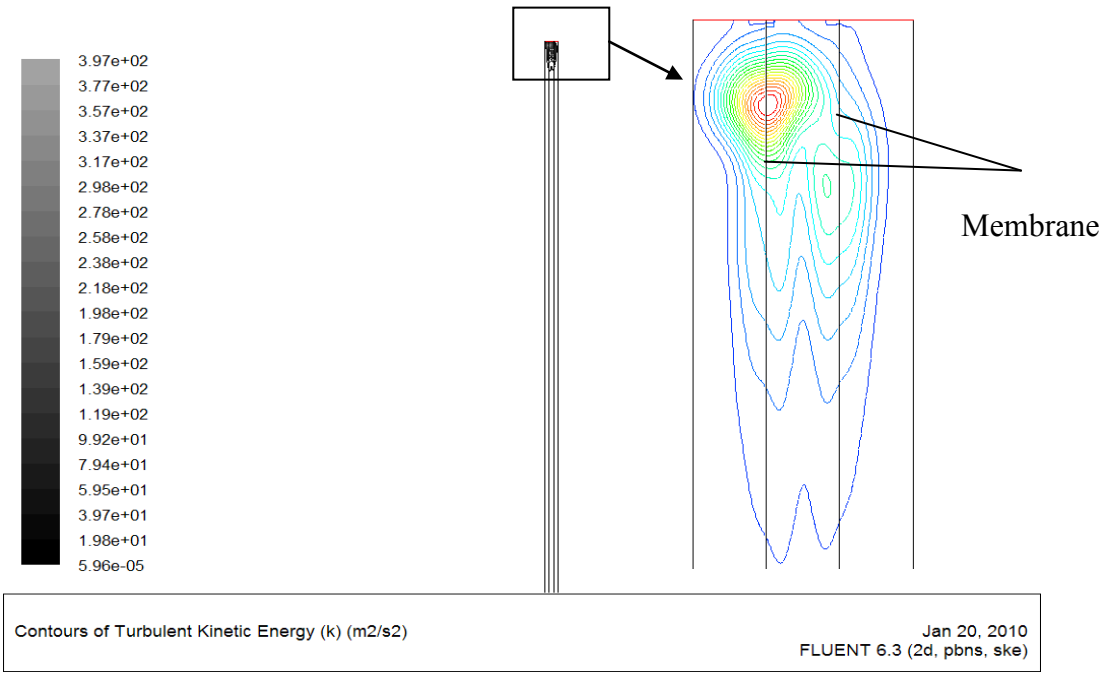

Figure 6.12 Contour of turbulent kinetic energy at DP 0.5 TMP 2.75 with turbulence intensity of 70%

In this study, by understanding the fluid flow pattern for 50 kDa MWCO membrane, other membranes with bigger pore size could be deduced. The trend of the fluid flow as a function of DP would be the same with different types of membrane i.e. lower DP will have higher turbulence intensity than higher DP. Though with bigger pore size, the turbulence created at low DP would be lesser than that created by smaller pore size. For the actual produced water, deposition of oil would appear on the membrane surface. However, since this study is to understand the fluid flow pattern in the membrane slit, simulation of DI water would suffice for the objective.

6.5 Conclusions

In this work, the computational fluid dynamic (CFD) modeling has been used to simulate the turbulence intensity of the fluid flow as a function of DP. From the simulation it can be seen that the differential pressure and velocity is inter-related. Lower DP produces more vortexes nearer to the retentate slit outlet thus contribute to higher turbulence intensities. This turbulence reduces the gel layer concentration at the membrane wall which was discussed in previous chapter. Therefore to enhance the dissolved oil separation and obtain a higher permeate flux, operating at lower DP is desirable.

Chapter 7: *Optimization of Dissolved Oil Separation*

7.1 Introduction

Crossflow pressure (DP) is an essential parameter to minimize fouling as well as to enhance the separation of dissolved oil from the produced water. From previous chapters, membrane filtration operating at low DP was found to achieve higher turbulence intensities which in turn help in the reduction of oil deposition on the membrane surface. As indicated in Chapter 4, low DP is required for higher dissolved oil concentration in permeate stream; whereas high DP is required for higher dispersed oil concentration in retentate stream. With this contradicting requirement, the best optimum DP needs to be determined to attain maximum of both dissolved and dispersed oil concentration in permeate and retentate stream respectively.

For this purpose, in this chapter, different DPs were studied for different material types and pore sizes of membranes. Optimum trans-membrane pressure (TMP) is operated throughout the experiment to achieve highest permeate flux. This multi-component optimization to maximize the oil separations are performed by RSM D-optimal design. Since this design is a multivariate technique, it offers some advantages over experimental one-factor–a-time (OFAT) approach by taking into account the interaction among the dominant factors [128]. Although there are two goals to achieve, the emphasis is given to "dispersed oil" as it is the component under oil-in-water regulation.

RSM D-optimal is a computer generated optimal design. It is designed in such a way that the factors are not set higher or lower than the upper and lower constraints. The standard RSM designs such as Central Composite Design (CCD) and Box-Behnken (BBD) do not suit the practicality of this experiment. This is because when choosing the axial points it will exceed the upper and lower limits which are the experimental constraints such as pressure settings. D-optimal design conforms to multifactor operating constraint for the actual process [129]. It is also time and cost-saving as it requires less number of runs as compared to CCD and BBD. In many researches, statistical analysis has proved to be an effective tool to investigate relationship between variables and formulation work. Regretfully, this D-optimal design has not been widely used in membrane sciences area except CCD and BBD [130, 131]. Therefore in this work, D-optimal design is used to optimize the separation of dissolved oil using physical parameters.

7.2 Materials and Methods

The membrane filtration set up has been described in Chapter 3.3 and shown in Figure 4.3. For this experiment, the set-up emphasises on the selection of operating pressure DP, TMP, membrane types and pore sizes for the separation of dissolved and dispersed oil.

7.2.1 Produced Water

The simulated produced water containing 100ppm crude oil was used in the experiments as the feed. The preparation and the choice of using have been discussed in Chapter 3. The methods of extractions and GCMS analysis before and after filtration are discussed in detail in section 3.5.

7.2.2 Membrane Selection

A preliminary study in Chapter 3 shows that the membrane with 0.01 μm pore size membrane is not suitable in the separation of dissolved oil. Therefore, 0.02 μm membrane and 0.2 μm membranes are selected for use.

7.2.3 Membrane Filtration Set-up

Experiment was performed by using different membrane filtrations at optimum TMP with the operating pressures illustrated in Table 7.1 where 100kDa-P is the 0.02 μm Polyethersulfone membrane, 100kDa-H is the 0.02 μm Hydrosart® membrane.

Table 7.1 Operating pressures for 100kDa-P, 100kDa-H, and 0.2μm Hydrosart® membrane

Pressure term (bar)				
P_f	P_r	P_p	DP	TMP
3.80	3.30	0.80	0.50	2.75
3.25	2.25	0.00	1.00	2.75
3.50	2.00	0.00	1.50	2.75
3.75	1.75	0.00	2.00	2.75

7.3 Optimization

7.3.1 2^k Factorial and RSM D-Optimal Design

In the first stage of experimental design, 2^k factorial design is performed to check for curvature term. If a significant curvature term is found in this first-order modeling, it indicates that quadratic or higher-level process model for RSM is required to be performed. Otherwise, the data will be analyzed by using linear process model [132]. There are a total of 13 runs for this factorial design. Table 7.2 shows the 2^k factorial designed for first-order modelling.

Table 7.2 2^k factorial design for modelling dissolved and dispersed oil response

Run	DP (bar)	Size (µm)	Type
1	1.0	0.2	Hydrosart®
2	0.5	0.02	Hydrosart®
3	1.0	0.02	PESU
4	2.0	0.2	Hydrosart®
5	1.3	0.02	Hydrosart®
6	1.5	0.2	Hydrosart®
7	1.5	0.02	Hydrosart®
8	0.5	0.02	PESU
9	1.0	0.02	Hydrosart®
10	2.0	0.02	PESU
11	0.5	0.2	Hydrosart®
12	2.0	0.02	Hydrosart®
13	1.5	0.02	PESU

After performing the first order-modelling, the data was augmented to RSM D-optimal design instead of conventional designs as it involved two responses and multi-level numerical factor. Conventional designs such as CCD and Box-Behnken require more number of runs which is a constraint in terms of cost and time for this experiment. In the analysis, the running sequences were randomized and analyzed with Design Expert 7.1.3. The Model Sum of Squares and the Model Summary Statistics under the Fit Summary were analyzed to select the appropriate model. Transformation of data will be done if necessary with Box-Cox plot.

Optimization for the process was then performed by setting the appropriate objective functions and constraints. The objective function is to maximize the dispersed oil in retentate and maximize dissolved oil in permeate. They are solved by using constrained optimization program supplied in the RSM optimization toolbox.

7.4 Results and Discussions

7.4.1 GC-MS Results for Different DPs at TMP 2.75

Figure 7.1 and 7.2 show the GC-MS spectra for the oils obtained from retentate and permeate respectively for 0.2 μm membrane filtration. Notice that the dispersed oil peaks, which can be seen in Figure 7.1 as cyclohexasiloxane, dodecane, hexadecane, heptadecane and octadecane, disappeared from the permeate spectrum in Figure 7.2 indicating that the dispersed oil size is in fact bigger than the pore size of 0.2 μm. Therefore, the dispersed oil would either be in the retentate or deposited on the membrane surface.

Table 7.3 shows that for all types of membranes, the dissolved oil content in the permeate is the highest when filtration is operating at DP 0.5 bar. Among these membranes in Table 7.3, 0.2 μm membrane gives the highest percentage of 26.2% dissolved oil in permeate. However, for dissolved oil, some of it is retained by the smaller pore size 100 kDa membrane, and therefore the dissolved oil in permeate is less. Nevertheless, by increasing the DP, more dispersed oil will be rid from the membrane surface into the retentate solutions. This indicates that, lower DP is prefer for higher dissolved oil content in permeate whereas higher DP is required for higher dispersed oil in retentate content.

Therefore to achieve this contradictory objective functions where the dissolved oil is maximum in permeate and dispersed oil is maximum in the retentate, the optimum DP is sought. The experimental results in Table 7.3 were analyzed by 2^k factorial design for first-order modeling.

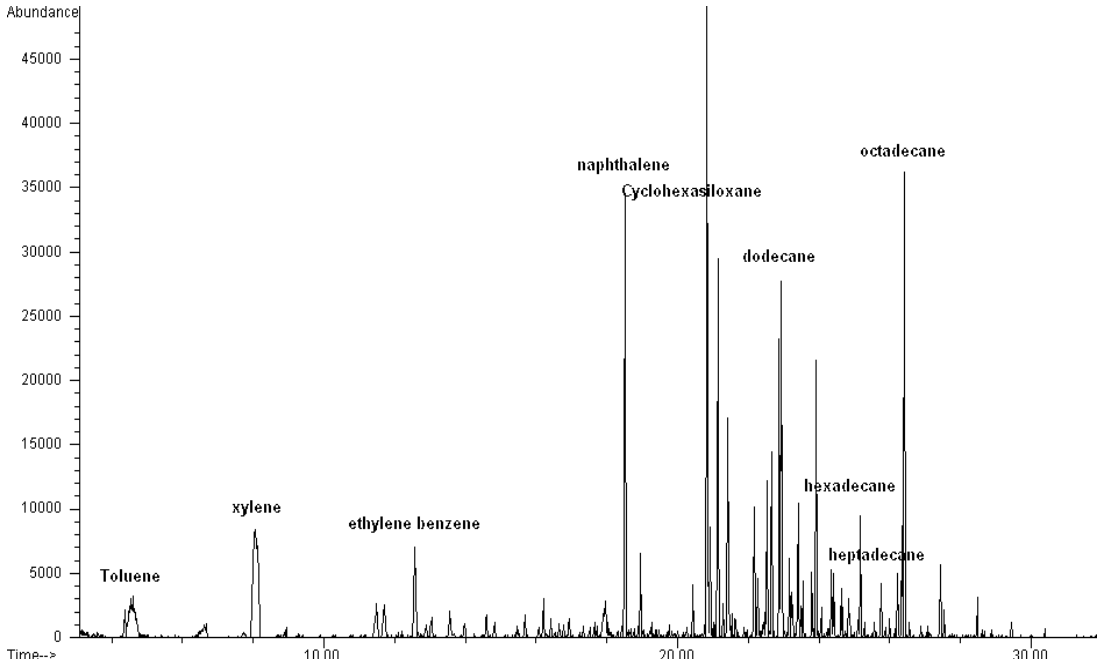

Figure 7.1 Dispersed and dissolved oil spectrum in retentate for 0.2 μm membrane filtration at DP 0.5 bar

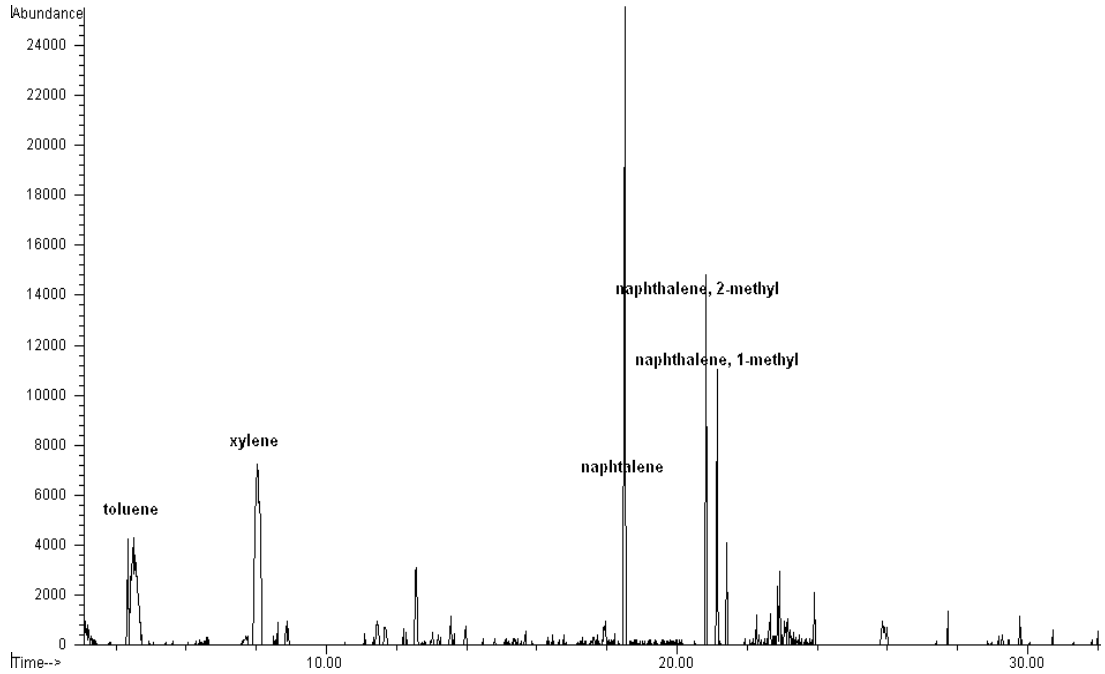

Figure 7.2 Dissolved oil spectrum in permeate for 0.2 μm membrane filtration at DP 0.5 bar

Table 7.3 Results for separation of oil for different membranes at different DPs without replication

DPs	Oil content in %	100kDa-H	100kDa-P	0.2µm-H
DP0.5	Dispersed oil in retentate	18.2	25.8	16.9
	Dissolved oil in permeate	9	1.3	26.2
DP1.0	Dispersed oil in retentate	10.9	7.3	31
	Dissolved oil in permeate	7.5	1	20.7
DP1.5	Dispersed oil in retentate	1.6	4.4	17.3
	Dissolved oil in permeate	4.4	2	15.8
DP2.0	Dispersed oil in retentate	11.4	7.5	44.8
	Dissolved oil in permeate	5.5	3.4	13.7

7.4.2 ANOVA Results from 2^k Factorial Design Analysis

Analysis of variance (ANOVA) performed for both dissolved and dispersed oil responses provided assurance that the models are significant with no curvature. These are shown in Table 7.4 and 7.5 where the p-values are < 0.05 for model term, whereas the p-values are > 0.05 for curvature term. Since there are no curvature terms, the design are therefore augmented to RSM D-optimal using linear process.

Table 7.4 Analysis of Variance (ANOVA) for dissolved oil component

Source	Sum of Squares	df	Mean Square	F Value	p-value	
Model	734.06	5	146.81	275.72	< 0.0001	significant
A-DP	25.62	1	25.62	48.11	0.0023	
B-Size	152.23	1	152.23	285.89	< 0.0001	
C-Type	24.63	1	24.63	46.25	0.0024	
AB	20.77	1	20.77	39.02	0.0033	
AC	8.45	1	8.45	15.87	0.0163	
Curvature	6.46	3	2.15	4.05	0.1052	Not significant
Residual	2.13	4	0.53			
Cor Total	742.65	12				

Table 7.5 Analysis of Variance (ANOVA) for dispersed oil component

Source	Sum of Squares	df	Mean Square	F Value	p-value	
Model	1270.76	4	317.69	8.13	0.0205	significant
A-DP	85.44	1	85.44	2.19	0.1994	
B-Size	1069.42	1	1069.42	27.36	0.0034	
C-Type	6.03	1	6.03	0.15	0.7106	
AB	499.37	1	499.37	12.77	0.0160	
Curvature	344.00	3	114.67	2.93	0.1384	Not significant
Residual	195.46	5	39.09			
Cor Total	1810.22	12				

7.4.3 Optimization using RSM D-optimal Design

After determining that the process can be represented by linear order, RSM D-optimal design is employed to determine the optimum condition for dissolved and dispersed oil separation. There are all together 26 runs for the analysis and their dissolved and dispersed oil results are shown in Table 7.6. Tables 7.7 to 7.10 show the model sum of squares, model summaries statistics and ANOVA respectively for the model derived from experimental data. Table 7.7 and 7.8 both suggested that the linear model is suitable for the process. By analysing the diagnostic plots, box-cox

plot suggested a natural log transformation for both dissolved and dispersed oil components as shown in Figure 7.3 and 7.4.

Table 7.6: Statistical experiment design by D-optimal method with Block 2 as replication

Run	Block	Factor			Response	
		DP	Size	Type	Dissolved oil	Dispersed oil
1	Block 1	1	0.02	Hydrosart®	7.46	10.90
2	Block 1	1.5	0.02	PESU	1.96	4.43
3	Block 1	1.3	0.02	Hydrosart®	7.65	5.19
4	Block 1	2	0.02	PESU	3.44	7.53
5	Block 1	1.5	0.02	Hydrosart®	4.36	1.55
6	Block 1	1	0.02	PESU	0.99	7.34
7	Block 1	2	0.2	Hydrosart®	13.65	44.81
8	Block 1	0.5	0.02	Hydrosart®	9.05	18.21
9	Block 1	0.5	0.02	PESU	1.32	25.79
10	Block 1	1	0.2	Hydrosart®	20.74	31.03
11	Block 1	2	0.02	Hydrosart®	5.53	11.42
12	Block 1	1.5	0.2	Hydrosart®	15.78	17.29
13	Block 1	0.5	0.2	Hydrosart®	26.21	16.94
14	Block 2	1.5	0.02	PESU	4.03	2.21
15	Block 2	2	0.2	Hydrosart®	26.63	33.04
16	Block 2	0.5	0.02	PESU	3.07	15.10
17	Block 2	1.5	0.2	Hydrosart®	35.69	12.93
18	Block 2	2	0.02	PESU	2.80	3.50
19	Block 2	1	0.02	Hydrosart®	10.51	2.58
20	Block 2	0.5	0.2	Hydrosart®	45.24	9.52
21	Block 2	2	0.02	Hydrosart®	5.58	5.17
22	Block 2	0.5	0.02	Hydrosart®	14.88	9.82
23	Block 2	1.5	0.02	Hydrosart®	5.32	3.90
24	Block 2	0.5	0.02	Hydrosart®	6.93	5.00
25	Block 2	1	0.2	Hydrosart®	34.26	11.21
26	Block 2	1	0.02	PESU	1.94	3.25

Table 7.7 Model Sum of Squares

Source	Sum of Squares	df	Mean Square	F Value	p-value	
Mean vs Total	19.67	1	19.67			
Block vs Mean	0.22	1	0.22			
Linear vs Block	4.51	3	1.50	61.45	< 0.0001	Suggested
2FI vs Linear	0.20	2	0.10	6.22	0.0084	Aliased

Table 7.8 Model Summary Statistics

Source	Std. Dev.	R-Squared	Adjusted R-Squared	Predicted R-Squared	PRESS	
Linear	0.1564	0.8977	0.8831	0.8416	0.7955	Suggested
2FI	0.1278	0.9382	0.9219	0.8809	0.5981	Aliased

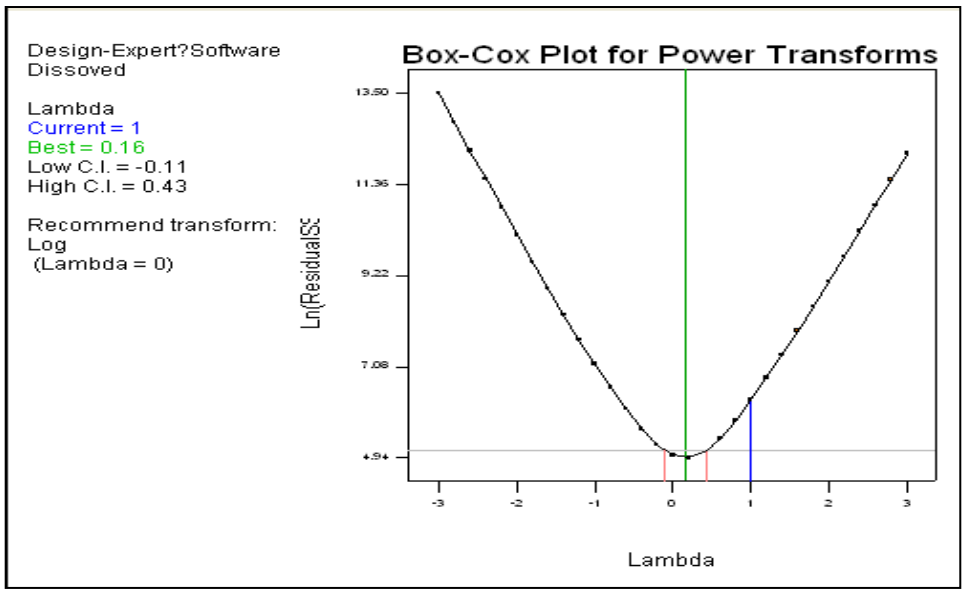

Figure 7.3 Diagnostic box-cox plots for dissolved oil component

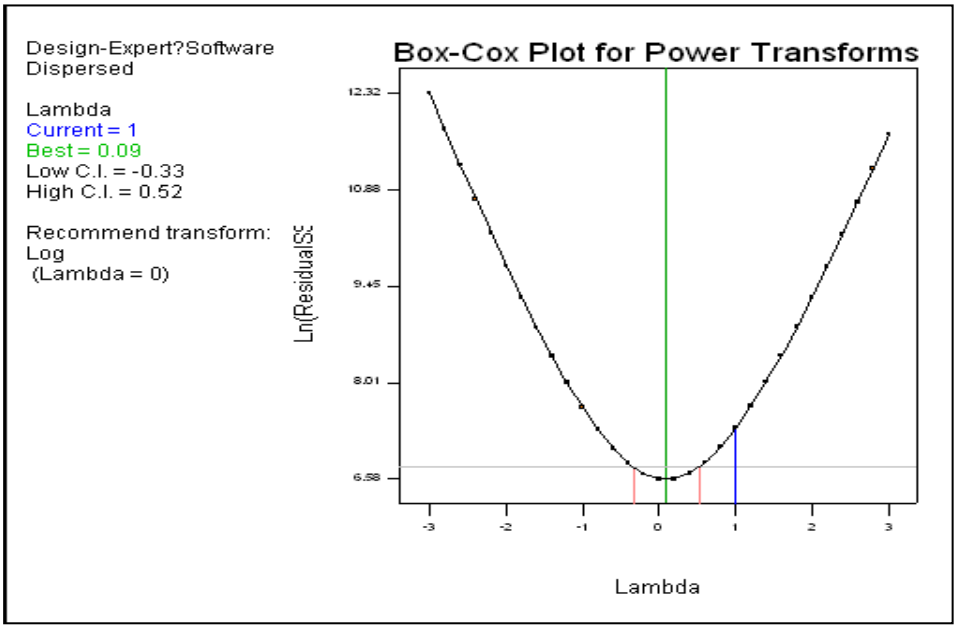

Figure 7.4 Diagnostic box-cox plots for dispersed oil component

Therefore a data transformation using natural log (*ln*) was performed to improve the normality of the data. From ANOVA results (Table 7.9 and 7.10), the p-value shows that, at 95% confidence level the process fitted with the model. It is important to note that the model is significant with no lack of fit (LOF). The model p-value also shows that membrane pore size is the main factor for both dispersed and dissolved oil responses. The DP is a more significant factor for the dissolved oil separation compared with dispersed oil separation. Table 7.9 and 7.10 also show that the type of membrane is significant for dissolved oil separation but not significant for dispersed oil separation. Hydrosart® membrane allows more dissolved oil to pass through than Polyethersulfone (PESU) membrane. This might be due to its cellulosic properties which are less adsorptive for oil. Moreover, the dissolved oil might cause interporous plugging within PESU membrane pores resulting in lower dissolved oil concentration in permeate.

Table 7.9 ANOVA for RSM Linear Modeling with ln Transformation for dissolved oil component

Source	Sum of Squares	df	Mean Square	F Value	p-value	
Block	1.16	1	1.16			
Model	23.90	3	7.97	61.45	< 0.0001	significant
A-DP	0.16	1	0.16	1.27	0.2721	
B-Size	7.07	1	7.07	54.57	< 0.0001	
C-Type	6.09	1	6.09	46.98	< 0.0001	
Residual	2.72	21	0.13			
Lack of Fit	2.43	20	0.12	0.42	0.8631	not significant
Pure Error	0.29	1	0.29			
Cor Total	27.79	25				

Table 7.10 ANOVA for RSM Linear Modeling with ln Transformation for dispersed oil component

Source	Sum of Squares	df	Mean Square	F Value	p-value	
Block	1.87	1	1.87			
Model	7.96	3	2.65	5.75	0.0049	significant
A-DP	0.50	1	0.50	1.09	0.3078	
B-Size	6.46	1	6.46	14.01	0.0012	
C-Type	0.03	1	0.03	0.07	0.7870	
Residual	9.68	21	0.46			
Lack of Fit	9.46	20	0.47	2.07	0.5050	not significant
Pure Error	0.23	1	0.23			
Cor Total	19.51	25				

Optimization by numerical analysis was performed on the data subject to the constraints stipulated in Table 7.11. Four solutions were generated for 4 combinations of categorical factor (Table 7.12). From the analysis, the most desirable optimum operating conditions to maximize both the responses listed below:

DP= 0.5 bar,
Membrane Pore Size= 0.2 μm
Membrane Type= Hydrosart®

When operating at DP 0.5 bar, the crossflow velocity is lower compared to the crossflow velocity at higher DP thus allowing more dissolved oil to have more time to pass through the membrane into the permeate. The higher DPs are not able to improve the separation of dispersed oil in retentate. This might be due to adsorption of oil inside the membrane pores where crossflow effect is not critical. Compared with 0.02 μm membrane, the bigger pore size membrane, 0.2 μm, can prevent dispersed oil while allowing more dissolved oil to pass through into the permeate. The optimum condition simulated is verified again in experiment and the result is shown in Table 7.13.

Table 7.11 Constraints for optimization of dissolved oil separation using RSM D-optimal

Constraints						
Name	Goal	Lower Limit	Upper Limit	Lower Weight	Upper Weight	Importance
DP (bar)	is in range	0.5	2	1	1	3
Size (μm)	is in range	0.02	0.2	1	1	3
Type	is in range	Hydrosart®	PESU	1	1	3
Ln(Diss)	maximize	-0.005383	3.811947	1	1	4
Ln(Disp)	maximize	0.441136	3.80243	1	1	5

Table 7.12 Simulated optimized solution from empirical models

Solutions						
Number	DP	Size (μm)	Type	ln(Dissoved)	ln(Dispersed)	Desirability
1	0.5	0.2	Hydrosart®	3.34	3.14	0.84
2	0.5	0.2	PESU	2.17	3.23	0.7
3	0.5	0.02	Hydrosart®	2.08	1.94	0.49
4	0.5	0.02	PESU	0.91	2.02	0.35

7.4.4 Validation of Simulated Optimum Conditions

Solution number 1 from Table 7.12 is selected as the optimum conditions for maximum dissolved oil separation as the desirability is closest to 1. Validation of the optimum condition is done by using Hydrosart® membrane with pore size 0.2 μm, operated at DP 0.5 bar. Whereas the TMP of the operation was performed at 1.00 bar instead of TMP of 2.75 bar. This is the optimum TMP for 0.2 μm Hydrosart® membrane as referred to Figure A.4 in Appendix A. By increasing the TMP, the permeate flux remains constant. At this TMP, the dissolved oil concentration is 19.2% less than the simulated results (Table 7.13). However, the dispersed oil in the retentate improved by 57.84%. This is because when performed at TMP 1.00 bar, less dispersed oil is being trapped in the pores of the membrane as lower pressure exerting the solution in membrane direction. Unfortunately, this also causes less dissolved oil to penetrate the membrane into the permeate. Dissolved oil content in permeate has to be forfeited to achieve higher dispersed oil content in retentate as dispersed oil is the main parameter under regulation.

Table 7.13 Experimental verification with optimized values

0.2μm Hydrosart® membrane at DP 0.5 bar	**Simulation**	**Experimental**
Dispersed oil (%) in retentate	23.10	36.46
Dissolved oil (%) in permeate	28.22	22.80

7.5 Conclusions

In this chapter, optimization was performed by using RSM D-optimal design and the optimum DP for maximum dissolved and dispersed oil in permeate and retentate was found to be at 0.5 bar. This is in accordance with the findings from Chapter 6, where DP 0.5 was found to have greater turbulence intensity, and therefore, this helps in removing the dispersed and dissolved oil which were attached on the membrane surface. The linear model produced by RSM was at 95% confidence level. The optimum conditions to achieve high dispersed oil in retentate and high dissolved oil in permeate is obtained and validated experimentally. By using this optimum setting by physical approach, 22.8% of dissolved oil will be eliminated in the permeate therefore lowering the oil-in-water content during monitoring for the disposal of produced water. However, there is only 36% of dispersed oil retrieved from the retentate, whereas 64% of it was still within the membrane. Therefore further enhancement steps need to be performed to recover the rest of the dispersed and dissolved oil from the membrane. This issue will be addressed in the following chapter.

Chapter 8: *Enhancement of Dissolved Oil Separation by Integrated Physical and Chemical Treatment*

8.1 Introduction

For decades, researchers have been investigating numerous means to solve the problem caused by fouling in membrane filtration system. In Chapter 7, studies to avoid deposition of oils and to optimize the dissolved oil separation by altering the differential pressures (DP) are reported. An improvement of the separation can be seen; however, the accumulation of oil on the surface or interporous plugging of the membrane is inevitable despite this approach. Therefore the most suitable solution for accurate measurement is to clean out the dispersed and dissolved oil attached on the membrane either physically, chemically [133] or both [134] and these oil concentrations with the first measurement are combined.

Besides that, chemical pre-treatment process is integrated before filtration process to study its effect on the enhancement of dissolved oil separation. Membranes are passive entity as they perform exactly what they are able to do under given circumstances. Pre-treatment for the feed prior to membrane filtration is therefore an extremely important process. For the purpose of our study, pre-treatment process should be able to change the affinity of the oils in the feed towards the membrane without changing the oil concentration. Poulopoulos and co-workers [135] reported their pre-treatment process for oily waste water by using physical approach which is by nitrogen stripping operated at different temperatures. The stripping technique however changes the concentration of oil which is not suitable in this application of analytical study. Chemical pre-treatment is therefore being considered as the next appropriate pre-treatment approach.

In this chapter, combined techniques of the physical and chemical treatment including DP, TMP, chemical pre-treatment, and chemical cleaning are studied for their efficiency to enhance the dissolved oil separation. The process of integrated studies is summarized in Figure 8.1. These techniques are investigated through experiments where a process optimization was done by using statistical analysis i.e. response surface method (RSM). The obtained optimum results are verified experimentally.

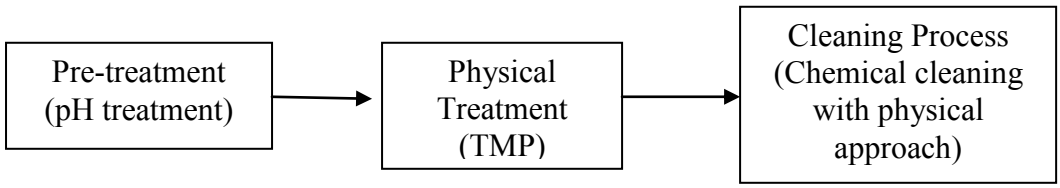

Figure 8.1 Integrated physical and chemical treatment

8.1.1 Effect of Chemical Pre-treatments

Chemical pre-treatment such as coagulation or oxidation might cause unnecessary fouling of membrane from the chemicals used if not done properly [76]. For example, the divalent or trivalent cations such as Ca^{2+} or Al^{3+} which are often used in coagulation process will form a foulant layer on the membrane and should be avoided [136-138]. Notably, dispersed oil properties should also remain undissolved when chemical pre-treatment is involved so that the quantity of dispersed oil will not be altered for the accuracy of measurement. Kurt reported his study of beef emulsification by using Chitosan [139]. In his research, Chitosan was found to possess a positive ionic charge which gives it the ability to chemically bind with negatively charged fats and oils. However, the charge binding properties of Chitosan is not selective and may cause both changes in dispersed and dissolved oil concentration.

With regards to solubility in water, hydrophilic species tend to dissolve readily in water and are usually polar molecules. Dissolved oil such as BTEX and PAH are relatively hydrophilic in nature. Although they are non-polar molecules, they are polarizable when present in water by dipole-induced dipole interaction due to the aromatic ring present [140]. Hydrophobic species such as dispersed oils are non-polar and do not dissolve in water because the molecule has no net electrical charge across it and thus it is not attracted to water molecules. To increase the solubility of oil, pH adjustment is one of the pre-treatment methods [75]. A study by Caldero *et. al.*, showed that the diffusion rate of the oil particle is affected by the pH of the emulsion [141]. On the other hand, studies also show that pH can affect the charges of the membrane surface thus resulting in electrostatic interactions or repulsions between the membrane wall and solutes [76]. Ang and co-workers [79] investigated the use of EDTA and SDS for cleaning RO membrane fouled by effluent organic matter. The study showed that the cleaning performance for both solutions improved in caustic environment. This also shows the correlation between pH, organic matter and membrane surface.

Therefore, from all these literature findings, altering the pH of the feed could change the affinity of oil towards the membrane without changing the concentration of dissolved and dispersed oil. HCl and NaOH used in these experiments are strong acid and base by which only a small amount is needed to change the pH.

8.1.2 Effect of Chemical Cleaning and Circulation Time on the Separation of Oils

Cleaning is an important stage of membrane filtration as fouling is unavoidable. Chemical cleaning can be done to eliminate the stubborn foulant deposited on the membrane which otherwise could not be removed by physical cleaning [77, 78]. Studies suggest that an alkaline solution such as NaOH does not only increase the pH of the solution, but it can hydrolyse and emulsify the organic molecules [79, 80]. Through emulsifying the foulant particles on the membrane, the foulant is dispersed into the solution. Membrane manufacturers recommend that 1M NaOH be used to clean this type of membrane [104]. Besides identifying chemical cleaning agents,

optimizing the chemical cleaning procedure is equally vital because excessive cleaning will not only result in adverse effect on membrane life, it will also increase the cost of chemicals used and the amount of water required [75].

This work is done by simultaneous approach, where the four factors, pH, TMP, volume of chemical used and circulation time are analysed together. However, for accuracy of oil measurement, dissolved and dispersed oil quantifications were done in two stages, i.e. pre-treatment stage and cleaning stage. Oils that are being extracted from these two stages are quantified and added up together to represent one run of experiment. After oil quantification of all the runs are done, optimized values for each of the variables i.e. differential pressure (DP), trans-membrane pressure (TMP), pH, circulation time and volume of chemical used are being determined by D-optimal design and the result is verified experimentally.

8.2 Experimental Set-up

8.2.1 Membrane

The membrane used in this experiment is 0.2 μm Hydrosart® membrane (3051860701W—SG, Sartorius AG.) which, from Chapter 7 is found to be the most suitable membrane for the separation of both the dissolved and dispersed oil. It is a hydrophilic membrane with polar affinity. Choosing a hydrophobic or hydrophilic membrane depends on the properties of the suspensions with minimal fouling as the main interest [142]. Hydrophilic membranes prevent non-polar dispersed oil from attaching to it, therefore minimizing the possibility of oil fouling. But on the other hand, it allows hydrophilic dissolved oils to pass through easily. The dispersed oil attached on the surface of hydrophilic membrane can be washed out using chemical cleaning process. During cleaning process, this membrane can withstand a pH range of 2 to 13.

8.2.2 Chemical Cleaning Agent

Caustic solution is very efficient in washing out the oils from membrane surface [76, 143]. Sodium hydroxide (NaOH) solution is typically used as cleanser for organic matter. NaOH solutions and oils react to produce soaps and glycerol. These soap molecules have both properties of non-polar and polar at opposite ends of the molecule which can "bridge" the non-polar oil with polar water molecules. Thus it is able to carry the oil deposited on the membrane surface into retentate. Another factor to consider is the ionic strength of the cleaning agent. 1M is recommended from the manufacturer mainly due to the resistant limit of this type of membrane [104]. Some studies show that NaOCl is used together with NaOH [76] to enhance the cleaning by oxidation. However, NaOCl is not used in this case, because it changes the chemical properties of the oils, and will in turn cause changes to the oils concentration.

8.2.3 Pre-treatment

Temperature and pH can affect the solubility of organic compounds [144] and the hydrolysis of oils [76]. However, the experiment in this work is performed at ambient temperature for consistency in the implementation in standard test method. NaOH solution is physically smooth with lubricating effect. Therefore feed pre-treated with NaOH may enhance the smoothness of flow and reduces oil attachment on the surface along the flow channel and the membrane. Therefore, enhancing dissolved oil separation by using HCl and NaOH to alter the pH is explored.

8.2.4 Design of Experiment (DOE)

Similar to Chapter 7, the experiment is designed by 2^k factorial design and RSM D-optimal design [129] for pre-treatment and cleaning stages. The experimental design for the pre-treatment are summarised in Table 8.2. Optimum differential pressure (DP) of 0.5 bar, established in Chapter 7, is used throughout the experiment. A total of 10 runs with 4 replicates of experiments are performed.

8.3 Analytical Method

Analysis was performed as described in Section 3.5. Examples of calculation for dispersed and dissolved oil content are showed in Table 8.1(a) and Table 8.1(b) show an example of the calculation.

8.3.1 Clean Water Flux (CWF)

Prior to every run, the membrane is thoroughly cleaned with 1N of NaOH and the CWF before and after experiments are measured to ensure that the membrane quality is standardized before each run (Figure 8.2). The low oil concentrations in the pseudo-produced water enable the membrane to be reusable.

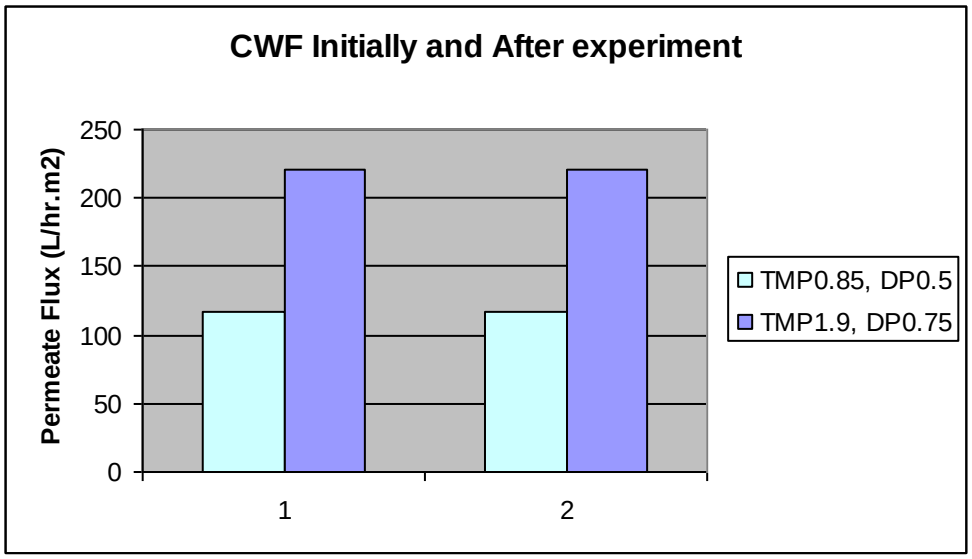

Figure 8.2 CWF before (1) and after (2) experiments for 0.2µm Hydrosart® membrane at two different TMPs

Table 8.1(a) Example of calculation for Run 1 (pre-treatment stage)

Run 1	Crude Oil		conc %	Retentate		conc	Permeate		conc	Total %
TMP0.55	Area	ppm		Area	ppm	%	Area	ppm	%	
Dissolved	3.98E+07	20.01	100	8.85E+06	4.45	22.3	5.73E+06	2.88	14.4	36.70
Dispersed	1.59E+08	79.99	100	1.98E+07	9.97	12.5	0	0	0	
Total Crude	1.99E+08	100		2.87E+07						

Table 8.1(b) Example of calculation for Run 1 (cleaning stage)

Run 1	R2		conc %	Retentate+	P2		conc %	Permeate+
TMP0.55	Area	ppm		R2 total in	Area	ppm		P2 total in
Dissolved	1.48E+07	7.44	37.19	59.44	1.61E+06	4.05	20.24	34.65
Dispersed	2.84E+07	14.31	17.89	30.35	3.59E+06	2.26	2.82	2.82
Total Crude	4.32E+07				5.20E+06			

8.4 Results and Discussions

8.4.1 Combined Pre-treatment and Cleaning Stage Results

Results for dissolved and dispersed oil concentration retrieved by combining pre-treatment and cleaning process are shown in Table 8.2. Block 1, 2 and 3 are experiments done at different sessions. Results from Table 8.2 are analyzed by ANOVA for RSM D-optimal design.

The fit summary for dissolved oil component in Table 8.3 suggested a 2FI model. By using 2FI model, the significant factors can be identified by their p-value. From Table 8.4, 2FI model has no lack of fit. This model shows that all four factors have interaction with one another.

An interaction of circulation time with the TMP, which would influence the separation of dissolved oils, can be seen in Figure 8.3. At long circulation time, TMP should be set high to achieve good dissolved oil separation. The factor interactions between TMP and pH in Figure 8.4 show that when TMP is high, pH is not significant for dissolved oil separation. However, when TMP is low, pH plays a significant role instead. When TMP is low, the velocity of fluid passing through the membrane is low; therefore the chances of interporous adsorption of oils on the membranes are higher. Consequently, the pH for the membrane environment is very important where at higher pH, less dissolved oil will be trapped inside the membrane. From Figure 8.5, the longer the circulation time, the better separation of dissolved oil. Figure 8.6 shows that cleaning should be done at longer circulation time, with lower volume of NaOH for better dissolved oil separation in permeate.

Table 8.2 Experiment data for integrated physical and chemical approach in enhancement of separation of dissolved oil in produced water

Run	Block	TMP (bar)	pH	Time (mins)	Vol (L)	Dissolved	Dispersed
1	Block 1	0.55	2.00	5.00	0.70	34.65	30.35
2	Block 1	2.75	13.00	5.00	0.70	43.77	55.72
3	Block 1	0.55	2.00	20.00	2.00	19.79	16.53
4	Block 1	2.00	13.00	20.00	2.00	31.69	90.56
5	Block 1	2.00	13.00	5.00	0.70	40.08	89.12
6	Block 1	2.00	2.00	5.00	2.00	18.60	45.33
7	Block 1	2.00	2.00	20.00	0.70	57.64	37.81
8	Block 1	1.25	7.50	12.50	1.35	44.96	26.08
9	Block 1	0.55	13.00	20.00	0.70	49.36	82.37
10	Block 1	0.55	13.00	5.00	2.00	60.96	94.18
11	Block 2	2.75	2.00	15.00	1.50	25.94	36.63
12	Block 2	2.75	2.00	7.50	1.25	22.11	3.85
13	Block 2	2.75	7.00	5.00	1.50	5.03	11.39
14	Block 2	2.75	2.00	10.00	0.50	24.58	16.87
15	Block 2	2.75	7.00	10.00	1.50	13.71	8.53
16	Block 2	2.75	7.00	10.00	1.50	5.03	11.39
17	Block 1	1.25	7.50	12.50	1.35	40.84	10.27
18	Block 3	2.20	5.00	9.00	1.00	17.56	68.38
19	Block 3	0.55	2.00	5.00	2.00	25.90	65.26

Table 8.3 Fit summary for dissolved oil component

Source	Sum of Square	df	Mean Square	F Value	p value Prob > F	
Mean vs Total	17840.057	1	17840.057			
Block vs Mean	2441.5966	2	1220.7983			
Linear vs Block	584.67040	4	146.1676	1.00407	0.4430	
2FI vs Linear	1412.9009	6	235.48349	4.23020	0.0514	Suggested
Quadratic vs 2FI	287.84035	4	71.960089	3.11764	0.2573	
Cubic vs Quadratic	0	0				Aliased
Residual	46.163106	2	23.08155316			
Total	22613.22838	19	1190.169915			

Table 8.4 Model Sum of Square for dissolved oil component

Source	Sum of Square	df	Mean Square	F Value	p value Prob > F	
Block	2441.596553	2	1220.798276			
Model	1997.571334	10	199.7571334	3.588414314	0.0657	significant
A-tmp	11.49948448	1	11.49948448	0.206575425	0.6654	
B-pH	188.6861843	1	188.6861843	3.389537049	0.1152	
C-time	81.86666335	1	81.86666335	1.470643384	0.2708	
D-vol	586.0643091	1	586.0643091	10.52799226	0.0176	
AB	80.27140554	1	80.27140554	1.441986355	0.2751	
AC	375.1803339	1	375.1803339	6.739696638	0.0409	
AD	166.102714	1	166.102714	2.983850171	0.1348	
BC	8.170325235	1	8.170325235	0.146770789	0.7148	
BD	25.39455	1	25.39455	0.456184794	0.5246	
CD	75.39750677	1	75.39750677	1.354432194	0.2887	
Residual	334.0034611	6	55.66724351			
Lack of Fit	287.8403548	4	71.96008869	3.117644996	0.2573	not significant
Pure Error	46.16310631	2	23.08155316			
Cor Total	4773.171348	18				

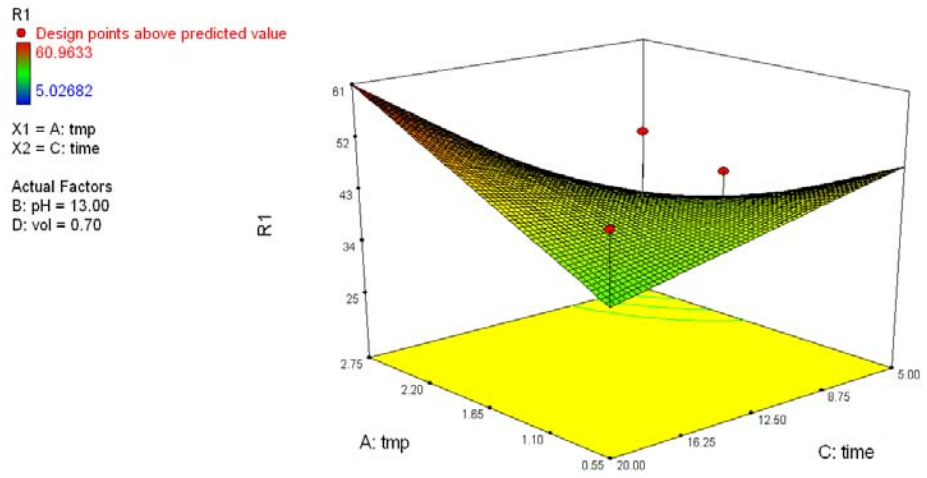

Figure 8.3 Factor interactions between TMP and circulation time for dissolved oil

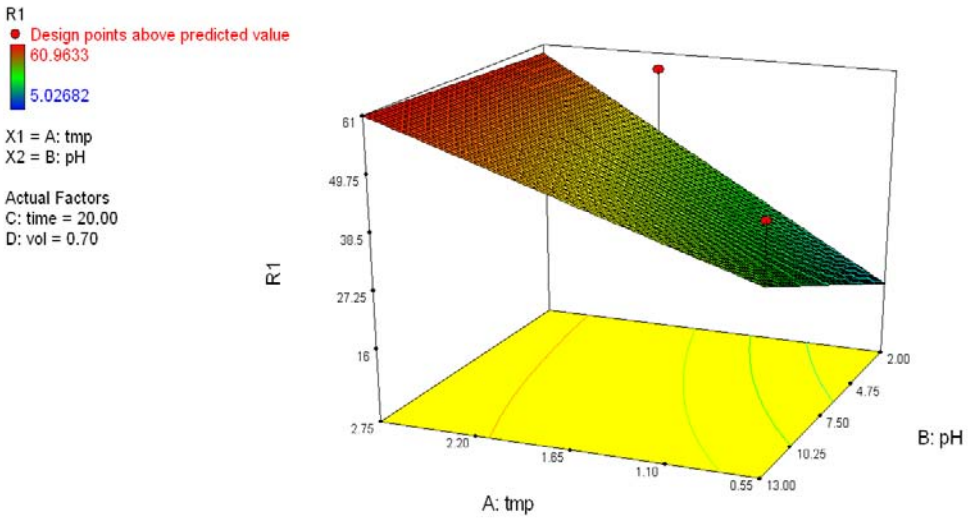

Figure 8.4 Factor interactions between TMP and pH for dissolved oil

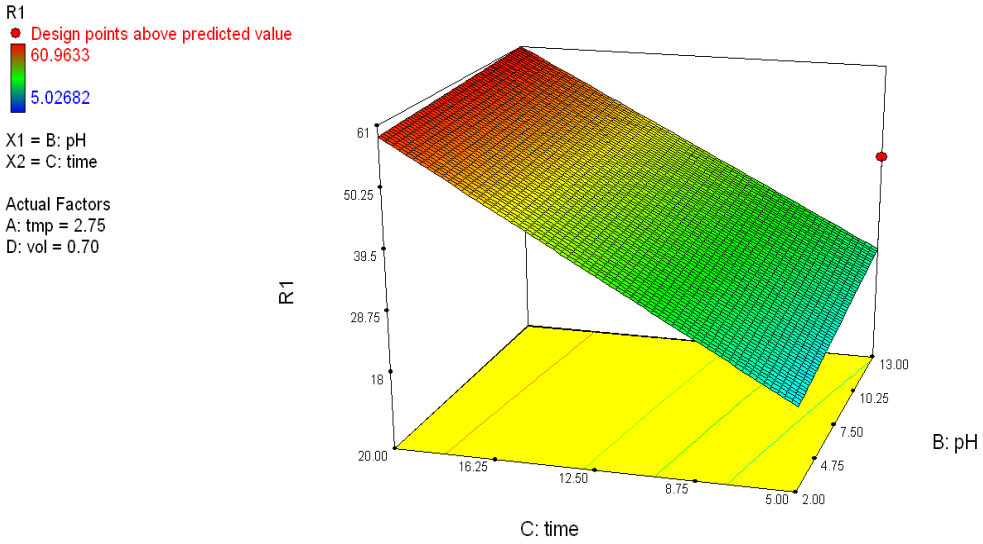

Figure 8.5 Factor interactions between time and pH for dissolved oil

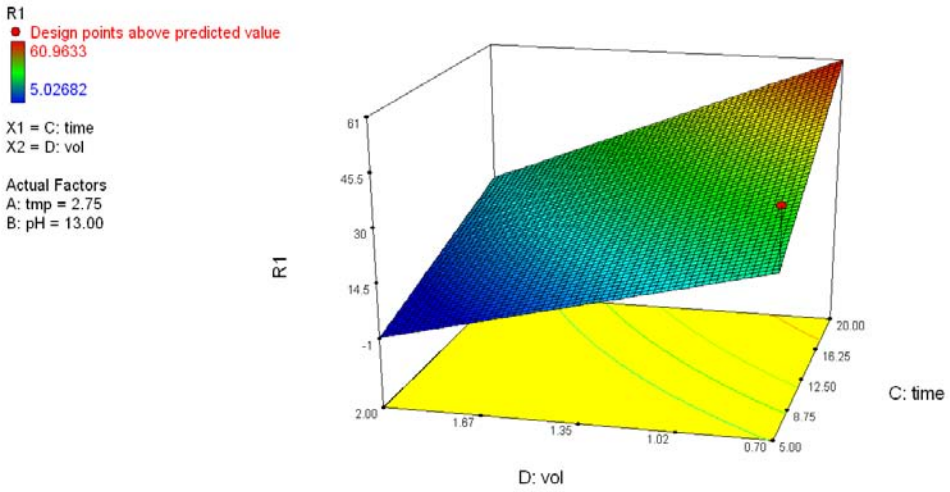

Figure 8.6 Factor interactions between volume and time for dissolved oil

On the other hand, the fit summary (Table 8.5) for dispersed oil component suggested a quadratic model. Contrary to dissolved oil component, pH factor is a significant factor for the dispersed oil separation with a p-value of 0.12 while other factors are not critical. Therefore, to achieve the maximum dissolved oil and

dispersed oil in permeate and retentate respectively, a numerical optimization was performed and is outlined in the next section.

Table 8.5 Fit Summary for dispersed oil component

Source	Sum of Square	df	Mean Square	F Value	p value Prob > F	
Mean vs Total	33737.95096	1	33737.95096			
Block vs Mean	6907.535401	2	3453.7677			
Linear vs Block	4657.940859	4	1164.485215	2.34	0.1141	
2FI vs Linear	2617.879445	6	436.3132408	0.78	0.6144	
Quadratic vs 2FI	3225.10827	4	806.2770674	12.49	0.0755	Suggested
Cubic vs Quadratic	0	0				Aliased
Residual	129.0728621	2	64.53643106			
Total	51275.4878	19	2698.709884			

Table 8.6 Model Sum of Square for dispersed oil component

Source	Sum of Sq	df	Mean Sq	F Value	p value Prob > F	
Block	6907.535401	2	3453.7677			
Model	10500.92857	14	750.0663267	11.62237072	0.0820	significant
A-tmp	28.73401132	1	28.73401132	0.445237068	0.5733	
B-pH	458.8433253	1	458.8433253	7.10983421	0.1166	
C-time	12.97997552	1	12.97997552	0.20112633	0.6977	
D-vol	36.6849751	1	36.6849751	0.568438237	0.5296	
AB	105.1284285	1	105.1284285	1.628978033	0.3300	
AC	69.05641225	1	69.05641225	1.070037669	0.4096	
AD	28.84002408	1	28.84002408	0.446879749	0.5726	
BC	15.85448377	1	15.85448377	0.245667191	0.6692	
BD	47.34569495	1	47.34569495	0.733627413	0.4820	
CD	58.88902073	1	58.88902073	0.912492677	0.4403	
A^2	0.039842578	1	0.039842578	0.000617366	0.9824	
B^2	0.226067968	1	0.226067968	0.003502951	0.9582	
C^2	35.96147935	1	35.96147935	0.557227581	0.5332	
D^2	419.1337142	1	419.1337142	6.494528862	0.1256	
Pure Error	129.0728621	2	64.53643106			
Cor Total	17537.53684	18				

8.4.2 Optimization

Numerical optimization was done using the constraints stipulated in Table 8.7. These constraints are bound by the limit available to the membrane filtration instrument used in the experiments. Four solutions with the highest desirability were obtained in Table 8.8. Desirability function can be used to combine multiple responses into one response using mathematical transformation. Desirability functions of 1 means that all the product characteristics are on target. A higher pH will result in an increase of dissolved oil in permeate. Contrary, it will cause the dispersed oil to be lower. Moreover, the desirability for pH 11 is closest to 1; therefore, it is chosen to be the optimum operating pH for pre-treatment.

Table 8.7 Constraints for process optimization

Name	Goal	Lower Limit	Upper Limit	Lower Weight	Upper Weight	Importance
TMP	is in range	0.55	2.75	1	1	3
pH	is in range	2	13	1	1	3
time	is in range	5	20	1	1	3
vol	is in range	0.7	2	1	1	3
Dissolved	maximize	5.027	60.96	1	1	3
Dispersed	maximize	3.85	94.18	1	1	3

Table 8.8 Solution for process optimization

Number	TMP	pH	Time (mins)	Vol (L)	Dissolved oil	Dispersed oil	Desirability	
1	2.75	11	20	0.7	60.58	81.8	0.925824	Selected
2	2.75	12	20	0.7	60.77	81.25	0.924064	
3	2.75	13	20	0.7	60.89	80.73	0.921991	
4	2.75	5	20	0.7	59.55	81.35	0.914449	

Figure 8.7 shows the interactions of TMP and pH factors towards the desirability function for numerical optimization. To achieve high desirability, TMP and pH should be high, and cleaning circulation time is set at 20mins with 0.7 L of NaOH.

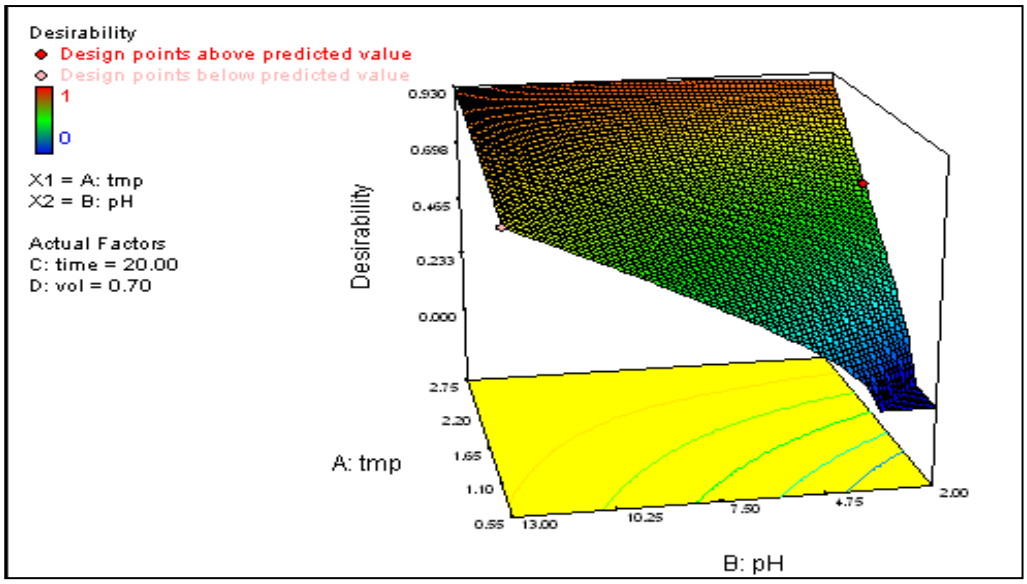

Figure 8.7 Optimization 3D surface view for dissolved and dispersed oil response

Pre-treatment method improves both the separation of dispersed and dissolved oil into retentate and filtrate respectively. Moosemiller and co-workers [145] reported that the maximum permeability for alumina membrane is at caustic environment. Results obtained from this study are in consistent with Moosemiller study where the optimum pH is at 11 which is in caustic environment. According to Hua et al [59], at high pH, the oil deposition layer on the membrane surface became porous due to the inter-droplet repulsion, and this increased the permeability resulting in higher dissolved oil passing through the membrane. This can be explained by the fact that at high pH, the membrane matrix would be at a more expanded state due to the inter-membrane electrostatic repulsion. Therefore, the membrane pore size is larger than normal because the negative charges of the polymer chains in the three-dimensional

network of the surface repel each other and make the surface layer more ‗open' [146]. Moreover, as pH increases, the wettability of the membrane surface increases because the degree of dissociation of the groups that interact with water is higher [146].

Meanwhile, according to Galjaard and colleagues [147], the zeta-potential surface charge measured for hydrophilic membrane is from -40 to -100mV. Moreover from Shim and co-workers' [148] findings, at high pH, the zeta-potential at membrane surface becomes more negatively charged. This increase in negative charge causes more charge repulsion for both negatively charged dissolved oil and the membrane surface resulting in lower fouling and more dissolved oil in the filtrate.

For this experiment, the TMP is varied over a range of 0.55 bar to 2.75 bar. The general consensus from Figure 8.3 and 8.4 would be that as the TMP increases, more dissolved oil is observed in the permeate. According to Blanpain-Avet and coworkers [149], the higher the TMP, the higher is the permeation flux. The higher the permeate flux, the higher the convective mass transport coefficient to the membrane wall [150]. Thus, with higher permeation rates, more dissolved component are transported through membrane pores by the bulk fluid.

For the chemical cleaning experiment, the interaction between circulation time and TMP factors is significant for dissolved oil separation (Figure 8.3). Some dissolved oil may have adsorbed in the pores of membrane which can be improved by high TMP with longer circulation time. But for dispersed oil, both factors are not significant for the separation (Table 8.6). This shows that not much of hydrophobic dispersed oil deposits on the hydrophilic membrane justifying the claim from the manufacturer, that the Hydrosart® membrane possessed patented properties which have low fouling for hydrophobic substances.

From Table 8.4 and 8.6, the p-values show that the volume used for cleaning is significant for dissolved oil component but not significant for dispersed oil component. However, for dissolved oil separation, this factor is involved in an interaction as shown in Figure 8.8. Dissolved oil increases at high TMP with

decreasing volume. This shows that the high TMP pushes the dissolved oil adsorbed in the interporous membrane into the reagent. Whereas at low TMP, the effect of reagent volume towards the dissolved oil separation is insignificant. This shows that in fact the dissolved oil is not at saturation point when 0.7 L of cleaning reagent is used.

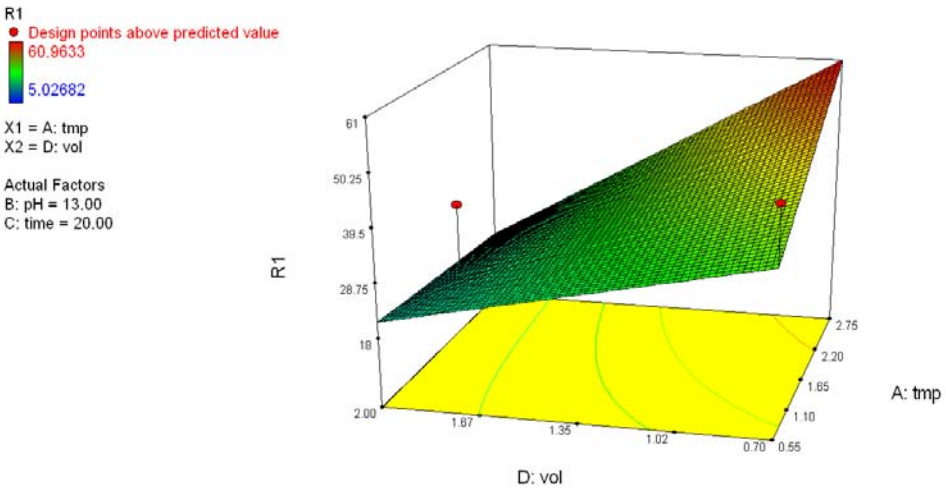

Figure 8.8 Factor interactions between TMP and Volume for dissolved oil response

8.4.3 Confirmation Run

A confirmation run was performed to verify the simulated results. Pre-treatment was done at DP 0.5 bar, TMP 2.75 bar with pH 11. Oils from permeate and retentate were extracted and analyzed by GCMS and the oil concentrations were recorded from the first stage results. Cleaning process was done by using 0.7 L of NaOH with 20 mins circulation time. Oils concentrations were obtained again from the GCMS analysis. Dissolved oils in permeate and dispersed oils in retentate are added and the results are compared with the simulated results as shown in Table 8.9.

Table 8.9 Confirmation run for optimum value simulated

Run	TMP (bar)	pH	Time (mins)	Vol (L)	Dissolved oil in permeate	Dispersed oil in retentate
Simulated	2.75	11.00	20.00	0.70	60.58	81.80
Experimental	2.75	11.00	20.00	0.70	50.50	93.80

The experimental run using optimum value simulated shows that there are 50.5% of dissolved oil being discarded from permeate. Moreover, the recovery of dispersed oil concentration improves from 36% (Chapter 7) to 93.8%, with combined pre-treatment and chemical cleaning approach.

8.5 Conclusions

In this chapter, the separation of dispersed and dissolved oil in produced water were further been enhanced by combining pre-treatment and cleaning process using both physical and chemical approach. Four factors such as TMP, pH, chemical volume and cleaning circulation time are analysed simultaneously for the optimization of the oils separation. Feed pre-treatment in caustic environment has proved to enhance the separation of both dissolved and dispersed oil. The optimum TMP for dissolved oil separation is at 2.75 bar which not only gives higher dissolved oil in permeate but also higher permeate flux. The circulation time has significant effect on the separation. The longer the circulation time, the more dissolved and dispersed oil are washed out. The cleaning reagent volume for the response of dissolved oil component is involved in an interaction where its degree of significance is largely depends on TMP.

With this combination of physical and chemical treatment on the oils separation by membrane filtration, dispersed oil content retained from the separation is 93.8%, whereas dissolved oil eliminated is 50.5%. The recovery of dispersed oil improved from 36.46% to 93.8%; whereas elimination of dissolved oil also improved from 22.8% to 50.5%. In conclusions, this result is very promising and has justified the

integration of membrane filtration technique into the standard analysis method of oil-in-water. With this new strategy, 50% of the dissolved oil will not be measured whereas nearly all dispersed oil is being monitored. This combined technique shows remarkable improvement in the results compared with only physical treatment applied.

Chapter 9: Conclusions and Recommendations

9.1 Conclusions

To improve current standard analytical method for oil-in-water analysis, the removal of dissolved oil is critical. This thesis has shown that the incorporation of membrane filtration for dissolved oil separation prior to the GC-FID analysis is possible. However, the deposition of oils on the membrane surface may affect the accuracy of measurement. Therefore, an enhanced separation method for dissolved oil by membrane filtration was presented through physical and chemical means. This study gives significant insight into: (1) the modeling of fluid transport inside the membrane cartridge, (2) Mathematical modeling of gel concentration and (3) process optimization in the removal of dissolved oil using experimental design and statistical analysis.

Contributions from this work are summarized as:

- Hydrosart® microfiltration and Polyethersulfone ultrafiltration membranes of pore size 0.2 μm and 0.02 μm respectively were proven feasible for the separation of dissolved oil from produced water (Chapter 4).

- A novel approach in predicting MTC and gel layer concentration was established by using modified film theory model. According to the modified film theory model, DP has to be lower for lesser attachment of oil on the membrane surface. Finally, the optimum DP was found to be at 0.3 bar which is at the lowest DP operable for this instrument (Chapter 5).

- Fluid flow behavior inside the membrane cartridge was analyzed at different DPs using CFD modeling. Different operating conditions are simulated and lower DP with high inlet pressure and high outlet pressure has been found to be able to have increased the turbulent intensities. The shearing effect created by this turbulence will reduced the fouling on the membrane. (Chapter 6).

- Optimum DP for dissolved oil separation is found and verified experimentally. Process optimization is done through statistical analysis with the aid of experimental designs which is D-optimal design. Hydrosart membrane material with 0.2 μm pore sized has been identified to be able to maximize the dissolved oil separation. The optimum trans-membrane pressure (TMP) is at 2.75 bar, and the optimum differential pressure (DP) is at 0.5 bar. Adjustable inlet pressure is at 3 bar and outlet pressure at 2.5 bar (Chapter 7).

- A combined Physical and Chemical Treatment for the enhancement of dissolved oil separation was performed by studying 4 factors such as pH, TMP, volume of chemical used and circulation time. The optimum operating factors are summarized as TMP at 2.75 bar, DP at 0.5 bar with inlet pressure at 3.0 bar and outlet pressure at 2.5 bar; 0.2 μm Hydrosart membrane type; pre-treatment at pH 11; NaOH chemical cleaning with 0.7 ml in volume and 20 mins circulation. The results are verified experimentally and found to be in close proximity. From the experimental data, at the optimum operating condition, about 50% of dissolved oil has been eliminated from the produced water. A total of 93.80% dispersed oil is retrieved from the separation unit. The rest of the 6% of dispersed oil might still be trapped inside the membrane cartridge. However, this result is very promising and has justified the integration of membrane filtration technique into the standard analysis method of oil-in-water (Chapter 8).

9.2 Recommendations

Although the strategies developed for the removal of dissolved oil in simulated produced water by membrane filtration have been shown to be successful in this work, this methodology has not been applied in the actual produced water samples. Further study can be performed using the actual produced water from the field in order to have a comprehensive understanding of other constituent inside the produced water that might have an effect on the fouling of membranes.

Furthermore, the cost analysis associated with the incorporation of membrane filtration into the current standard test method has not been performed. Further study can include the estimation of initial capital cost and operational cost such as cleaning of membrane, changing of new membrane etc. This costing study can be associated with the savings gained from abiding to the Standards thus avoiding penalty being imposed. With these insights, the economical aspect of this technique can be a substantial support for this operation.

Moreover, with the removal of dissolved oil in permeate, this "waste" can be further study either for possible regeneration purposes or for proper disposal. Studies on dissolved oil from the permeate can be done by reprocessing it into concentrate that can be reused as renewable energy.

Further work on the study of the chemistry of oil interaction with membrane material can be investigated to have further insight in how the dissolved oil plugged within different membrane materials such as PESU and Hydrosart® membranes for this dissolved oil separation purpose. With this knowledge, an improved membrane suitable for this process can be fabricated.

Lastly, in Chapter 7, simultaneous approach was used in the factor analysis for optimum dissolved and dispersed oil separation. However, another method can be explored in the analysis that is by two stage approach, which is analysing pre-treatment factors first and find the optimum values for the factors and then incorporating these optimum values to perform the second cleaning stage. With this

two stage approach, the optimum values might be different from that of the simultaneous approach done in Chapter 7. These findings would be interesting to compare the reliability of both optimum values.

References

1. Mondal, S., Wickramasinghe, S.R., *Produced Water Treatment by Nanofiltration and Reverse Osmosis Membranes.* Journal of Membrane Science, 2008. **322**: p. 162-170.

2. Kemmer, F.N., *NALCO Water Handbook*. 2nd ed. 1988: McGraw-Hill.

3. Arnold, K., Stewart, M., *Produced Water Treating Systems*, in *Surface Production Operations - Design of Oil-Handling Systems and Facilities (2nd Edition)* M.E. Whitworth, Editor. 1999, Elsevier.

4. Veil, J.A., Puder, M.G., Elcock, D. Redweik, Jr., R.J., *A white paper describing produced water from production of crude oil, natural gas and coal bed methane.* 2004.

5. Ming, Y. *Review of Oil-on-water Monitoring Technology*. in *Oil pollution Detection and Monitoring Seminar* 2001.

6. Green, D., Naimimohasses, R, Smith, PR, Thomason, H *In-situ measurement and classification of oil pollution.* Environemt International, 1995. **21**(2): p. 245-250.

7. YANG, M., *Oil in produced water analysis and monitoring in the North Sea*, in *SPE Annual Technical Conference and Exhibition*. 2006: San Antonio, Texas U.S.A.

8. YANG, M., MacGillivray, *Oil in Water Measurement Training Course*. 2008: Kuala Lumpur Malaysia.

9. Ehrhardt, M., Knap A., *A direct comparison of UV fluorescence and GC/MS data of lipophilic open-ocean seawater extracts.* Marine Chemistry, 1989. **26**: p. 179-188.

10. Lambert, P., Goldthorp, M, Fieldhouse, B, Wang, Z, Fingas, M, Pearson, L, Collazzi, E *Field Fluorometers as Dispersed Oil-in-water Monitors.* Journal of Hazardous Materials, 2003. **102**: p. 57-79.

11. Schomburg, G., *Analytical chemistry*. Gas chromatography, ed. R. Kellner, Mermet, J.-M., Otto, M., Widmer, H.M. 2000, New York: Wiley-VCH.

12. Stephenson, M.T., *A Survey of Produced Water Studies*. Produced Water, ed. J.P. Ray, Englehart, F.R. 1992: Plenum Press, New York.

13. Arnold, K., Stewart, M., *Surface Production Operations - Design of Oil-Handling Systems and Facilities* 1999, Elsevier. p. 194-196.

14. OGP, *Guidelines for Produced Water Injection*, in *Report No. 2.80/302*. 2000: January 2000.

15. OGP, *Aromatics in produced water: Occurence, fate & effects and treatments*, in *Report No. 1.20/324*: January 2002.

16. Hansen, B.R., Davies, R.H., *Review of Potential Technologies for the Removal of Dissolved Components from Produced Water*, in *Trans IChemE*. 1994. p. 176-188.

17. *Mass, Weight, Density, or Specific Gravity of Bulk Materials*. 1996; Available from: http://www.simetric.co.uk/si_materials.htm.

18. Ilia Anisa, A.N., Nour, A.H., *Affect of Viscosity and Droplet Diameter on water-in-oil (w/o) Emulsions: An Experimental Study.* World Academy of Science, Engineering and Technology, 2010. **62**: p. 691-694.

19. Stewart, M., Arnold, K. , *Emulsions and Oil Treating Equipment: Selection, Sizing and Troubleshooting*. 2009, London: Elsevier Inc. .

20. Khor, E.H., Samyudia, Y. . *Review on Produced Water Treatment Technology*. in *21st Symposium of Malaysian Chemical Engineers* 2007. Kuala Lumpur, Malaysia.

21. OSPAR, C. *Addendum to the OSPAR Background Document Concerning Techniques for the Management of Produced Water from Offshore Installations* 2006 [cited 2010 29 November]; Available from: http://www.ospar.org/documents/dbase/publications/p00295_factsheets%20for%20produced%20water.pdf.

22. Ranck, J.M., Bowman, R.S., Weeber, J.L., Katz, L.E., Sullivan, E.J., *BTEX Removal from Produced Water using Surfactant - Modified Zeolite.* Journal of Environmental Engineering, 2005. **131**(3): p. 434-442.

23. Price, G., *Failures of the global measurement system. Part 2: institutions, instruments and strategy*, in *Berita IKM- Chemisty in Malaysia*. 2010, Sept Institut Kimia Malaysia: Malaysia.

24. Tao, F.T., Curtice, S., Hobbs, R.D., Sides, J.L., Wieser, J.D., Dyke, C.A., Tuohey, D., and Pilger, P.F., *Reverse osmosis process successfully converts oil field brine into freshwater.* Oil and Gas Journal, 1993. **91**(38): p. 88-91.

25. Santos, S.M., Wiesner, M.R., *Ultrafiltration of Water generated in oil and gas production.* Water Environment Research, 1997. **69**(6): p. 1120-1127.

26. Richardson, J.F., Harker, J.H., Backhurst, J.R., *Ultrafiltration, membrane separation processes*, in *Coulson's and Richardson's Chemical Engineering*. 2002, Butterworth-Heinemann: Great Britain. p. 446-448.

27. Wijmans, J.G., Baker, R. W. , *The solution-diffusion model: a review* Journal of Membrane Science, 1995. **107**(1-2): p. 1-21.

28. Khor, E.H., Samyudia, Y., *The Study of Mass Transfer Coefficient in Membrane Separation for Produced Water.* International Journal of Chemical Engineering, 2009. **2**(2-3 (May-Dec 2009)): p. 143-152.

29. Yang, M., *Oil-in-Produced Water Measurement Training Course*. 2008, Kuala Lumpur, Malaysia.: TUV NEL Ltd. .

30. Azetsu-Scott, K., Yeats, P.,Wohlegeschaffen, G.,Dalziel, J., Niven, S., Lee, K. , *Precipitation of Heavy Metals in Produced Water: Influence on Contaminant Transport and Toxicity.* Marine Environmental Research, 2007. **63**: p. 146-167.

31. Khatib, Z., Verbeek, P. , *Water to Value - Produced Water Management for Sustainable Field Development of Mature and Green Fields.* Journal of Petroleum Technology, 2003: p. 26-28.

32. EPA, *Development Document for Effluent Limitations Guidelines and New Source Performance Standards for the Offshore Subcategory of the Oil and Gas Extraction Point Source Category.* U.S. Environmental Protection Agency, 1993. **EPA 821-R-93-003**.

33. Ali, S.A., Henry,L.R., Darlington, J.W., Occapiniti, J., *Novel Filtration Process Removes Dissolved Organics from Produced Water and Meets Federal Oil and Grease Guidelines*, in *9th Produced Water Seminar*. 1999: Houston, TX.

34. Tjeerdema, R.S., Anderson, B.S., Singer, M.M., Viant, M.R., *Accute and chronic effects of crude oil and dispersed oil on Chinook Salmon Smolts*. 2009: University of North Hampshire.

35. Philly, *Largest Oil Spill Ever*. 2004.

36. Ma, X., Cogswell, A., Li, Z., Lee, K., *Particle size analysis of dispersed oil and oil-mineral aggregates with an automated ultraviolet epifluorescence microscopy system.* Environ. Technol, 2008. **29**: p. 739-748.

37. Shinnar, R., *On the behaviour of liquid dispersions in mixing vessels.* Journal of Fluid Mechanics, 1961. **10**: p. 259-275.

38. Neff, J.M., Sauer, T.C., Jr., *Aromatic hydrocarbons in produced water*, in *Produced water 2: Environmental issues and mitigation technologies*, M. Reed, Johnsen, S., Editor. 1996, Plenum: New York. p. 163-175.

39. Viator, C.L., Gilley, G.E., Gracy, D., *Method of removing dissolved oil from produced water*, U.S. Patent, Editor. 1988: United States.

40. OSPAR, C. *OSPAR reference method of analysis for the determination of the dispersed oil content in produced water*. 2009; Available from: http://www.ospar.org

41. Yang, M., McEwan, D., *OIL-IN-WATER ANALYSIS METHOD (OIWAM) JIP*. 2005.

42. Niessen, W.M.A., *Principles and Instrumentation of Gas Chromatography-Mass Spectrometry*, in *Current Practice of Gas Chromatography-Mass Spectrophotometry*. 2001, Marcel Dekker. p. 1-29.

43. *Standard methods for examination of water and waste water*. 21 ed, ed. A.D. Eaton, Clesceri, L.S., Rice, E.W., Greenberg, A.E., Franson, M.A.H. 2005: American Public Health Association.

44. Sartorius, S.B., *Ultrafiltration Product Catalog*.

45. *Sartorius microfilters: Product overview*, Sartorius AG: Germany.

46. Song, L., *Flux Decline in Crossflow Microfiltration and Ultrafiltration: Mechanisms and Modeling of Membrane Fouling.* Journal of Membrane Science, 1998. **139**: p. 183-200.

47. Rautenbach, R., Albrecht, R. , *Membrane Processes*. 1989, England: John Wiley & Sons Ltd.

48. Baker, R.W., *Microfiltration*, in *Membrane Separation Systems - Recent Developments and Future Directions*. 1991. p. 337.

49. Noble, R.D., Stern, S.A., *Membrane Separations Technology. Principle and Applications*. 2nd ed. 1999: Elseviers

50. Yazhen, X., Dodds, J., Leclerc, D., *Cake Characteristics in Crossflow and Dead-end Microfiltration.* Filtration and Separation, 1995(Sept 1995): p. 795-798.

51. Mulder, M., *Basic Principles of Membrane Technology*. 1996: Kluwers Academic Publishers.

52. Choong, H.R., Martyn, P.C., Kremer, J.G., , *Removal of oil and grease in oil processing wastewaters* S.D.o.L.A. County, Editor. 1987: Los Angeles.

53. Choong, H.R., Martyn, P.C., Kremer, J.G., , *Removal of oil and grease in oil processing wastewaters* S.D.o.L.A. County, Editor. 1989: Los Angeles.

54. Lee, S., Aurelle, Y., Roques, H., *Concentration polarization membrane fouling and cleaning in ultrafiltration of soluble oil.* Journal of Membrane Science, 1983. **19**: p. 23-38.

55. Lobo, A., Cambiella, A., Benito, J.M., Pazos, C., Coca, J., *Ultrafiltration of oil-in-water emulsions with ceramic membranes: Influence of pH and crossflow velocity.* Journal of Membrane Science, 2006. **278**: p. 328-334.

56. Ricq, L., Pierre, A., Bayle, S., Reggiani, J., *Electrokinetic characterization of polyethersulfone UF membranes.* Desalination, 1997. **109**: p. 253-261.

57. Claudia, N.L., Amy, G.L., Jekel, M., *Understanding the Size and Character of Fouling-Causing Substances from Effluent Organic Matter (EfOM) in Low-Pressure Membrane Filtration.* Environ. Sci. Technol, 2006. **40**: p. 4495-4499.

58. Droste, R.L., *Theory and Practice of Water and Wastewater Treatment*. 1997, United States of America: John Wiley & Sons, Inc.

59. Hua, F.L., Wang, Y.J., Tsang, Y.F., Chan, S.Y., Sin, S.N., Chua, H., *Study of microfiltration behaviour of oily wastewater.* Journal of Environmental Science and Health, 2007. **42**: p. 489-496.

60. Rosenberger, S., Evenblij, H., S. te Poele, Wintgens, T., Laabs, C., *The Importance of Liquid Phase Analyses to Understand Fouling in Membrane Assisted Activated Sludge Processes-Six Case Studies of Different European Research Groups.* J. of Memb Sc, 2005. **263**: p. 113-126.

61. Yazhen Xu-Jiang, J.D.a.D.L., *Cake Characteristics in Crossflow and Dead-end Microfiltration.* Filtration and Separation, 1995(Sept 1995): p. 795- 798.

62. Yazdanshenas, M., Tabatabaee-Nezhad, S.A.R., Soltanieh, M., Roostaazad, R., Khoshfetrat A.B., *Contribution of fouling and gel polarization during ultrafiltration of raw apple juice at industrial scale* Desalination, 2010. **258**(1-3): p. 194-200.

63. Song, L., *A new model for calculation of the limiting flux in ultrafiltration.* Journal of Membrane Science, 1998. **144**: p. 173-185.

64. Spellman, F.R., ed. *Handbook of Water and Wastewater Treatment Plant Operations*. 2003, Lewis Publishers: Boca Raton.

65. Field, R.W., Wu, D., Howell, J.A. & Gupta, B.B. , *Critical Flux Concept for Microfiltration Fouling.* Journal of Membrane Science, 1995. **100**(3): p. 256-272.

66. Crespo, J.G., Böddeker, K. W., *Membrane processes in separation and purification* 1994, Boston: Kluwer Academic Publisher.

67. Nystrom, M., Pihlajamaki, A., Ehsani, N. , *Characterization of Ultrafiltration Membranes by Simultaneous Streaming Potential and Flux Measurements.* Journal of Membrane Science, 1994. **87**: p. 245-256.

68. Vyas, H.K., Bennett, R.J., and Marshall, A.D., *Performance of Crossflow Microfiltration during Constant Transmembrane Pressure and Constant Flux Operations.* International Dairy Journal, 2002. **12**(5): p. 473-479.

69. Anderson, J.D.J., *Computational fluid dynamics*. 1995, Singapore: McGraw-Hill.

70. Rahimi, M., Madaeni, S.S., Abbasi, K., *CFD modeling of permeate flux in cross-flow microfiltration membrane.* Journal of Membrane Science, 2005. **255**: p. 23-31.

71. Mo, L., Huang, X., and Wu, J., *Effect of Operational Conditions on Membrane Permeability in A Coagulation–Microfiltration Process for Water Purification.* J. Environ. Sci. Health, 2002. **37**: p. 273-285.

72. Howell, J.A., *Sub-critical flux operation of microfiltration.* Journal of Membrane Science, 1995. **107**: p. 165-171.

73. Pollice, A., Brookes, A., Jefferson, B., Judd, S. , *Sub-critical flux fouling in membrane bioreactors - a review of recent literature.* Desalination, 2005. **174**: p. 221-230.

74. Vela, M.C.V., Blanco, S.Á., García, J.L., Gozálvez-Zafrilla, J.M., Rodríguez, E.B., *Utilization of shear induced diffusion model to predict permeate flux in the crossflow ultrafiltration of macromolecules.* Desalination, 2007. **206**(1-3): p. 61-68.

75. Wagner, J., ed. *Membrane Filtration Handbook Practical Tips and Hints*. 2nd ed. 2001, Osmonics, Inc.

76. Liu, C., Caothien, S., Hayes, J., Caothuy, T., Otoyo, T., Ogawa, T. *Membrane Chemical Cleaning: From Art to Science*. Available from: http://www.pall.com/pdf/mtcpaper.pdf.

77. Mohammadi, T.M., S.S; Moghadam, M.K., *Investigation of Membrane Fouling.* Desalination, 2002. **153**: p. 155.

78. Madaeni, S.S., Mohammadi, T., Moghadam, M.K., *Chemical Cleaning of Reverse Osmosis Membranes.* Desalination 2001. **134**: p. 77-82.

79. Ang, W.S., Lee, S., Elimelech, M., *Chemical and Physical Aspects of Cleaning of Organic-Fouled Reverse Osmosis Membranes.* Journal of Membrane Science, 2006. **272,**: p. 198-210.

80. Grabosch, M., ed. *Cleaning Handbook: A Guide to Cleaning Membrane Filter Systems*. 2008, Sartorius AG, Separationstechnik.

81. Kim, K.J., Fane, A.G., Nystrom, M., Pihlajamaki, A., Bowen, W.R., Mukhtar, H., *Evaluation of Electroosmosis and Streaming Potential for Measurement of Electric Charges of Polymeric Membranes.* Journal of Membrane Science, 1996. **116**: p. 149-159.

82. Brink, L.E.S., Romijn, D.J. , *Reducing the Protein Fouling of Polysulfone Surfaces and Polysulfone Ultrafiltration Membranes: Optimization of the Type of Presorbed Layer.* Desalination, 1990. **78**: p. 209-233.

83. Gekas V., H., B. , *Microfiltration Membranes, Cross-Flow Transport Mechanisms and Fouling Studies.* Desalination, 1990. **77**: p. 195-218.

84. Taniguchi M., K.J.E., Belfort G., *Low Fouling Synthetic Membranes By UV-Assisted Graft Polymerization: Monomer Selection To Mitigate Fouling By Natural Organic Matter.* Journal of Membrane Science, 2003. **222**: p. 59-70.

85. Taniguchi M., B.G., *Low Protein Fouling Synthetic Membranes by UV-Assisted Surface Grafting Modification: Varying Monomer Type.* Journal of Membrane Science, 2004. **231**: p. 147-157.

86. Wavhal D.S., F.E.R., *Membrane Surface Modification by Plasma-Induced Polymerization of Acrylamide for Improved Surface Properties and Reduced Protein Fouling.* Langmuir, 2003. **19**: p. 79-85.

87. Good, K., Escobar, I., Xu, X., Coleman, M., Ponting, M., *Modification of Commercial Water Treatment Membranes by Ion Beam Irradiation.* Desalination, 2002. **146**: p. 259-264.

88. Hunter, J.S., *Design and Analysis of Experiments*, in *Juran's Quality Control Handbook*. 1999, Mc-Graw-Hill.

89. Tanco, M., Elisabeth, V., Laura, I., Maria, J.A., *Implementation of Design of Experiments Projects in Industry.* Applied Stochastic Models in Business and Industry, 2009. **25**(4): p. 478-505.

90. Soravia, S., Orth, A., *Design of Experiments*, in *Ullmann's Encyclopedia of Industrial Chemistry*. 2009.

91. Hahn, G.J., Patterson, A.N. , *Design of Experiments*, in *Kirk-Othmer Encyclopedia of Chemical Technology*. 2002.

92. Box, G.E.P., Cox, D.R.. Journal of the Royal Statistical Society, 1964. **Series B, 26**: p. 211.

93. Khuri, A., *Response Surface Methodology and Related Topics*. 2006: World Scientific Publishing Co.

94. Myers, R.H., Montgomery, D.C., *Response Surface Methodology*. 2nd ed. 2002, New York: John Wiley & Sons.

95. Montgomery, D.C., *Design and Analysis of Experiment*. 1984, New York: John Wiley & Sons.

96. Mannarswamy, A., Munson-McGhee, S.H., Steiner, R., Anderson, P.K., *D-Optimal Experimental Designs for Freundlich and Langmuir Adsorption Isotherms.* Chemometrics and Intelligent Laboratory Systems, 2009. **97**(2): p. 146-151.

97. Aguiar, P.F.D., Bourguignon, B., Khots, M.S., Massart, D.L., Phan, R.T.L., *D-Optimal Designs.* Chemometrics and Intelligent Laboratory Systems, 1995. **30**(2): p. 199-210.

98. Kruijf, S.D., Tee, T.D. , *Online oil-in-water analysers in Shell's EP operations units*, in *NEL's 4th Oil-in-water Monitoring Workshop*. 2002: Aberdeen, UK.

99. Ithnin, I.B., et al *The Discharge of Produced Water from Oil and Gas Production: Legislation Requirement in Malaysia*, in *NEL's 1st Produced Water- Best Management Practices*. 2006: Kuala Lumpur.

100. Agilent, *GC columns Stationary Phase Application Guide*. p. 315.

101. NRB, *Analytical Detection Limit Guidance & Laboratory Guide for Determining Method Detection Limits*, D.o.N.R. (DNR), Editor. 1996: Wisconsin.

102. Gbadebo, A.M., Taiwo, A.M., Ola, O.B. , *Effects of Crude Oil on Clrias garpinus: A Typical Marine Fish.* American Journal of Environmental Sciences 2009. **5**(6): p. 753-758.

103. Singer, M.M., Jacobson, S., Tjeerdema, R.S., Sowby, M. *Accute effects of fresh versus weathered oil to marine organisms: California findings*. in *Proceedings of 2001 International oil spill conference*. 2001. Tampa, Florida.

104. Sartorius, A.G., *Sartocon Cassettes and Sartocon Slice Cassettes: Directions for Use*, in *Sartorius Biotech GmbH*. 2006: Germany.

105. Johnson, R.A., ed. *Miller & Freund's Probability and Statistics for Engineers*. 7th ed. 2005, Prentice Hall.

106. Wijmans, J.G., Nakao, S., van den Berg, J.W.A., Troelstra, F.R., and Smolders, C.A., *Hydrodynamic resistance of concentration polarization boundary layers in ultrafiltration.* Journal of Membrane Science, 1985. **22**: p. 117-135.

107. Jonsson, G., *Boundary layer phenomena during ultrafiltration of dextran and whey protein solutions.* Desalination, 1984. **51**: p. 61-77.

108. Petala, M.D., Zouboulis, A.I., *Vibratory shear enhanced processing membrane filtration applied for the removal of natural organic matter from surface waters.* Journal of Membrane Science 2006. **269**(1-2): p. 1-14.

109. Cheng, T.W., Lee, Z.W. , *Effects of aeration and inclination on flux performance of submerged membrane filtration.* Desalination, 2008. **234**(1-3): p. 74-80.

110. Gekas, V., Hallstrom, B., *Mass Transfer in the membrane concentration polarization layer under turbulent cross flow. 1. Critical literature review and adaptation of existing sherwood correlations to membrane operations* Journal of Membrane Science, 1987. **30**: p. 153-170.

111. van den Berg, G.B., Smolder, C.A., *Mass transfer coefficients in cross-flow ultrafiltration.* Journal of Membrane Science, 1989. **47**: p. 25-51.

112. Khor, E.H., Samyudia, Y., *The Study of Mass Transfer Coefficient in Membrane Separation for Produced Water.* International Journal of Chemical Engineering, 2009. **2**(2-3): p. 143-152.

113. Murthy, Z.V.P., Gupta, S.K., *Estimation of Mass Transfer Coefficient using a Combined Nonlinear Membrane Transport and Film Theory Model.* Desalination, 1997. **109**: p. 39-49.

114. Pusch, W., Ber. Bunsenges. Physik. Chem., 1977. **81**(269).

115. Khor, E.H., Samyudia, Y. *Optimization of Dissolved Oil Separation for Produced Water Analysis*. in *5th International Symposium on Design, Operation and Control of Chemical Processes (PSE Asia)*. 2010. Singapore.

116. Box, G., Hunter, W., *Statistics for Experimenters*. 2006, Wiley Interscience.

117. Porter, M.C., *Concentration Polarization with Membrane Ultrafiltration.* Ind. Eng. Chem. Prod. Res. Develop. , 1972. **11**(3): p. 234 - 248.

118. Huang, L., Morrissey, M.T., *Fouling of membranes during microfiltration of surimi wash water: Roles of pore blocking and surface cake formation.* Journal of Membrane Science, 1998. **144**: p. 113-123.

119. Song, L., Elimelech, M., *Particle deposition onto a permeable surface in laminar flow* Journal of Colloid and Interface Science, 1995. **173**: p. 165-180.

120. Damak, K., Ayadi, A., Zeghmati, B., Schmitz, P., *A new Navier-Stokes and Darcy's law combined model for fluid flow in crossflow filtration tubular membranes.* Desalination, 2004. **161**: p. 67-77.

121. Nassehi, V., *Modelling of combined Navier-Stokes and Darcy flows in crossflow membrane filtration.* Chem. Eng. Sci., 1998. **53**: p. 1253-1265.

122. Pak, A., Mohammadi, T., Hosseinalipour, S.M., Allahdini, V., *CFD modeling of porous membranes.* Desalination, 2008. **222**: p. 482-488.

123. Ghidossi, R., Veyret, D., Moulin, P. , *Computational fluid dynamics applied to membranes: State of the art and opportunities*. Chemical Engineering and Processing 2006. **45**: p. 437-454.

124. Ahmad, A.L., Lau, K.K., *Modeling, simulation, and experimental validation for aqueous solutions flowing in nanofiltration membrane channel.* Ind. Eng. Chem. Res. , 2007. **46**: p. 1316-1325.

125. Belfort, G., Nagata, N., *Fluid mechanics and crossflow filtration: some thoughts.* Desalination, 1985. **53**: p. 57-79.

126. Ansys, I., *FLUENT 6.3 User-guide.* 2006.

127. Launder, B.E., Spalding, D.B. , ed. *Lectures in Mathematical Models of Turbulence*. 1972, Academic Press: London, England.

128. Bezerra, M.A., Santelli, R.E., Oliveira, E.P., Villar, L.S., Escaleira, L.A. , *Response surface methodology (RSM) as a tool for optimization in analytical chemistry.* Talanta, 2008. **76**: p. 965- 977.

129. Anderson, M.J., Whitcomb, P.J., ed. *RSM Simplified: Optimizing Processes using Response Surface Methods for design of Experiment*. 2005, Productivity Press: New York.

130. Madaeni, S.S., Saedi, Sh., Rahimpour, F., Zereshki, S., *Optimization of Chemical Cleaning for Removal of Biofouling Layer.* Chemical Product and Process Modeling, 2009. **4**(1, Article 16).

131. Ahmad, A.L., Ismail, S., Bhatia, S. , *Optimization of Coagulation−Flocculation Process for Palm Oil Mill Effluent Using Response Surface Methodology.* Environ. Sci. Technol., 2005. **39**(8): p. 2828-2834.

132. Ting, H.T., Abou-El-Hossein, K.A., Chua, H.B., *Prediction of etching rate of aluminosilicate glass by RSM and ANN.* Journal of Scientific & Industrial Research, 2009. **68**: p. 920-924.

133. Lee, S., Aurelle, Y., Roques, H., *Concentration polarization, membrane fouling and cleaning in ultrafiltration of soluble oil.* Journal of Membrane Science, 1984. **19**: p. 23-38.

134. Farahbakhsh, K., Szrcek, C., Guest, R.K., Smith, D.W., *A review of the impact of chemical pretreatment on low-pressure water treatement membranes.* Journal of Environmental Engineering and Science, 2004. **3**: p. 237-253.

135. Poulopoulos, S.G., Voutsas, E.C., Grigoropoulou, H.P., Philippopoulos, C.J., *Stripping as a pretreatment process of industrial oily wastewater.* Journal of Hazardous Materials, 2005. **B117**: p. 135-139.

136. Grant, G.T., Morris, E.R., Rees, D.A., Smith, J.C., Thom, D., *Biological interaction between polysaccharides and divalent cations: the eggbox model.* FEBS Letter, 1973. **32**: p. 195-198.

137. Rees, D.A., *Polysaccharide shapes and their interactions- some recent advances.* Pure Applied Chemistry, 1984. **53**: p. 1-14.

138. Jacangelo, G.J., Laine, J.M., Cummings, E.W., Deutschmann, A., Malevialle, J., Wiesner, M.R., *Evaluation of ultrafiltration membrane pre-treatment and nanofiltration of surface waters*. American Water Works Association Research Foundation, Denver, Colo. 1994.

139. Kurt, S., *Effects of pH and chitosan on beef emulsion properties.* International Journal of Food Science and Technology, 2010. **45**: p. 140-146.

140. Lopes, P.E.M., Lamoureux, G., Roux, B., MacKerell, A.D., *Polarizable Empirical Force Field for Aromatic Compounds Based on the Classical Drude Oscillator.* Journal of Physical Chemistry, 2007. **111**(11): p. 2873-2885.

141. Calderó, G., García-Celma, M. J., Solans, C., Pons, R. , *Effect of pH on Mandelic Acid Diffusion in Water in Oil Highly Concentrated Emulsions (Gel Emulsions).* Langmuir, 2000. **16**(4): p. 1668-1674.

142. Chen, W., Parma, F., Patkar, A., Elkin, A., and Sen, S., *Selecting Membrane Filtration Systems*, in *CEP Magazine*. 2004.

143. Hydranautics, *Foulants and cleaning procedures for composite polyamide RO membrane elements*, in *Technical service bulletin*. 2010.

144. McFarlane, J., Bostick, D.T., Luo, H. *Characterization and Modeling of Produced Water*. in *Ground Water Protection Council Produced Water Conference*. 2002. Colorado Springs, CO.

145. Moosemiller, M.D., C.G., Hill JR., M.A., Anderson, *Physicochemical properties of supported γ -Al2O3 and TiO2 ceramic membranes.* Separation Science and Technology, 1989. **24**: p. 641-657.

146. Manttari, M., Pihlajamaki, A., Nystrom, M., *Effect of pH on hydrophilicity and charge and their effect on the filtration efficiency of NF membranes at different pH.* Journal of Membrane Science, 2006. **157**(1-3): p. 369-375.

147. Galjaard, G., Kruithof, J., Kamp, P.C. , *Influence of NOM and Membrane Surface Charge on UF-membrane fouling*, in *Membrane Technology Conference,*. 2005, AWWA: Phoenix, Arizona.

148. Shim, Y., Lee, H-J., Lee, S., Moon, S-H, Cho, J., *Effects of Natural Organic Matter and Ionic Species on Membrane Surface Charge.* Environmental Science Technology, 2002. **36**: p. 3864-3871.

149. Blanpain-Avet, P., Doubrovine, N., Lafforgue, C., Lalande, M., *The effect of oscillatory flow on crossflow microfiltration of beer in tubular mineral membrane system- Membrane fouling resistance decrease and energetic considerations.* Journal of Membrane Science, 1999. **152**(3): p. 151-174.

150. Gesan-Guiziou, G., Boyaval, E., Daufin, G., *Critical stability conditions in crossflow microfiltration of skimmed milk: Transition to irreversible deposition.* Journal of Membrane Science, 1999. **158**(5): p. 211-222.

Appendix

Appendix A shows the results from a preliminary experimental study for determining the optimum TMP in the cross-flow filtration system. All the experiments were conducted at the optimum TMP found in this appendix unless specified otherwise. The produced water feed is filtered through each of the membranes namely 50kDa-PESU, 100kDa-PESU, 100kDa-H and 0.2μm-H membranes by changing the TMP. The permeate fluxes are recorded. The TMP at which the flux does not change by increasing the TMP is the optimum TMP.

Appendix B shows the calculations in the experiment for determining the k values in Chapter 5.

APPENDIX A:

DETERMINATION OF OPTIMUM TMP FOR CROSSFLOW SYSTEM

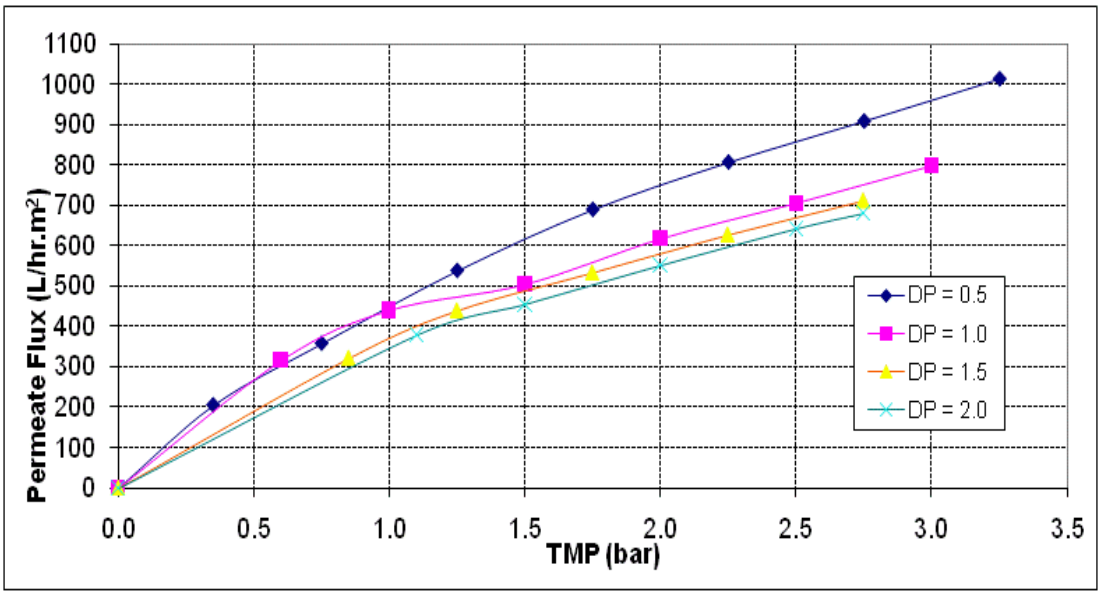

Figure A.1 Flux vs. TMP for 50kDa PESU membrane

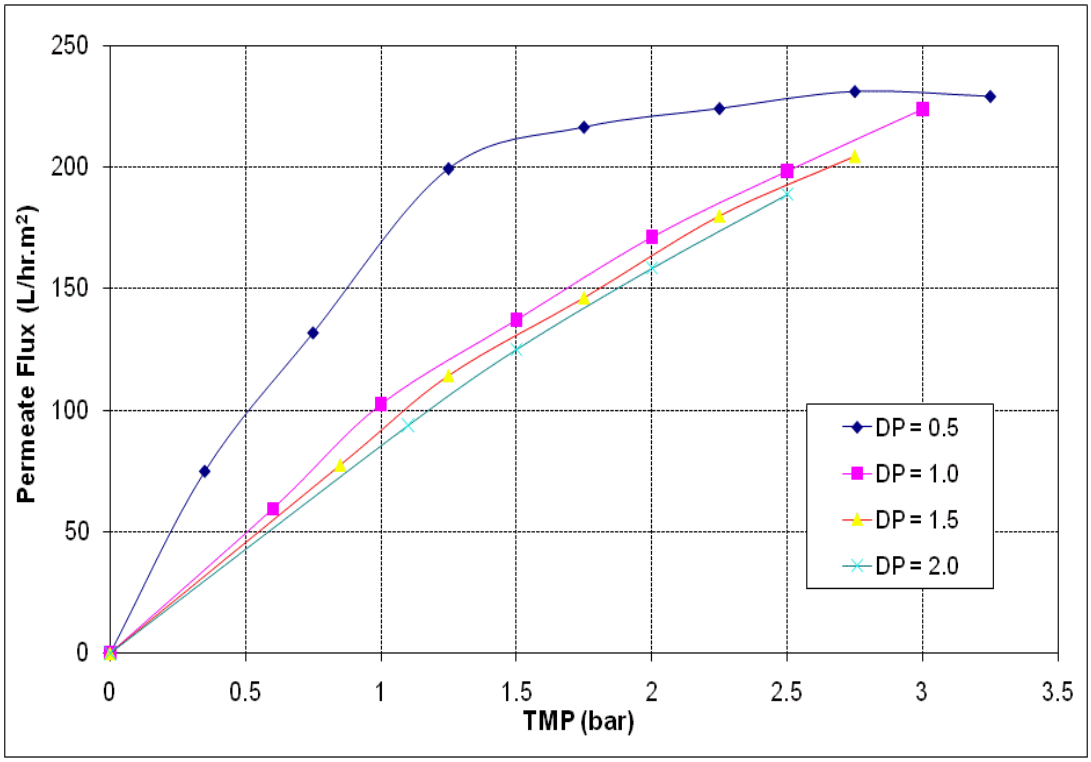

Figure A.2 Flux vs. TMP for 100kDa PESU membrane

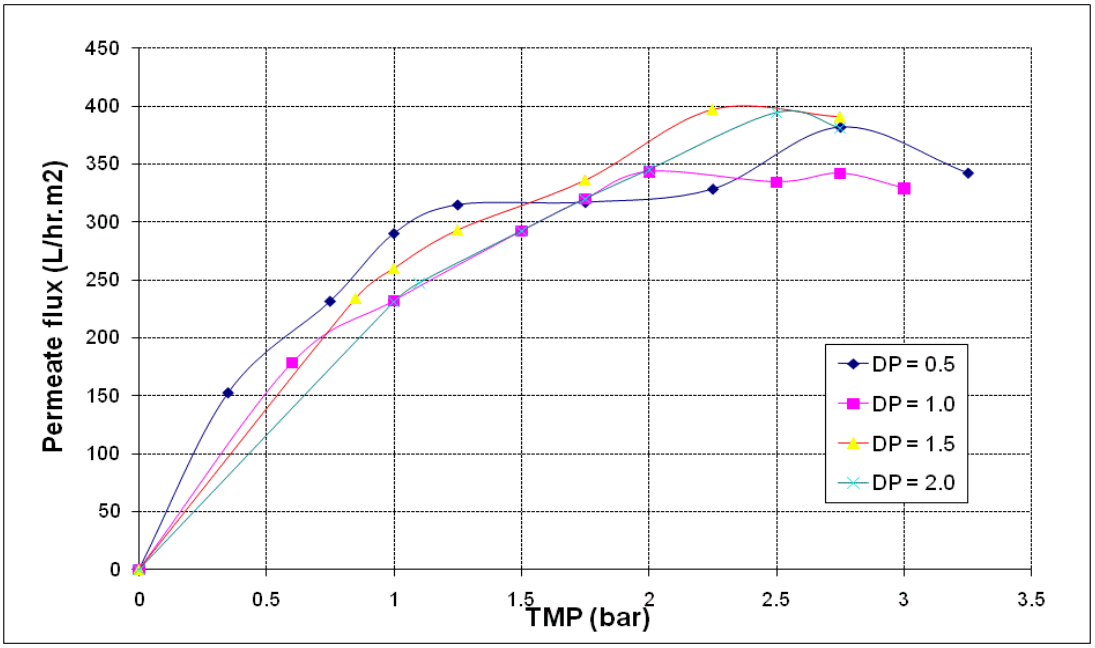

Figure A.3 Flux vs. TMP for 100kDa Hydrosart® Membrane

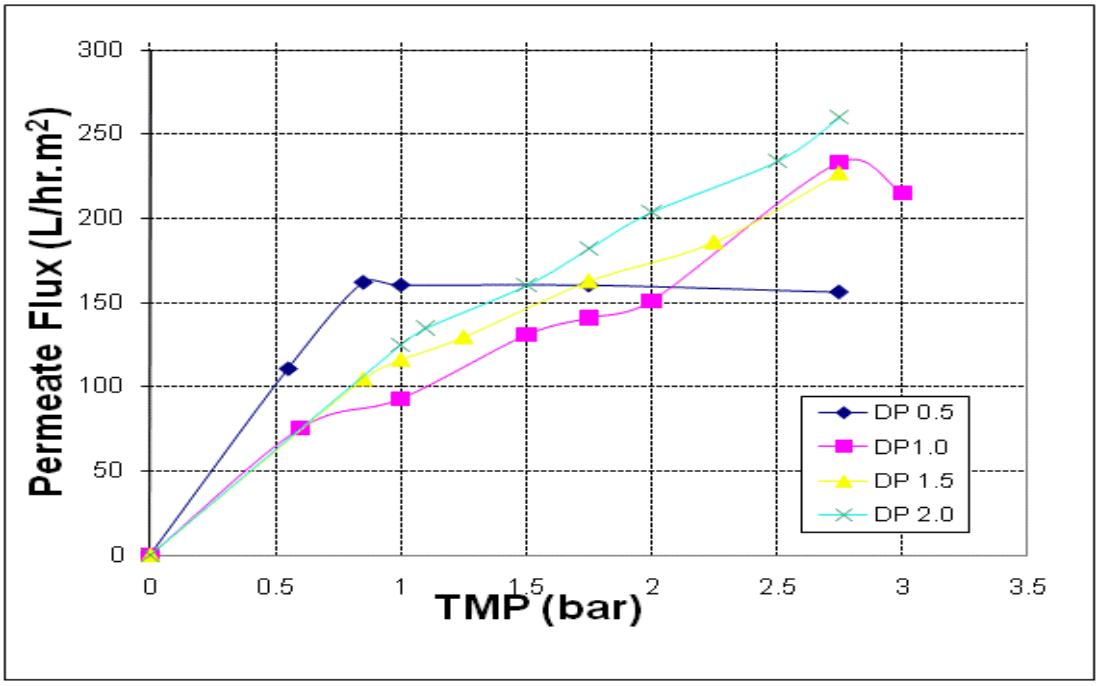

Figure A.4 Flux vs. TMP for 0.2µm Hydrosart® membrane

APPENDIX B:

CALCULATIONS FOR THE DETERMINATION OF K VALUES IN CHAPTER 4

DP = Feed Pressure (P_F) – Outlet Pressure (P_R)

TMP = $[(P_F + P_R)/2] – P_p$

Weight of 100ml DI water (A) = Weight of Beaker with 100ml DI water – Weight of Beaker

Weight of 100ml feed water (B) = Weight of Beaker with 100ml feed water – Weight of Beaker

Initial Feed concentration g/ml = (B-A)/100

Weight of permeate (C) = weight of cylinder with 100ml permeate – weight of cylinder

Permeate concentration g/ml = (C-A)/100

Flux = Flow rate calculated/ Effective area of membrane

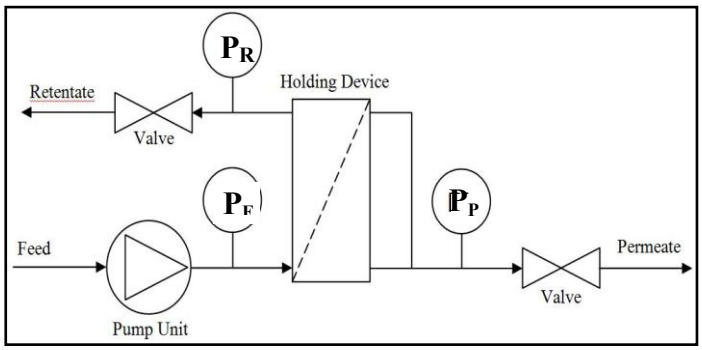

Figure B.1 Schematic diagram of membrane filtration unit

APPENDIX C:

FLUENT MODEL

C1: Parameters defined in FLUENT at Differential Pressure 0.5bar

- Defined Material Used: Water
- Density: 998.2 kg/m3
- Cp (Specific Heat): 4182 j/kg-k
- Thermal Conductivity: 0.6 w/m-k
- Viscosity: 0.001003 kg/m-s
- Molecular Weight: 18.0152 kg/kgmol

- Defined Boundary conditions
- In-velocity: mass flow-rate at 0.0495 kg/s, with turbulence intensity 70%, anti- gravitational flow.
- Wall: Stationary wall with no slip condition.
- Porous membrane: Face Permeability 1.65002e-16m^2 with 0.1mm thickness
- Permeate outlets: zero gauge pressure, targeted mass flow 0.0229kg/s each
- Retentate outlet: Gauge Pressure 253313pascal, targeted mass flow 0.00368kg/s

- Defined Solver: Pressure based
- Implicit, Steady, Standard k-epsilon turbulence model

- Defined Solution Controls
- Solve for flow and turbulence equation.

- Define Initial Conditions
- Initial Gauge Pressure 303975pascal
- Y-velocity: 0.05m/s

C2: Parameters defined in FLUENT at Differential Pressure 1.0bar

- Defined Material Used: Water
- Density: 998.2 kg/m3
- Cp (Specific Heat): 4182 j/kg-k
- Thermal Conductivity: 0.6 w/m-k
- Viscosity: 0.001003 kg/m-s
- Molecular Weight: 18.0152 kg/kgmol

- Defined Boundary conditions
- In-velocity: mass flow-rate at 0.0691kg/s, with turbulence intensity 40%, anti- gravitational flow.
- Wall: Stationary wall with no slip condition.
- Porous membrane: Face Permeability 1.65002e-16m^2 with 0.1mm thickness
- Permeate outlets: zero gauge pressure, targeted mass flow 0.0223kg/s each
- Retentate outlet: Gauge Pressure 233048pascal, targeted mass flow 0.0251kg/s

- Defined Solver: Pressure based
- Implicit, Steady, Standard k-epsilon turbulence model

- Defined Solution Controls
- Solve for flow and turbulence equation.

- Define Initial Conditions
- Initial Gauge Pressure 334372.5pascal
- Y-velocity: 0.07m/s

C3: Parameters defined in FLUENT at Differential Pressure 1.5bar

- Defined Material Used: Water
- Density: 998.2 kg/m3
- Cp (Specific Heat): 4182 j/kg-k
- Thermal Conductivity: 0.6 w/m-k
- Viscosity: 0.001003 kg/m-s
- Molecular Weight: 18.0152 kg/kgmol

- Defined Boundary conditions
- In-velocity: mass flow-rate at 0.08504kg/s, with turbulence intensity 13%, anti- gravitational flow.
- Wall: Stationary wall with no slip condition.
- Porous membrane: Face Permeability 1.65002e-16m^2 with 0.1mm thickness
- Permeate outlets: zero gauge pressure, targeted mass flow 0.02116kg/s each
- Retentate outlet: Gauge Pressure 202650pascal, targeted mass flow 0.04271kg/s

- Defined Solver: Pressure based
- Implicit, Steady, Standard k-epsilon turbulence model

- Defined Solution Controls
- Solve for flow and turbulence equation.

- Define Initial Conditions
- Initial Gauge Pressure 354638pascal
- Y-velocity: 0.085m/s

C4: Parameters defined in FLUENT at Differential Pressure 2.0bar

- Defined Material Used: Water
- Density: 998.2 kg/m3
- Cp (Specific Heat): 4182 j/kg-k
- Thermal Conductivity: 0.6 w/m-k
- Viscosity: 0.001003 kg/m-s
- Molecular Weight: 18.0152 kg/kgmol

- Defined Boundary conditions
- In-velocity: mass flow-rate at 0.09375kg/s, with turbulence intensity 10%, anti- gravitational flow.
- Wall: Stationary wall with no slip condition.
- Porous membrane: Face Permeability 1.65002e-16m^2 with 0.1mm thickness
- Permeate outlets: zero gauge pressure, targeted mass flow 0.01911kg/s each
- Retentate outlet: Gauge Pressure 151988pascal, targeted mass flow 0.05553kg/s

- Defined Solver: Pressure based
- Implicit, Steady, Standard k-epsilon turbulence model

- Defined Solution Controls
- Solve for flow and turbulence equation.

- Define Initial Conditions
- Initial Gauge Pressure 303975pascal
- Y-velocity: 0.09392m/s

APPENDIX D:

GRID DIAGRAM FOR CFD SIMULATION

Grid diagram below shows the boundaries for fluid flow simulations inside the membrane as explained in Appendix C.

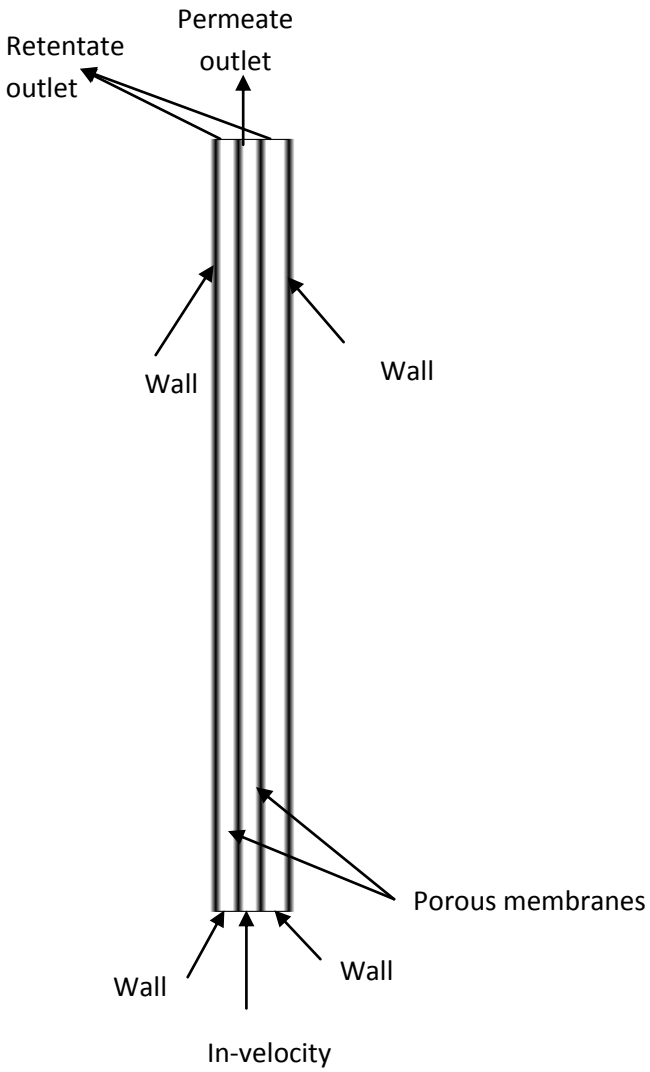

APPENDIX E:

Calculation for Section 3.5 on one experimental run

Sample volume	1µl Crude Oil Feed			1µl Retentate			1µl Permeate		
	Area	ppm	%	Area	ppm	%	Area	ppm	%
Dissolved Oil	C_{ss}	$K*C_{ss}$	100	R_{ss}	$K*R_{ss}$	$(K*R_{ss}/K*C_{ss})*100$	P_{ss}	$K*P_{ss}$	$(K*P_{ss}/K*C_{ss})*100$
Dispersed Oil	C_{sp}	$K*C_{sp}$	100	R_{sp}	$K*R_{ss}$	$(K*R_{sp}/K*C_{sp})*100$	N.D.	N.D.	
Total Crude	C_t	100							

$K=100/C_t$

"*" means multiply

Integration of total spectrum area from Crude Oil = C_t

Integration of dissolved oil spectrum area from Crude Oil = C_{ss}

Integration of dispersed oil spectrum area from Crude Oil = C_{sp}

Since C_t = 100ppm,

Concentration for dissolved oil for Crude oil is K * C_{ss} and this is 100% of dissolved oil in the feed.
Similarly, concentration for dispersed oil for Crude oil is K * C_{sp} and this is 100% of dispersed oil in the feed.

The retentate and permeate is calculated in the similar way as shown in the table.

APPENDIX F:

Sample of quantification reports for Chapter 4

Quantification Report for Feed (for 0.02 μm membrane)

Data Path : C:\msdchem\1\DATA\
Data File : KHOR26.D
Acq On : 15 Oct 2009 12:30
Operator : Chong
Sample : Crude Oil 100ppm (Feed)

ALS Vial : 1 Sample Multiplier: 1

Quant Time: Mar 09 16:29:26 2010
Quant Method : C:\msdchem\1\METHODS\Crude Oil.M
Quant Title : Crude oil
QLast Update : Fri Oct 30 14:40:52 2009
Response via : Initial Calibration

Compound	R.T.	QIon	Response	Conc	Units
Target Compounds					
1) Eicosane	30.404	57	585	1.64	ppm #
2) Xylene	8.008	106	528	2.84	ppm #
3) Ethylbenzene	7.745	91	162	12.62	ppm #

(#) = qualifier out of range (m) = manual integration (+) = signals summed

Ref: Crude Oil.M Tue Mar 09 16:29:26 2010

Quantification Report for Retentate (for 0.02 μm membrane)

Data Path : C:\msdchem\1\DATA\
Data File : KHOR27.D
Acq On : 15 Oct 2009 14:25
Operator : Chong
Sample : Crude Oil 100ppm (Retentate)
Misc :
ALS Vial : 1 Sample Multiplier: 1

Quant Time: Mar 09 16:18:15 2010
Quant Method : C:\msdchem\1\METHODS\Crude Oil.M
Quant Title : Crude oil
QLast Update : Fri Oct 30 14:40:52 2009
Response via : Initial Calibration

Compound	R.T.	QIon	Response	Conc	Units
Target Compounds					
1) Eicosane	0.000	0		N.D.	
2) Xylene	8.008	106	234	1.42	ppm
3) Ethylbenzene	7.745	91	6	0.42	ppm

(#) = qualifier out of range (m) = manual integration (+) = signals summed

Ref: Crude Oil.M Tue Mar 09 16:18:15 2010

Quantification Report for Permeate (for 0.02 μm membrane)

Data Path : C:\msdchem\1\DATA\
Data File : KHOR28.D
Acq On : 15 Oct 2009 15:40
Operator : Chong
Sample : Crude Oil 100ppm (Permeate)
Misc :
ALS Vial : 1 Sample Multiplier: 1

Quant Time: Mar 09 16:29:45 2010
Quant Method : C:\msdchem\1\METHODS\Crude Oil.M
Quant Title : Crude oil
QLast Update : Fri Oct 30 14:40:52 2009
Response via : Initial Calibration

Compound	R.T.	QIon	Response	Conc	Units
Target Compounds					
1) Eicosane	0.000	0		N.D.	
2) Xylene	8.008	106	102	0.39	ppm
3) Ethylbenzene	7.745	91	3	0.07	ppm

(#) = qualifier out of range (m) = manual integration (+) = signals summed

Ref: Crude Oil.M Tue Mar 09 16:29:45 2010